ASSESSING THE VEGETATION AND SOIL SHEAR TESTER (VASST) AS A TOOL TO MEASURE VEGETATED SOIL SHEAR STRENGTH

BY

CASEY D. CAMPBELL

THESIS

Submitted in partial fulfillment of the requirements
for the degree of Master of Science in Agricultural and Biological Engineering
in the Graduate College of the
University of Illinois at Urbana-Champaign, 2014

Urbana, Illinois

Adviser:

Professor Prasanta Kalita

ABSTRACT

The degradation of military training lands due to vehicular traffic presents a challenge for land managers trying to optimize training capacity while reducing impacts. The Optimal Allocation of Land for Training and Non-Training Uses (OPAL) Program aims to provide a model for land managers to predict impacts of training under a range of land management regimes utilizing soil, vegetation, and climatic data. In general, OPAL's intended purpose is to help land managers optimize training land carrying capacity.

As part of OPAL, the Vegetation And Soil Shear Tester (VASST) was developed as a new method of in-situ measurement for shear strength of vegetated soils. During this research, data on vegetation and soil parameters was collected concurrently with VASST measurements at five geographic locations to determine if the VASST effectively measured soil shear strength. Additionally, as part of this study, a Python program was developed to automate the process of conditioning and analyzing VASST outputs to reduce human bias and dramatically decrease processing times of raw data.

Evaluating the VASST against calculated soil shear strength as well as other common in-situ strength measurements such as cone index, drop-cone value, and Clegg impact values, confirmed that the VASST shear measurements were moderately to strongly correlated with one another. An investigation into potential associations of soil parameters to strength measurements obtained with the VASST was conducted. VASST measures were taken in high plasticity (clayey) and non-plastic (sandy) soils where soil strengths were dictated by particle size, aboveground biomass, and root weight. Results also indicated that soil moisture content influenced VASST measured soil shear strength in high plasticity soils.

ACKNOWLEDGEMENTS

I would like to thank Heidi Howard of the United States Army Corps of Engineers Engineer Research Development Center- Construction Engineering Research Laboratory (ERDC-CERL) for giving me the opportunity to pursue a master's degree and providing guidance throughout my research. Also, I would like to thank Daniel Koch (ERDC-CERL) and Andrew Fulton (ERDC-CERL) for providing me with valuable input and support during my graduate studies and research. I also appreciate the many people within CERL and the Cold Regions Research and Engineering Laboratory (CRREL) who provided direct assistance with data collection, sample processing, as well as input on my research. In particular, I would like to thank Kelly McDonald (CRREL), Taylor Leahy of the University of Illinois at Urbana-Champaign (UIUC), Jeff Mifflin (CERL), Nick Wendling (UIUC), Paul Schumacher (UIUC), and August Metzler (UIUC).

I thank Dr. Prasanta Kalita (UIUC) for serving as my advisor through my undergraduate and graduate studies at UIUC. I greatly appreciate Dr. George Gertner (UIUC/CERL) who provided me with advice on the statistical analysis of my research, as well as mentored me in SAS programming procedures. I express my gratitude to Dr. Bhattarai (UIUC) for his feedback on the presentation of my research and for serving on my committee. Thank you to Paul Davidson (UIUC) for also serving on my committee.

Funding and support for this work was provided by ERDC-CERL under the Army 6.2 A896 program and as a part of the OPAL Work Package.

TABLE OF CONTENTS

CHAPTER 1: INTRODUCTION

1.1 Motivation

The Army's mission requirements often include the use of heavy armored equipment, some weighing up to 70 tons (Rostam-Abadi et al., 1993), on naturally vegetated soils within training lands. Due to repeated traffic on training areas, land degradation is likely to occur. Land degradation can lead to increased soil erosion, hazardous training conditions, decreased mobility and realism, and costly land rehabilitation. It is important for the Army to understand the soil mechanics leading to this type of land degradation in order to improve the quality of training lands and optimize land rehabilitation (Guretzky et al., 2005).

Since the publishing of Army Regulation (AR) 210-21 in 1997, The United States Army has been researching methods to reduce its environmental impact from repeated training activities on training lands. The motivation for increasing environmental conservation is addressed in AR350-19 which assigns responsibilities and provides policy and guidance for the management and operation of ranges and training lands. AR350-19 supports U.S. Army long-term sustainability and utility to meet the national defense mission with core programs such as the Army's Sustainable Range Program (SRP), Range and Training Lands Program (RTLP), and Integrated Training Area Management (ITAM) Program. These programs enable the Army to manage and maintain training lands to meet mission requirements while striving to minimize negative effects of military activity on the environment (U.S. Department of the Army, 2005).

1.2 Background

The Mohr-Coulomb failure criterion is used throughout engineering practices to calculate the shear strength of homogeneous materials. When dealing with engineered soil (non-vegetated), Equation 1.1 describes soil shear strength.

$$\tau = c + \sigma \tan \phi \qquad \text{Eq.1.1}$$

τ = shear strength

c = particle cohesion

σ = applied normal force

ϕ = the internal angle of friction

However, roots commonly present in vegetated soils have shown a measurable effect on soil shear strength (Waldron, 1977; Abe and Ziemer 1991). Roots from vegetated soil are unaccounted for in the Mohr-Coulomb failure criterion for homogenous materials.

One of the first studies on the shear strength of root permeated soil columns was conducted by Endo and Tsuruta (1969). Endo's research on the soil reinforcement of properties of tree roots was done using a rigid box with a normal load applied at the soil surface and a shearing load applied perpendicular to the normal load.

Figure 1.1: Schematic of Endo and Tsuruta (1969) experimental apparatus (Endo, 1980)

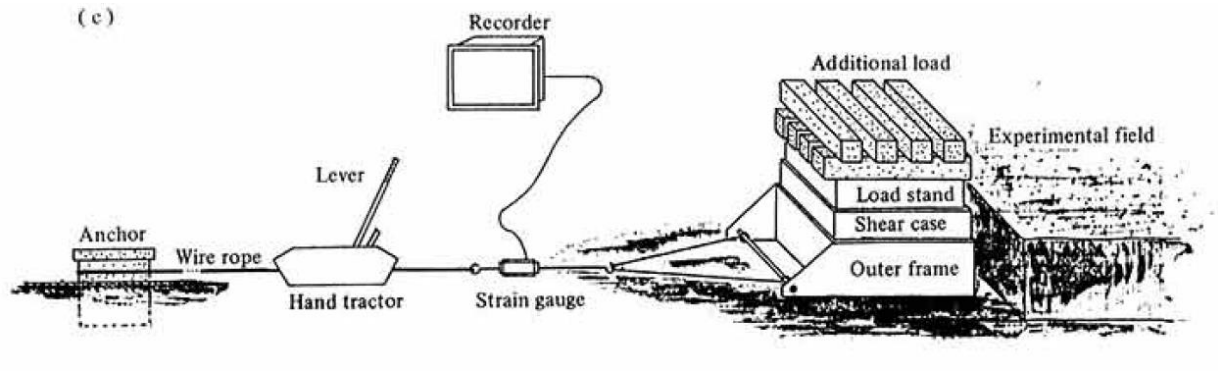

Although the test was performed in-situ, it simulated a direct shear test commonly conducted under laboratory conditions. The results of this study showed that roots in the soil matrix increase soil shear strength. Later studies confirmed Endo's findings of the reinforcing effects of roots on soil (Waldron, 1977; Gray and Leiser, 1982; Gray and Sotir, 1996; Pollen and Simon, 2005; Zhang, et al. 2010).

In 1977, L. J. Waldron proposed a modified Mohr-Coulomb failure criterion in order to describe the effects of roots on soil shear strength. Results from Waldron's testing showed that soils containing roots can be analyzed as a composite material, with the roots acting as high tensile strength fibers distributed in a lower tensile strength material (1977). The equation he used to describe vegetated soil shear strength is Equation 1.2.

$$\tau = c + \Delta s + \sigma \tan \phi \qquad \text{Eq. 1.2}$$

The addition of Δs to the basic equation accounted for the increase in shear strength due to the reinforcing effect of roots and has been adopted as a common way of describing the shear strength of vegetated soils.

Current research at the Engineering Research Development Center (ERDC) led to the development of a device that tests soil strength by mimicking a direct shear test. The device, known as the VASST, was designed and built as a tool to quantify soil mobility and

trafficability, with the reinforcing effects of vegetation present (MacDonald, et al. 2012). The VASST is advantageous over previous methods due to its ability to perform relatively quick, in-situ tests with minimal ground disturbance, while simulating horizontal forces at the soil surface seen during vehicle trafficking.

1.3 Purpose

Many studies describing the effects of roots on shear strength have been disclosed in previous studies. However, most research has addressed root reinforcement for slope stability rather than trafficability. The VASST provides shear strength measurements analogous to horizontal shearing occurring at the soil surface during typical vehicle maneuvers; providing a perspective on the role roots play in laterally reinforcing the soil surface. By investigating the role roots play in trafficability, the Army plans to incorporate belowground biomass into current land carrying capacity models and the NATO Referenced Mobility Model (NRMM). The addition of root influence on soil shear strength, as measured by the VASST, will aid the Army's conservation efforts by identifying training land conditions that may lead to accelerated land degradation or areas which have a higher land carrying capacity for training maneuvers. As a result, the Army will be able to more effectively utilize training lands by decreasing the down time needed to rehabilitate vegetation and soil between training events.

CHAPTER 2: RESEARCH OBJECTIVES

The goal of this research was to develop a vegetated soil shear strength equation specific to measurements taken with the VASST, based on the modified Mohr-Coulomb failure criterion. The research focus was to develop a relationship between soil strength and potential of vegetation rooting effects on soil trafficability using the VASST. The hypothesis was tested using field-measured data to estimate vegetation rooting effects on soil trafficability.

These were the specific objectives:

1. Develop a model based on the modified Mohr-Coulomb failure criterion to describe direct shear forces measured by the VASST tests.
2. Create an automated approach to computing critical soil shearing force resulting from VASST tests.
3. Validate the model from Objective 1 using field-collected vegetation and soil data and compare the VASST test results to in-situ measurements associated with soil trafficability.

CHAPTER 3: LITERATURE REVIEW

In order to understand how the VASST may build on previous research of vegetated soil strength, an in-depth literature review was performed. The history and past research presented in this thesis served as valuable resources for the development of Mohr-Coulomb as it relates to measurements obtained with the VASST.

3.1 Discovery of Mohr-Coulomb Failure Criterion

To fully understand the complexities of soil shear strength and how to calculate it, a review of the Mohr-Coulomb failure criterion initial development was performed. The Mohr-Coulomb failure criterion, as explained by Holtz et al. (2010) arose from the combining of ideas from Christian Otto Mohr and Charles-Augustin de Coulomb. Mohr hypothesized that materials fail when shear stress on a failure plane reached a critical value which depended on the normal stress. This idea is shown in the following equation:

$$\tau_{ff} = f(\sigma_{ff}) \qquad \text{Eq. 3.1}$$

τ = shear strength

σ = applied normal force

With this function, Mohr had developed a method of predicting shear failure in homogeneous materials.

In the 18th century, Coulomb was interested in the sliding friction characteristics of various soils and observed both a stress-independent component and a stress-dependent component of shear strength. The stress dependent component behaved similar to sliding friction; Coulomb identified this stress as internal angle of friction, denoted as ϕ in Equation 3.2. The symbol *c* was given to the independent component that seemed related to intrinsic cohesion.

The combining of Mohr and Coulomb's theories and observations led to the realization of the Mohr-Coulomb Failure Criterion, shown in Equation 3.2, which is currently used to determine the shear strength of engineered soils.

$$\tau_{ff} = c + \sigma_{ff} tan\, \phi \qquad \text{Eq. 3.2}$$

τ = shear strength

c= cohesion of soil particles

σ = applied normal force

ϕ = internal angle of friction

3.2 Adaption of Mohr-Coulomb Failure Criterion for Vegetated Soil

Although the Mohr-Coulomb Failure Criterion effectively estimates the shear strength of engineered soil, it does not account for the reinforcing qualities of roots in the soil matrix. Plant roots provide reinforcement to a soil matrix by increasing the soil matrix's tensile strength, a property that unvegetated soil lacks (Greenway, 1987). A reinforced soil matrix comprised of roots transfers the stress to roots as a soil is loaded, thus increasing the soil shear strength (Thorne, 1990).

There are several methods of testing the shear strength of the soil matrix with roots acting as reinforcing members. These methods include direct shear test, triaxial load test, and the root strength method. For the purpose of this research, the direct shear test will be reviewed in detail as it shares the most similarities to the mechanical behavior of the VASST, mainly the application of a load to the soil matrix in a single direction. The triaxial compression test will be discussed only briefly to gain further insight on root-soil interactions under unconstrained failure plane conditions.

3.2.1 Direct Shear Test Method

Pioneering the quantification of root influence on soil shear strength was a composite study by Endo and Tsuruta (1969) and Endo 1980. Results were published after each phase of the study. The study used 50 cm X 50 cm plots with 1 to 2 tree seedlings planted as yearlings. After two growing seasons, the plots containing the 3-year-old trees were subjected to an in-situ direct shear test at depths of 25 cm and 30 cm. In order to perform the test, the plots were incased with a rigid box and surrounding soil was excavated. The plot, or soil column, had a normal load applied to the soil surface. With the normal load applied, a horizontal load was gradually applied to the box using a cable come-along. A strain gauge recorded the force which tended to gradually increase to a certain maximum, then decrease thereafter. After failure had occurred along the shear plane, all exposed roots were collected, and diameters of the cut root ends were measured. The test apparatus is illustrated in Figure 1.1.

Endo (1980) concluded that the effect of roots in a soil matrix increase shear strength of soil. Endo proposed that the cohesion variable in Mohr-Coulomb Failure Criterion is the sum of the cohesion capacity of the soil itself and the effect of the root system. The composite report stated that the total cohesion could be equated using Equation 3.3 or alternatively Equation 3.4.

$$C = c + bR \qquad \text{Eq. 3.3}$$

c = cohesion from the soil particles

b = an experimental coefficient

R = the root weight per unit soil volume

$$C = c + b'D \quad \text{Eq. 3.4}$$

c = cohesion from the soil particles

b' = an experimental coefficient

D = total cross-sectional area of roots at shearing plane

Waldron (1977) applied concepts from Endo and Tsuruta's initial study to create a laboratory experiment to measure the reinforcing effects of roots in a soil matrix. Waldron created four types of engineered soils that were contained in rigid, 25.4 cm diameter cardboard tubes. The tubes were planted with barley, alfalfa, and yellow pine and allowed to grow for 3 months, 12 months, and 16 months respectively. A direct shear test was performed at 15, 30, and 45 cm to determine the amount of reinforcement the roots provided to the soil matrix. Waldron found that all species had reinforcing qualities in the soil matrix. The most important result of the research was Waldron's resulting modification of the Mohr-Coulomb Failure Criterion to account for the reinforcing effect of roots. Waldron created a modified Mohr-Coulomb Failure Criterion by adding Δs as a parameter to describe the effect of roots on shear strength, shown in Equation 1.2. He found that roots' effect on shear strength could be described with Equation 3.5.

$$\Delta s = T_r(\sin\theta + cos\theta \tan\phi)(A_R/A) \quad \text{Eq. 3.5}$$

T_r = average tensile strength per root area

θ = angle of distortion in the shear zone

A_R= cross-sectional area of roots at the shearing plane

A = total cross-sectional area of the shearing plane

Waldon's (1977) model, shown in Equation 1.2, had some assumptions which severely limited its applicability to the real-world scenarios of slope stability. The first assumption was the limitation of the direct shear method, which only measured shear strength along a

predetermined plane, horizontal in this case, not the weakest shear plane. Also, the model assumed that roots are flexible, linearly elastic, and uniform in size, type, and ordination, unlike roots found in naturally vegetated soils. Furthermore, the tensile strain on the root was said to be low enough that root length did not change during loading. Lastly, the assumption was made that the soil's internal angle of friction, ϕ, does not change due to roots. However, this last assumption was previously verified by Gray (1974) who reported that roots had little effect on internal angle of friction.

Wu et al. (1979) studied the strength of tree roots and their relation to soil shear strength. Wu focused on root decay's influence on reducing soil strength after deforestation. Wu's testing procedures and initial findings validated previous studies by Endo and Waldron. Similar to Waldron, cylindrical samples of vegetated soil were submitted to both saturated and unsaturated direct shear tests under laboratory conditions. However, Wu et al. (1979) collected samples from naturally vegetated soil, a key in capturing the natural root structures of plants. Wu et al. also tested the reinforcing action of roots during in-situ tests analogous to Endo (1969). Results of the in-situ test compared to the laboratory test showed some differences between test types on unsaturated samples. However, the data was highly scattered and no conclusions could be drawn about the difference in the in-situ and laboratory tests.

Further analysis by Wu et al. (1979) showed that Waldron's model for describing the effect of roots on shear strength, shown in Equation 3.5, could be simplified. After performing a sensitivity analysis on Δs, it was found that the effect of roots in the modified Mohr-Coulomb Failure Criterion was relatively unaffected by variations in θ in the range of 40 to 90 degrees and ϕ in the range of 25 to 40 degrees. With the value of Δs between 1.0 and 1.3 for these ranges of

θ and ϕ, Wu et al. (1979) selected 1.2 as a substitute for the angle term. The simplified way of determining the increase in shear strength due to roots became

$$\Delta s = T_r(A_R/A) * 1.2 \qquad \text{Eq. 3.6}$$

T_r = average tensile strength per root area

A_R= cross-sectional area of roots at the shearing plane

A = total cross-sectional area of the shearing plane

The implication of this adjustment to the modified Mohr-Coulomb Failure Criterion, also called the simplified perpendicular root model, is that the magnitude of reinforcement is solely dependent on the root area ratio and strength of roots in the soil (Pollen and Simon, 2006).

Ziemer (1981) also used an in-situ direct shear method to determine the increase in soil shear resistance due to the reinforcing effect of roots in vegetated sands of Northern California. But unlike previous research, the shear plane was oriented perpendicular to the surface. The device Ziemer used was very similar to that used by Endo and Tsuruta in 1969; the main difference was that Ziemer's device could be disassembled into plate sections. The plate sections design was required to orient the box with the shearing surfaces perpendicular to ground surface without disturbing the shearing surfaces. Once the shear box was in place, a mechanical jack was used to apply a shearing force to the box at a speed of 1.27 cm/min and a proving ring was used to measure the resistive force every second over a 7-minute period. Results of Ziemer's test found that 79% of the variation in soil shear strength could be accounted for by the dry weight of live roots less than 17 mm in diameter. However, Ziemer reported that because root orientation was not accounted for, his findings likely underestimated the true increase in soil strength due to the reinforcing effects of roots. The Ziemer's device was also successfully used by Wu et al.

(1988) across a range of soils including silty sand, silty sand to silty gravel, well-graded sand, and lean clay to silt with similar results to Ziemer's research.

Kato and Shuin (2002), developed an improved direct shear apparatus after reviewing flaws in calculating the reinforcement behavior of root systems based on individual root strength, mainly a group effect that emerges at high root densities. The direct shear device had several key features to observe shear deformation as a result of root-soil interactions under controlled soil moisture content. In order to observe shear deformation, acrylic beads were placed in vertical lines in an engineered sand column. The beads were suspended with string as soil was being placed in the column; the string was then removed once the beads were incased in sand. The beads were then measured for relative changes in position after the test was performed. This led to accurate deformation measurements throughout the soil column. Another key feature of the new device was its ability to control soil water content of the sample being sheared. This was accomplished by applying suction to the bottom of the sample using the magnitude of suction as control for the moisture content. Using the modified direct shear apparatus, Kato and Shuin showed the emergence of a group effect on shear strength as root area ratios increased.

3.2.2 Triaxial Compression Test

Zhang et al. (2010) used a triaxial compression test to observe the reinforcement qualities of roots on loess soil samples. The roots were oriented in vertical (VR), horizontal (HR), and vertical and horizontal, which was referred to in the study as cross (CR). All three orientations were tested at soil water contents of 12.7% and 20% to understand the relationship between soil water content and root reinforcement. To determine the shear strength of the samples, the modified Mohr-Coulomb failure criterion, Equation 1.2, was used. The results of the triaxial compression tests performed by Zhang et al. (2010) are presented in Table 3.1.

Table 3.1: Observation of triaxial compression test (Zhang et al., 2010)

Samples	12.7% Soil Water Content			20.0% Soil Water Content		
	ϕ	C	τ when σ=200 (kPa)	ϕ	C	τ when σ=200 (kPa)
Plain Soil	27	29	131	22.3	18	100
HR	26.6	40	140	25.3	22	117
VR	23	64	149	23.7	23	111
CR	23	74	159	26.2	26	124

The most significant increase in soil shear strength compared to plain soil was the cross rooted samples. The vertical and horizontal root orientations increased soil shear strength as well, but because they only acted as tension members in one direction, the reinforcing quality was limited. The data also validated the modified Mohr-Coulomb failure criterion by showing that as the roots present in the soil matrix increase *C*, total cohesion, they have little effect on ϕ, the internal angle of friction. The study also showed that as soil water content increased, the shear strength of soil decreased.

3.3 Effect of Soil Water Content on Soil Shear Strength

Roots, cohesion, and internal angle of friction are not the only soil matrix parameters that affect soil strength, soil water content (SWC) also impacts on soil strength. The effects of SWC are well documented and predate Waldon's 1977 modified Mohr-Coulomb failure criterion. In 1936, Terzaghi proposed a modification to the Mohr-Coulomb failure criterion to reflect the shear strength of soils under saturated conditions. Terzaghi (1936) found that the failure criteria for saturated soils should be

$$\tau = c' + (\sigma_n - \mu_w) \tan \phi' \quad \text{Eq. 3.7}$$

τ is shear strength

c' is the effective cohesion

ϕ' is the effective angle of internal friction

σ_n being the total normal stress on the plane of failure

μ_w is the pore-water pressure.

Although Terzaghi's equation is still used today, most in-situ measurements are performed in soils that are unsaturated. Fredlund and Morgenstern (1977) reported that two of three stress state variables $(\sigma_n - \mu_a)$, $(\sigma_n - \mu_w)$, and $(\mu_a - \mu_w)$ where μ_a is pore-air pressure and μ_w is pore-water pressure, describe the shear strength of unsaturated soils. With the realization of these stress states, Fredlund et al. (1977) described unsaturated soil shear strength as Equation 3.8.

$$\tau = c' + (\sigma_n - \mu_a) \tan \phi' + (\mu_a - \mu_w) \tan \phi^b \quad \text{Eq. 3.8}$$

ϕ^b = angle of relative change in shear strength compared to matric suction

ϕ' = angle of relative change in shear strength compared to net normal stress

Equation 3.8 can be rewritten as

$$\tau = c' + (\sigma_n - \mu_a) \tan \phi' + (\mu_a - \mu_w) \beta \tan \phi' \quad \text{Eq. 3.9}$$

$\beta = \tan \phi' / \tan \phi^b$= decrease in effective stress resistance as matric suction increases

Peterson (1988) proposed $\tau = c' + (\sigma_n - \mu_a) \tan \phi' + C_\Psi$ where C_Ψ is perceived as cohesion due to suction. The influence of soil suction on shear strength is dependent on soil water content. The cohesion component C_Ψ can be expressed as equal to $(\mu_a - \mu_w) \tan \phi^b$ making Petersons equation equivalent to Equation 3.8.

Fredlund et al. (1996) theorized that, unlike previous models, a nonlinear model would more accurately estimate the effect of SMC on soil shear strength. The equation, through theoretical development, became:

$$\tau = c' + (\sigma_n - \mu_a)\tan\phi' + (\mu_a - \mu_w)[\Theta(\mu_a - \mu_w)]^{\kappa}\tan\phi' \quad \text{Eq. 3.10}$$

$\Theta(\mu_a - \mu_w)$ = normalized volumetric water content

The normalized volumetric water content was based on saturation, residual conditions, and κ as a soil parameter based on soil type. Fredlund et al. (1996) concluded that a model using the soil-water characteristic curve and saturated soil shear strength properties effectively predicts the shear strength of unsaturated soil.

Although the effects of SMC on shear strength have been well documented and modeled, most models do not account for the effects of vegetation. Kato and Shuin (2002) used a modified direct shear test under varied soil moisture conditions to test the effect of vegetation on soil shear strength. Study results showed that as root area ratios increased, a group effect emerged. The observed group effect of roots increased as soil moisture decreased providing evidence of the importance of SMC's influence on vegetated soil shear strength. The SMC also played a key role in shear deformations not accounted for by conventional models such as the modified Mohr-Coulomb failure criterion.

Pollen (2007) showed that SMC affected mechanical properties of the soil and reinforcing capabilities of roots. Various root diameters where tested for tensile strength using an in-situ root pullout test. It was observed that roots could be described as failing one of two ways, breaking or slipping. A breaking failure was when the tensile strength of the root was exceeded, causing failure of the root fibers. Slipping failure occurred when the root was pulled from the soil matrix as a result of a failure at the root-soil interface. Observations made during Pollen's study showed

that as SMC increased, the threshold diameter for root pullout decreased. This information led to the suggestion that as SMC decreases, the frictional bonds at the root-soil interface increases resulting in more breaking failures. This conclusion echoed Peterson (1988) showing that apparent cohesion of the soil increases as the soil matric suction increases.

However, Pollen (2007) was only observing the effects of SMC on the available tensile strength of roots in the soil matrix. When applying an in-situ direct shear test similar to Endo (1980), Fan and Su (2008) found that additional peak shear strength from root reinforcement increases as SMC increases and calculated that roots can increase soil shear strength by up to 100% in soils having a degree of saturation between 80% to 85%.

3.4 Cone Index as a Measure of Soil Trafficability

Several methods has been developed to quickly measure the effect of key soil parameters on overall strength; these methods measure soil strength in terms of soil trafficability. The current standard for identifying terrain characteristics related to trafficability and mobility is the empirical measurement of cone index (CI). CI is the measurement of a soil's penetration resistance (Wong, 2001). CI has led to recent developments in the NRMM as CI has a proven correlation with vehicular performance, rutting, and slipping coefficients (Braunack, 1986; Muller et al., 1990; Godwin et al., 1991; Shoop, 1993; Nam et al., 2010).

3.4.1 Penetrometer Types

CI values are derived from tests performed with a penetrometer. There are three basic types of penetrometer: static cone, dynamic cone, and drop cone. These three types of penetrometers are defined by their operation. Static cone penetrometers measure the force applied to a metal cone as it is pushed at constant velocity through the soil. Dynamic cone penetrometers apply a known amount of kinetic energy to a metal cone causing the cone to

penetrate the soil. Drop-cone penetrometers are dropped from a known height and the penetration depth of the cone is measured (Godwin et al., 1991; Jones and Kunze, 2004). For the scope for this thesis, static and drop-cone penetrometers were used for field measurements.

3.4.2 Static Cone Penetrometers

The static cone penetrometer is one of the most popular tools for measuring the penetration resistance and is used extensively due to its simplicity, mobility, and measurement speed (Shoop, 1993). It has been used to predict the trafficability of off-road vehicles (Freitag and Richardson, 1968; Wismer and Luth, 1972).

The ERDC Geotechnical and Structures Laboratory (GSL) formerly Waterways Experiment Station (WES) has long identified CI values as a valuable measurement for soil strength used to determine soil trafficability. ERDC-GSL outlines the use of the static cone measurements for trafficability purposes as being a 30-degree circular cone with a cone base area of 3.23 cm^2 which is slowly pushed through the soil with a force of up to 68 kg as measured by a proving ring and deformation gauge (Meyer and Knight, 1961). However, a smaller cone option is available. The smaller cone has the same apex angle, but the base surface area is 1.30 cm^2. CI is calculated based on the area of cone and the amount of force applied to the cone; the force is measured incrementally as the cone passes through the soil profile. The standardization of the static cone penetrometer is found in ASABE Standard 313.2 (1992).

3.4.3 Drop-Cone Penetrometers

The drop-cone, currently used by CERL, was developed as a tool capable of quickly measuring penetration resistance, compared to previous penetrometers (Godwin et al., 1991). The drop-cone consists of a 2-kg, 30 degree cone that is dropped from a height of 1 meter. The depth of penetration into soil is then measured and used to describe penetration resistance. The

drop-cone, as described by Shoop (1993), applies a large force on the soil surface without the use of large weights or hydraulic equipment; this is advantageous for performing in-situ penetration tests.

When developing the drop-cone, Godwin et al. (1991) assessed the relationships between drop-cone penetration depth and cone type, soil moisture content, and shear strength. The cone types tested consisted of variations in mass and apex angle and were evaluated based on penetration depth and sensitivity. Results showed that a 2 kg mass with a 30 degree apex angle was most suitable for trafficability studies. Goodwin also showed the existence of a linear relationship between drop-cone measurements and soil moisture content for sandy loam, clay, and clay loam soils. Drop-cone and shear strength measurements as determined by an 18mm diameter shear vane were found to have a linear relation at soil shear strengths above 20 kPa. The drop-cone measurement was also found to be a good predictor of wheel rut depth for a range of wheel systems.

3.5 California-bearing Ratio as a Descriptor of Soil Shear Strength and Trafficability

Similar to penetration resistance measurements of CI, the California-bearing ratio (CBR) also uses the soil's resistance to vertical loading to measure trafficability. CBR is a standardized test to obtain a modulus of shearing resistance that is recognized by both the American Society for Testing and Materials (ASTM) and the United States Military (Semen, 2006).

3.5.1 Standard CBR Test

According to ASTM Standard D4429 (2009), the standard CBR test is performed by measuring the force required for the penetration of a cylinder with a 3-square-inch end surface area through the soil surface. The force measurements are taken in 0.025 inch increments until a

0.500 inch penetration is reached. To determine the CBR index value, the force measurements at 0.100 and 0.200 inch depths are divided by values of 1,000 psi and 1,500 psi (Semen, 2006).

3.5.2 Clegg Impact Hammer

An alternate method of measuring the CBR of soils and aggregates is the Clegg impact hammer which can be practically implemented in field and laboratory testing. The Clegg impact hammer is an easy to operate, portable, and cost-effective means of measuring the Clegg impact value (CIV) (Al-Amoudi et al., 2002).

One feature of the Clegg impact hammer similar to the drop-cone penetrometer is the much larger area of soil tested compared to the static cone penetrometer. The advantage of the large sample area is that variability from complex soil compositions is lowered between samples. However, some researchers have found that large sample areas were too insensitive (Shoop, 1993). Also, similar to the drop-cone penetrometer, the Clegg impact hammer is limited to taking measurements at the soil surface.

Although the Clegg impact hammer is typically used to assess the carrying capacity of unsurfaced roads (Mathur and Coghlan, 1987), it can also be used on vegetated soils for measures of trafficability. Koch et al. (2010) found that CIV and penetration resistance, as measured by a static penetrometer, are highly correlated measurements in vegetated, clayey soils. They also observed that CIV presents a lower variability in measurements compared to the drop-cone penetration test.

An investigation of the correlation of the CBR and CIV was carried out by Al-Amoudi et al. (2002). With tests conducted on 56 engineered samples of silty sands and silty gravels, they found a general model was able to estimate CBR from CIV with a coefficient of determination

(R^2) of 0.85. The general model, Equation 3.11, was similar to models reported in previous literature.

$$CBR = 0.1691(CIV)^{1.695} \quad \text{Eq. 3.11}$$

3.5.3 CBR from CI

It was found that the CBR was also highly related to CI for soil types other than silty sands and silty gravels. However, to better describe the CBR values of each soil type, the model needed soil specific coefficients and exponents. Shoop et al. (2008) evaluated 562 cases of coinciding CBR and CI measurements representing seven of the United Soil Classification System (USCS) soil types. It was found that CBR and CI are highly correlated for fine-grained soils but less correlated for course-grained soils. Similar to the model relating CIV to CBR proposed by Amoudi et al. (2012), Shoop et al. (2008) found the form of the Equation 3.12 with coefficients a and b per soil type listed in Table 3.2 could be used to describe the relationship across a broader range of soil types.

$$CBR = aCI^b \quad \text{Eq. 3.12}$$

Table 3.2: Coefficients and exponents for Equation 3.12 Shoop et al. (2008)

Soil Type	USCS Classification	Coefficients and Exponents		
		a	b	R^2
All Soils		0.2985	0.5358	0.4715
Clay, High Plasticity	CH	0.1264	0.6979	0.8516
Clay, Low Plasticity	CL	0.1266	0.6986	0.8701
Silt, High Plasticity	MH	0.0820	0.7174	0.7715
Silt, Low Plasticity	ML	0.1111	0.7390	0.5193
Coarse-Grained	SM + GP	1.1392	0.4896	0.3495
Fine-Grained	CH, CL, MH, ML	0.1305	0.6776	0.7724
High Plasticity	CH + MH	0.1460	0.6432	0.7741
Low Plasticity	CL+ ML	0.1281	0.6984	0.7962

3.6 Development of the VASST

The VASST was designed to quantify shear strength of vegetated soil at the soil surface (MacDonald et al., 2012). The motivation for the development of the VASST was to better understand the shear strength relationship between roots and soil at the ground surface, the section of the soil profile most susceptible to horizontal displacement. It was anticipated that the VASST tests could better predict vehicle mobility and trafficability in vegetated soils when compared to previously mentioned soil strength measurements (CI, CIV, and Drop-cone).

3.6.1 VASST Components and Operation

The VASST consists of the following major components: 1) tire analog/ shear surface, 2) rails/tubes, 3) load cell, 4) linear position transducer, 5) winch, and a data acquisition unit. The layout of the primary components of the VASST is shown in Figure 3.1.

Figure 3.1: Primary components of the VASST (Kelley et al., 2013)

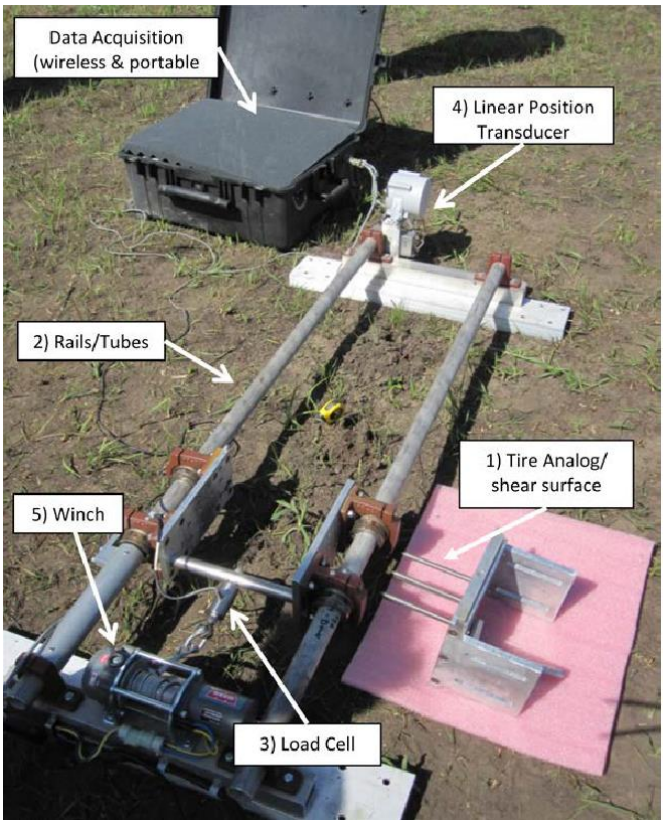

In order to test soil shear strength, the tire analog is inserted into the soil and pulled horizontally through the soil via the winch. Data on the force being applied to the tire analog and displacement of the tire analog is measured with the load cell and linear position transducer, respectively. The action of the tire analog during a VASST test is shown in Figure 3.2. Data also available from the VASST include time, temperature, equipment voltage, and event markers. All data is recorded on a 10 milliseconds interval using the data acquisition unit. An output file is then assembled from the sensor data and exported to a comma-separated values (CSV) file.

Figure 3.2: Tire analog during VASST test

3.6.2 Initial Test Results

MacDonald and Shoop (2013) tested the VASST alongside a Clegg impact hammer, static cone penetrometer, Drop-cone penetrometer, and a shear vane in reconstructed sand and clay. Tests of both vegetated and unvegetated sections were performed in each soil type. During initial VASST testing, they found that soil shearing data obtained with the VASST followed trends similar to common soil strength measures.

CHAPTER 4: MATERIALS AND METHODS

Materials and methods presented in this thesis were developed at the US Army Corps of Engineers ERDC-CERL and ERDC-CRREL. Standardized laboratory testing was achieved using ASTM Standards and ERDC-CERL testing protocols.

4.1 Site Selection and Typical Sampling Layout

The careful selection of sites was important to obtain results that would be meaningful when used as part of the OPAL work package; this required a wide range of soil types to be tested. Sampling protocol and layout was also important to maximize testing uniformity and improve spatial correlation between the soil strength tests and measured soil parameters.

4.1.1 Test Locations

Geographic locations were chosen based on soil, eco-regions and training land usage. Test locations were within Army installations in agreement with the OPAL program. Five locations for the study were: Champaign, Illinois; Ft. Benning, Georgia; Ft. Bragg, North Carolina; Ft. Hood, Texas; and Ft. Riley, Kansas.

4.1.1.1 Champaign, Illinois

Field testing was conducted at ERDC-CERL's campus in Champaign, Illinois. An existing monitored and controlled research site for trafficability studies was used. Soil at the location was Catlin silt-loam (Soil Survey, 2014). Existing plots had five vegetation treatments: bare soil, turf grass mixture, forbs mixture, native grasses mixture, and a mixture of forbs/grasses.

4.1.1.2 Ft. Benning, Georgia

Fort Benning, located at roughly 32.36° N, 84.97° W, is within the Sandhills region which contain deep, fluvial sands. Three sites were selected based on dominate soil type at Fort Benning; soils of the test sites were Nankin sandy clay-loam, Troup loamy sand, and Lakeland sand (USDA web Soil Survey, 2014). The vegetation in the three areas tested consisted primarily of scrub oaks, longleaf pines, and sparse grasses (Dilustro, 2002).

4.1.1.3 Ft. Bragg, North Carolina

Fort Bragg, located at approximately 35.14° N, 79.00° W, is positioned on the inner margin of the Atlantic Coastal Plain near the Sandhills region. Typical vegetation in the area consists of a longleaf pine, oak, and wiregrass communities (Sorrie, 1997). The soils determined to be representative of the area were Lakeland sand, Blaney loamy sand, and Candor sand (USDA web Soil Survey, 2014).

4.1.1.4 Ft. Hood, Texas

Fort Hood, located near 35.14° N, 79.00° W, is in the boundary region of the Cross Timbers and Prairies and Edwards Plateau eco-regions. The vegetation dominating the areas tested consisted of tallgrasses associated with the Blackland Prairie such as Little Bluestem, Indian Grass, Switch Grass, Eastern Gamagrass, etc. (Wootan, 2011). The area also contained some mixed forest-shrub communities generally dominated by Ashe Juniper and Live Oak (Directorate of Public Works Environmental Division, 2011). Soil studied at Ft. Hood included Nuff Series very stony clay loam and Georgetown clay loam (USDA web Soil Survey, 2014).

4.1.1.5 Ft. Riley, Kansas

Fort Riley, located at 39.11° N, 96.82° W, is within the Flint Hills tallgrass prairie with vegetation such as Big Bluestem, Indian Grass, and Switch Grass common (Kansas Sampler

Fountain, 2007). The area studied was an upland area with a soil taxonomy of Crete silty clay loam (USDA web Soil Survey, 2014).

4.1.2 Selection of Sites

The test sites within each location were chosen based on the following characteristics: representation of soils predominate on the installations, representative vegetation, and no history of vehicle traffic within the plot. To quantify the predominate soils at each location, ArcGIS was used to populate a list of soil types on the installation with information on area of coverage. The three most common soils by area were then identified and accessed based on training utilization. It was important for the purpose of this study that the sites had not been used for training activities that would have created compaction and/or been destructive to the vegetation. This criterion greatly narrowed down the site options greatly since the sites were within active training areas. The final site selection criterion was vehicle accessibility, an important factor due to the amount of equipment required to conduct field testing. A summary of the number of sites and total number of samples and tests performed at each location is shown in Table 4.1.

Table 4.1: Sampling quantities per location

Sampling Quantities per Location										
Location	Number of Sites	Soil Classification	TDR	Penetrometer	Clegg Impact Hammer	Drop-cone	VASST	Below Ground Biomass	Above Ground Biomass	Bulk Density
Ft. Bragg, North Carolina	3	9	45	51	45	81	75	9	9	9
Ft. Benning, Georgia	3	9	54	81	45	45	68	9	9	9
Champaign, IL	5	13	61	65	39	130	102	13	13	13
Ft. Hood, Texas	2	5	25	35	25	45	40	5	5	5
Ft. Riley, Kansas	1	3	3	3	3	9	16	3	3	3
Totals:	**14**	**39**	**188**	**235**	**157**	**310**	**301**	**39**	**39**	**39**

4.1.3 Replication Layout

Replications established at each site were chosen based on similarities in vegetation and soil characteristics as well as proximity to each other. For each replication, the tests performed and samples taken are listed in Table 4.2.

Table 4.2: Tests performed and samples taken per replication

Soil Tests	Soil Samples	Vegetation Samples
VASST	Soil Classification Sample	Above Ground Biomass
Clegg Impact Test	Bulk Density	Below Ground Biomass
Cone Penetration Test		
Drop-cone Penetration Test		
TDR		

These samples and tests were performed in a manner illustrated in Figure 4.1. Sample and test quantities for each replication can be found in Appendix A.

Figure 4.1: Typical sampling layout for field data collection

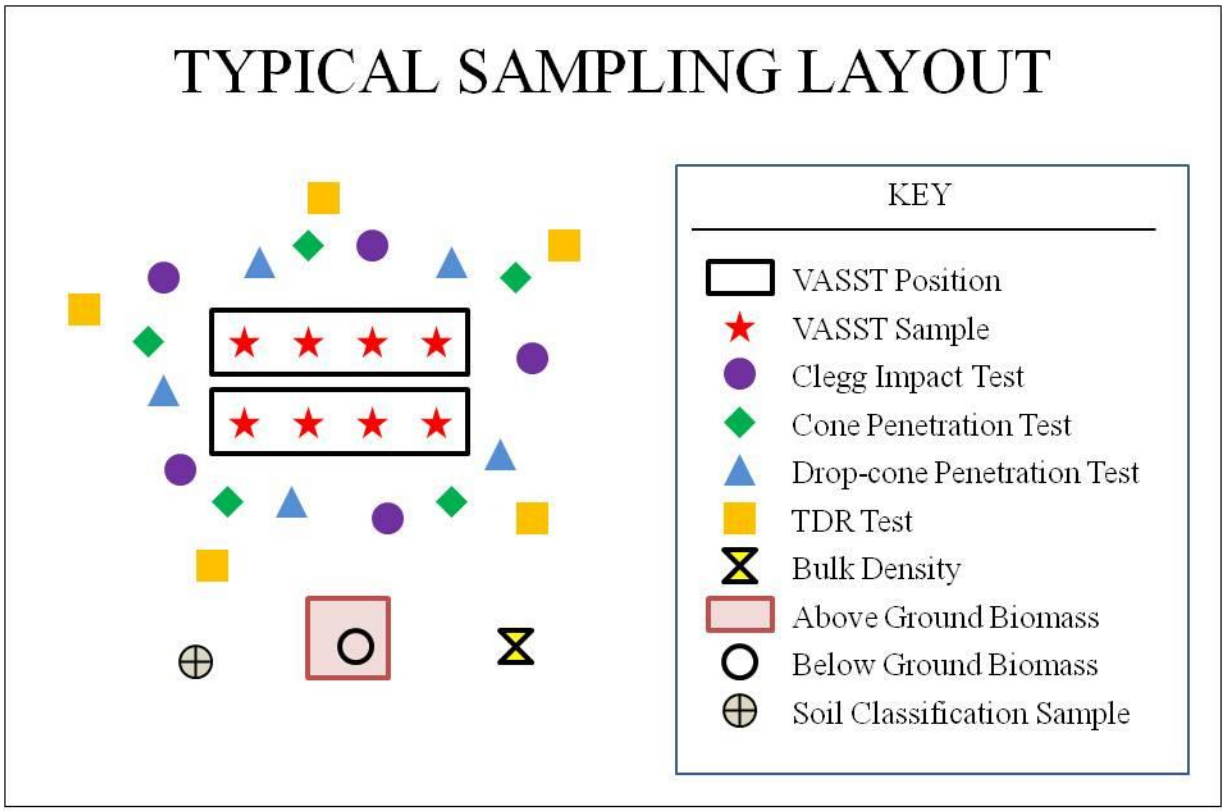

4.2 Field Sampling Methods

Field sampling was conducted during 2012 and 2013 with one sampling event per location. On location, sites were defined based on their soil classification, all in-situ measurements were taken, and soil and vegetation samples were collected for laboratory testing.

4.2.1 Soil Classification

Soils were initially classified using the soil data and information from the National Cooperative Soil Survey and the U.S. Department of Agriculture (USDA) and installation soil surveys. Information obtained about each soil included the soil name, USDA textural soil classification, distribution, and location. Soils were analyzed and classified using the USCS, commonly used in engineering applications. The soil classifications by the USCS were performed at ERDC-CERL on samples that were collected during field sampling; details of this process are described in section 4.3.1.

4.2.2 Soil Moisture

Soil moisture was measured in-situ using a Fieldscout TDR 300 (Spectrum Technologies Inc.) which measured SMC on a volumetric basis. The time domain reflectometry (TDR) probe used for this study was equipped with 20cm probes and the standard calibration setting was used as determined by the soil types tested. Figure 4.2 demonstrates the TDR being used to measure in-situ soil moisture.

Figure 4.2: Example of TDR test

The TDR measures soil moisture by injecting a step voltage in the soil in the form of a pulse. The velocity of the pulse is measured across a known distance to determine the soil moisture; slower pulse velocity indicates higher SMC. Evett (2003) explains the theory of TDR systems when used to make measurements in porous materials by converting measurements of time into length by using the relative propagation velocity factor, v_p, a fraction of the speed of light. The equation for calculating the relative propagation velocity factor is:

$$v_p = v/c_0 = (\varepsilon\mu)^{-0.5} \quad \text{Eq. 4.1}$$

v = propagation velocity of a pulse along the cable

c_0 = speed of light in a vacuum

ε = permittivity

μ = magnetic permeability of the dielectric material

The permittivity of soil is highly sensitive to water with soil type having a minimal influence on permittivity. This means that ε is an effective indicator of soil water content.

4.2.3 Soil Strength Tests

Soil strength was considered the key component in determining the impact of trafficability and was tested using several methods. Tests were conducted with the VASST, static cone penetrometer, drop-cone penetrometer, and Clegg impact hammer.

4.2.3.1 Vegetation and Soil Shear Tester (VASST)

At each test site, the VASST described in section 3.6 was set up in two adjacent positions with three to five tests per position. The test areas were prepared by clipping above ground biomass and removing organic debris. The VASST was then anchored via eight anchoring spikes inserted approximately 12 inches into the ground. Tests were performed with the tire analog inserted to a depth of 1.5 inches into the soil surface, a depth recommended by MacDonald et al. (2012). A load applied to the tire analog was increased until soil in contact with the tire analog was displaced; this was verified by visual inspection. Figure 4.3 shows where the soil has been displaced by the tire analog after two tests.

Figure 4.3: Soil displacement after two VASST tests (tests indicated by arrows)

Concerns about a depth of 1.5 inches being adequate to test soil shear strength were discussed at the beginning of this study. However, initial VASST testing at depths exceeding the recommended depth proved to be beyond the capabilities of the VASST. At a depth of 2 inches, in soil with high shear strength, the spikes deformed during the soil shearing, creating test data that was not replicable.

4.2.3.2 Static Cone Penetrometer

The static cone penetrometer used was a Field Scout SC 900 Soil Compaction Meter produced by Spectrum Technologies Inc. The penetrometer's cone had a 30° apex angle and a base area of 1.3 cm^2. It was equipped with sonar to measure penetration depth, a load cell to measure the force applied to the cone, and a data logger to record the average load applied over

2.5 cm distances. The SC 900 could have measured CI at depths of up to 45.0 cm, however, measurements at that depth were unnecessary and impractical for the purpose of this study. An example of the penetrometer being used is shown in Figure 4.4.

Figure 4.4: Example of static cone penetrometer test

In the field, the measurements using the SC 900 were taken adjacent to the VASST. The CI values recorded per depth were average forces per area on the cone. When the datasets from the SC 900 were uploaded to a computer, it was observed that the sonar had started measurements before the cone made contact with the soil. This was corrected by removing zero-force values at the start of the tests and adjusting the depth measurement so that the first positive force was at the zero depth reading. The depths utilized were at 0.0, 2.5, and 5.0 cm and deemed of the most interest due to the section of the soil profile tested by the VASST and drop-cone.

4.2.3.3 Drop-Cone Penetrometer

The drop-cone, built to the specifications of Godwin et al. (1991), had a 2 kg overall mass and a 30 degree apex angle cone. The cone was attached to a graduated rod and dropped through a poly-vinyl chloride (PVC) pipe from a height of 1 meter, illustrated in Figure 4.5. Once dropped, the graduations on the rod were read and processed to determine the penetration depth of the cone to the nearest millimeter. The drop-cone was performed at each replication between three and ten times depending on the location; number of repeated measurements can be found in Appendix A.

Figure 4.5: Example of drop-cone test

4.2.3.4 Clegg Impact Hammer

The Clegg impact hammer used for field testing was a 2.25 kg Clegg impact soil tester Model 95049A, produced Lafayette Instruments. The Clegg impact hammer, based on a modified Proctor hammer, contained a piezoelectric accelerometer and a digital output. Tests were performed per standard test protocol, with the hammer dropped four consecutive times in the same spot from a height of 45 cm, demonstrated in Figure 4.6; the peak CIV of the four tests was recorded.

Figure 4.6: Example of Clegg impact test

4.2.4 Soil Classification Sample

Samples taken for soil classification procedures were obtained by first removing above ground biomass and any organic debris on the soil surface. Then a spade was used to remove a sample from the first 6 inches of the soil profile that was approximately 170 cubic inches in volume. This was determined a sufficient amount of soil to perform both particle size analysis for all soils and Atterburg limits for fine grained soils, (procedures described in Section 4.3.1).

4.2.5 Biomass Sampling

To quantify the vegetation at each location, both aboveground and belowground biomass samples were taken at each plot.

4.2.5.1 Aboveground Biomass

U.S. Army Land Condition-Trend Analysis (LCTA) has laid out standards for accessing vegetation on military lands via a line intercept method (Diersing et al., 1992). However, to better suit the needs of this research, a modified Daubenmire frame or quadrat was used to measure ground cover adjacent to the location of the VASST. The advantage of the quadrat method over the methods described in LCTA was the area of sampling. The quadrat used for vegetation sampling was 2500 cm^2, a much larger sample area compared to the 60 cm^2 sampled per transect in the LCTA method.

The quadrate used in this study was constructed of 0.75 inch diameter PVC with sides measuring 50 cm which created a sampling area of 2500 cm^2. The quadrat also had a digital camera mounted at a height of 1m that aided in the documentation of the sample. The vegetation residing inside the frame was clipped at ground level and bagged in a pre-weighed paper bag, dried in a laboratory oven. A description of the drying process is in section 4.3.2.1.

4.2.5.2 Belowground Biomass

The quantification of belowground biomass was of major importance in achieving the goals of this research. However, quantifying belowground was difficult due to the root architecture and distribution throughout the soil profile. A soil core method was chosen to measure the amount of belowground biomass per volume of soil present near the soil surface. The use of soil core sampling methods was the only option suitable for use on active military lands due to speed of sampling and limited disturbance as not to interfere with future military activities.

The core samples taken for belowground biomass measurements were 5 cm in diameter and 25 cm deep. The samples were extracted using a split-core sampler driven into the ground using an 8.6 kg slide hammer; both the spilt-core sampler and slide hammer were manufactured by AMS, Inc. Once extracted, the soil core was placed in a sealable, gallon plastic bag, labeled and transported back to CERL's soils laboratory.

4.2.6 Bulk Density

Bulk density samples were taken with a 3 in. inside diameter by 3 in. deep ring as standardized by the Natural Resources Conservation Service (NRCS) in 2001. However, unlike procedures described in the NRCS (2001) method, the rings were driven into the ground using a modified slide hammer developed at CRREL. The slide hammer was designed to deliver impacts evenly across the edge of the ring ensuring the net force of the blow to be aligned with the central axis of the ring, in turn reducing sample compaction and variability.

To take a bulk density sample, a ring was loaded into the slide hammer and driven into the ground to a depth just over 3 inches. The volume of soil surrounding the sample was then removed using a spade. Soil surrounding the wall of ring was removed by hand; soil extending

past the open ends of the ring was removed using a knife creating clean, uniform bulk density sample. In order to transport the sample to the lab, it was placed in a sealed, quart plastic bag, and labeled.

4.3 Laboratory Methods

Laboratory testing and analysis was required to obtain soil parameters and quantify vegetation. All laboratory tests were conducted at CERL following ASTM Standards where applicable. Tests not defined by ASTM Standards were performed using Army Corp. of Engineers protocols.

4.3.1 Soil Classification

Soils were classified by USDA texture and the USCS. The tests used to describe the soils by the two classification systems were particle size analysis and Atterburg limits respectively.

4.3.1.1 Particle Size Analysis

Particle size analysis (PSA) was performed on soil samples as a way of quantifying their gravel, sand, silt, and fines content. ASTM Standard D422 (2007) procedures were followed for all PSA samples.

4.3.1.1.1 Sieve Analysis

Sieve analyses were performed on the sandy soils from Ft. Benning and Ft. Bragg as a method of classifying the soils by the USCS. The gradation of the particle sizes in the range of 4.75 mm (No. 4) to 75 μm (No. 200) was determined using ASTM Standard D422 (2007). The samples were passed through three stacks of 8 inch sieves. Samples first passed through U.S. Standard Sieve Sizes No. 4, 10, 16, 20, and 35, the second set was, 40, 60, 70, 100, 120, and 140 in size, and the final set 170, 200, and 325 in size.

A sub-sample of approximately 200 g of air-dried soil was shaken through each sieve stack for eight minutes via a mechanical sieve vibrating device. After each stack was shaken, the contents remaining on each sieve were weighed to an accuracy of 10 mg. The soil fraction passing through all the sieves in a stack was collected in a pan and loaded into the sieve stack containing the next smaller series of sieves. The process was repeated for all three stacks resulting in an accurate particle size gradation used to aid in the classification of coarse-grained soils.

4.3.1.1.2 Hydrometer Analysis

Particle size distribution analyses of soils consisting primarily of silt and clay were conducted using the ASTM Standard D422 (2007) hydrometer method. The hydrometer method relied on larger particles settling out of a liquid solution faster than smaller particles. Rates of sedimentation of various sized particles were captured with multiple hydrometer measurements in a time series. The 151H hydrometers used for the study were manufactured to meet ASTM Standard E100 (2010).

Concurrent with ASTM Standard D422 (2007), an air-dried sample weighing approximately 50 g was stirred into a hexametaphosphate solution (40 g/L) and allowed to sit more than 16 hours. The sample was then added to 500 ml of deionized water. The soil was then mixed with a soil blender for 8 minutes and transferred to a 1000 ml graduated cylinder. The total volume of the soil slurry was brought to 1000 ml with deionized water. Hydrometer and temperature measurements were taken at 1, 2, 4, 15, and 30 minutes followed by measurements at 1, 2, 4, and 24 hours.

4.3.1.2 Atterberg Limits

Atterberg limits were conducted on soils consisting primarily of silt and clay following ASTM Standard D4318 (2010). The liquid limit and plastic limit were used to define each sample's plasticity index, a parameter used to define fine-grained soils by the USCS.

4.3.1.2.1 Liquid Limits

The liquid limit for each plot was found using a sample of soil that had particles larger than Sieve Size No. 40 removed. The sample was hydrated and placed in an Atterberg device and cut by a standard grooving tool, illustrated in Figure 4.7. The cup was then dropped repeatedly a distance of 10 mm at a rate of two shocks per second. The number of blows used required to close or "seal" the groove over a distance 13mm was counted. The sample was weighed and then oven-dried at a temperature of 100°C for 24 hours to determine the SMC. This process was repeated three times at various soil moistures to determine a linear relationship between the number of blows and SMC. From the linear relationship, the SMC was found at which the gap would close after 25 blows, a descriptor of liquid limit outlined in ASTM Standard D4318 (2010).

Figure 4.7: Grooving of a liquid limit sample

4.3.1.2.2 Plastic Limits

The plastic limit for each plot was determined by ASTM Standard D4318 (2010). A small amount of the extra soil prepared for the liquid limit test was used for the plastic limit test. The sample weighed between 1 and 2 grams and was repeatedly rolled on a glass surface into a rod that was 3.2 mm in diameter. Each time a rod of the specified diameter was formed, it was broken into several threads and remolded allowing for the rod to be reformed by means previously described. Once the sample's SMC decreased to the point that a 3.2 mm rod could no longer be formed, the sample was weighed, oven-dried at a temperature of 100°C, and reweighed to determine the final SMC.

4.3.2 Biomass

The accurate quantification of biomass was critical to the scope of this research. Army Corp. of Engineers protocols for quantifying biomass were used to achieve accurate measurements.

4.3.2.1 Aboveground Biomass

Aboveground biomass was oven-dried at a temperature of 85°C in a convection laboratory oven for a period of 48 to 72 hours, depending on the volume and approximate water content of the vegetation. Once the mass of the vegetation was stable, indicating that no more water was being removed, the vegetation was weighed to determine a mass of vegetation per area.

4.3.2.2 Belowground Biomass

Belowground biomass samples were handled with great care so that root structures were not degraded as soil was being removed from the roots. In order to recover as many roots from the core samples as possible, the root washer and processing methods described in Fulton (2012) were employed.

The first step of the washing process was to transfer each soil core into a mesh bag with 125 µm openings. The samples were then soaked in water for 1 to 3 days or until the soil cores were thoroughly softened. Once the samples were softened, bagged samples were run through the root washing apparatus described by Fulton (2012). After a large portion of the samples' silt and clay fraction had been removed, the roots and remaining soil particles were separated by hand using a No. 18 sieve. The soil-free root samples were oven-dried at a temperature of 85° C to determine the dry mass of the belowground biomass.

4.3.3 Bulk Density

The bulk density samples were placed in pre-weighed ceramic drying dishes and weighed. The samples were then oven-dried in a convection laboratory oven at a temperature of 100°C for 24 hours or until all moisture was removed from the soil. After drying, the samples were allowed to cool in a desiccator to reduce convention currents from the samples which can affect scale readings. Samples were then weighed to determine the mass of soil contained in the known sample volume.

CHAPTER 5: COMPUTATIONAL APPROACH TO ANALYZING VASST DATA

The nature of this study resulted in a large and complex dataset that required simplification and data-mining to produce meaningful results. Data on VASST measured soil shear strength was derived from the data collected in the field; these measurements were tested against a theoretical model. The theoretical model developed from literature was based on the modified Mohr-Coulomb failure criterion (Waldon, 1977) and adjusted to describe the lateral shearing action produced by the VASST.

5.1 VASST Raw Data Analysis

During operation, the VASST created large amounts of data for each test that had to be refined to determine the breaking strength of the soil. A Python program was developed to quickly identify the force resulting in shear failure for each sample tested.

5.1.1 Previous Data Analysis Method

When the VASST was initially being tested by MacDonald et al. (2012), the output CSV file was imported into DIAdem, software that aids in the inspection, analysis, and reporting of data. However, the program could only be used to view the VASST outputs in the form of graphs and was not capable of identifying soil shear failure. Therefore, human input was required to identify the point at which shear failure occurred. Furthermore, using DIAdem to individually analyze datasets was a time consuming task. In order to remove human bias and reduce data processing time, a Python program to analyze the VASST data was developed as part of this thesis (Appendix B).

5.1.2 Algorithm for VASST Dataset Analysis Program

Creating a computational approach for analyzing raw data from the VASST was a complex process. To simplify the procedure, the following process was implemented:

1. Directory setup/import raw data
2. Validate dataset/condition the data
3. Determine force maximums
4. Determine points of interest other than maximums
5. Check for special cases (root breaks and event markers)
6. Output relevant information and attributes pertaining to the shear failure

5.1.2.1 Directory Setup

The first action taken by the program was to specify three file directories: code, data, and output. All three directories were user specified using the Tkinter package, a practical Graphical User Interface (GUI) toolkit for Python. The first input was the directory of the supporting program files which were sequentially executed from the main code during file processing. The next directory specified by the user was the location of the data files; the location was used so that all compatible data files in the directory could be processed without specifying each file individually. Finally, an output directory was designated to contain all files created by the program as outputs.

5.1.2.2 Importing Data / Compatibility Check

Once the data was located, a list of all CSV files in the directory was compiled. The list, displayed in the Python shell, informed the user which CSV files were found in the directory. Each file was then checked for size compatibility, meaning that files over 1 megabyte were not processed. This was important for two reasons: the large size could have been an indication of

bad data or the program may not have ran depending on the capabilities of the computer. Once a file's compatibility was verified, the program opened the file using Python's CSV module. Processing was performed in alphanumerical order based on file name.

5.1.2.3 Data Conditioning

Conditioning of raw data collected from the VASST removed unused data and checked for problems in the data sets. As the data were being read into a Python array, unnecessary header information was removed. Since raw data from the VASST used the same number of header rows, the rows were removed based on position rather than content.

If a second header was found within the dataset, it was an indication that multiple tests were exported as a single CSV file as shown in Figure 5.1. Once the program identified the existence of multiple tests in a single dataset, the program prompted the user to choose between continue using the first test data or skip to the next file. If the user chose to continue using the first test data, the program clipped the data so that only the first segment was used. If the user chose to skip to the next file, the system continued to next file.

Figure 5.1: Unedited dataset containing multiple tests

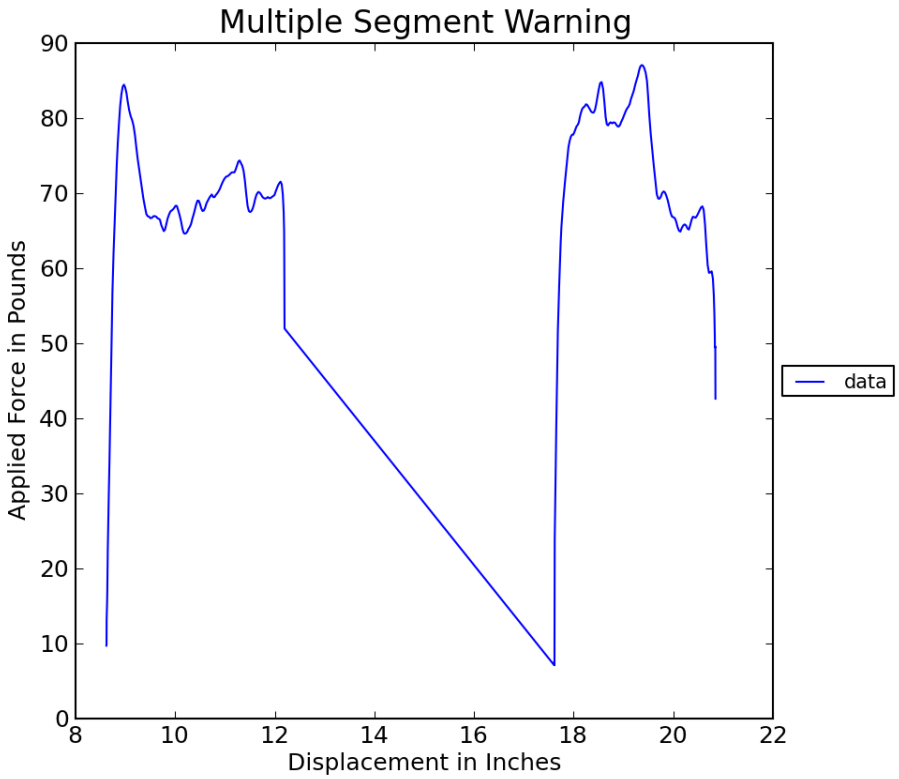

With the header removed and the data verified as being from a single test, the array consisting of floating numbers was tested for equipment failures associated with the linear position transducer and load cell. By comparing the maximum and minimum values recorded by each of the two VASST components, failures could be detected. If the differences in the maximums and minimums were less than 5 lb. or 0.25 in. respectively, the failure was reported as an error and program skipped to the next file. Examples of both failures are shown in Figure 5.2 and 5.3.

Figure 5.2: No load cell detected

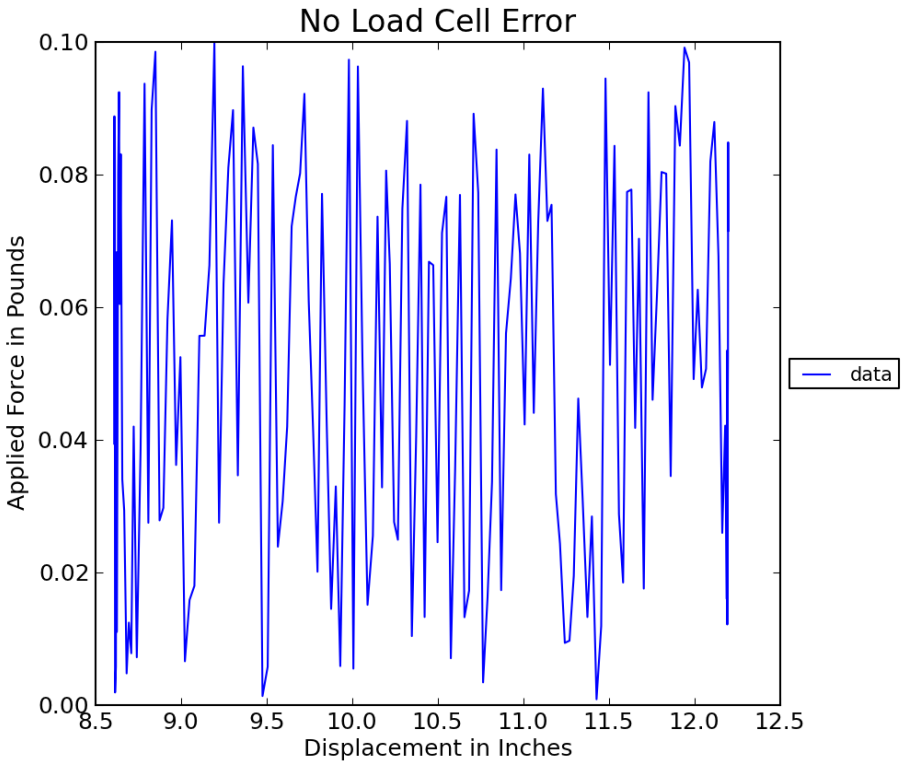

Figure 5.3: No linear positon transducer detected

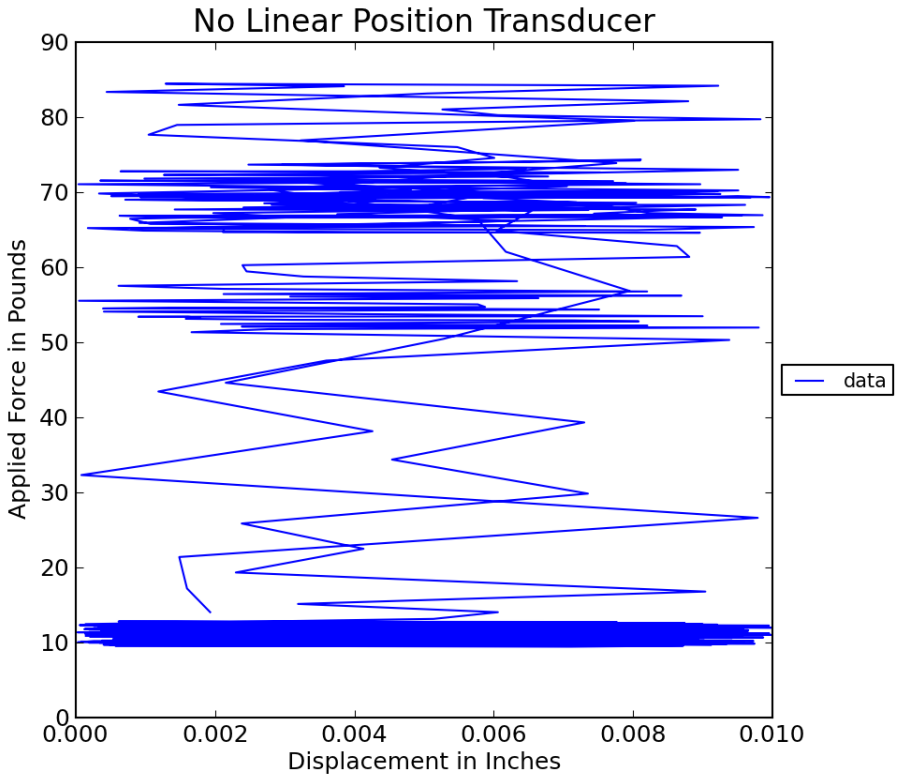

The event marker was checked for failures resulting from the momentary switch short-circuiting. A short-circuit displayed a marker signal throughout the entire test, as shown in Figure 5.4. Similar to when multiple data segments were found, if an event marker failure occurred, the program prompted the user to either continue with the current file or skip to the next file. However, there were two continue options which allowed the user to decide whether the field marker should or shouldn't be displayed on the output graph.

Figure 5.4: Event marker short-circuit warning

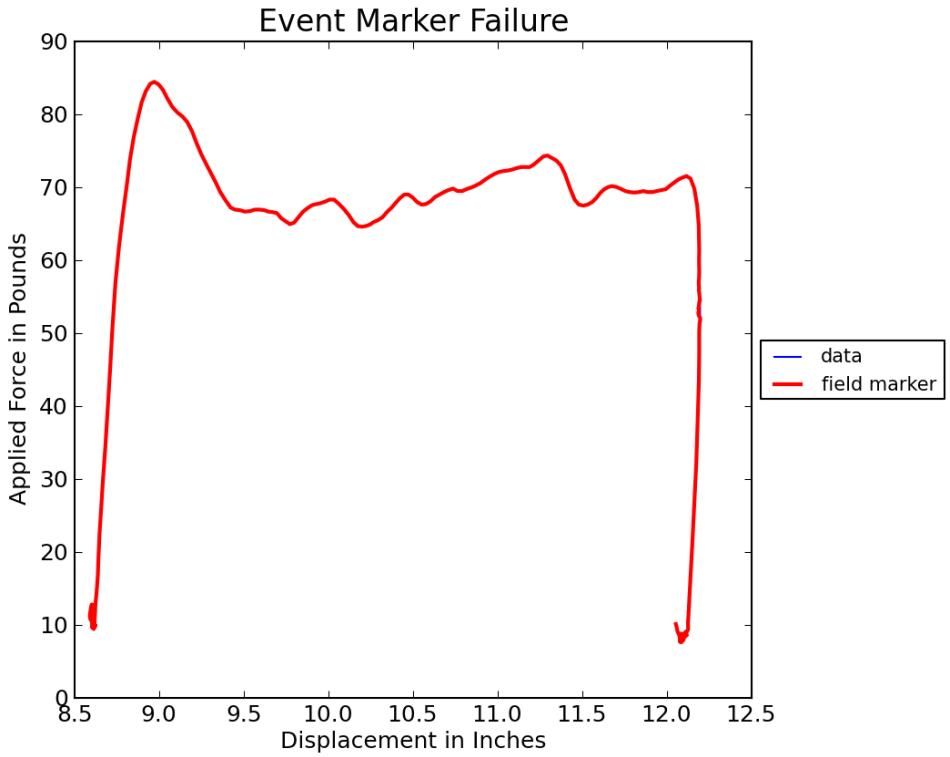

Next, the data array was trimmed from the duration of the recording to contain only data being recorded while a load was being applied as illustrated by Figure 5.5. Because data was recorded at a higher precision than available from the sensors on the VASST, negative loads and reverse movement were often indicated before the test started and after it ended; by removing these readings, the dataset size was greatly reduced. Also, the VASST readings were limited to a

maximum position of just over 37.5 in.; thus load cell readings at a distance in excess of the maximum position could be removed.

Figure 5.5: Untrimmed dataset with noise at beginning and end

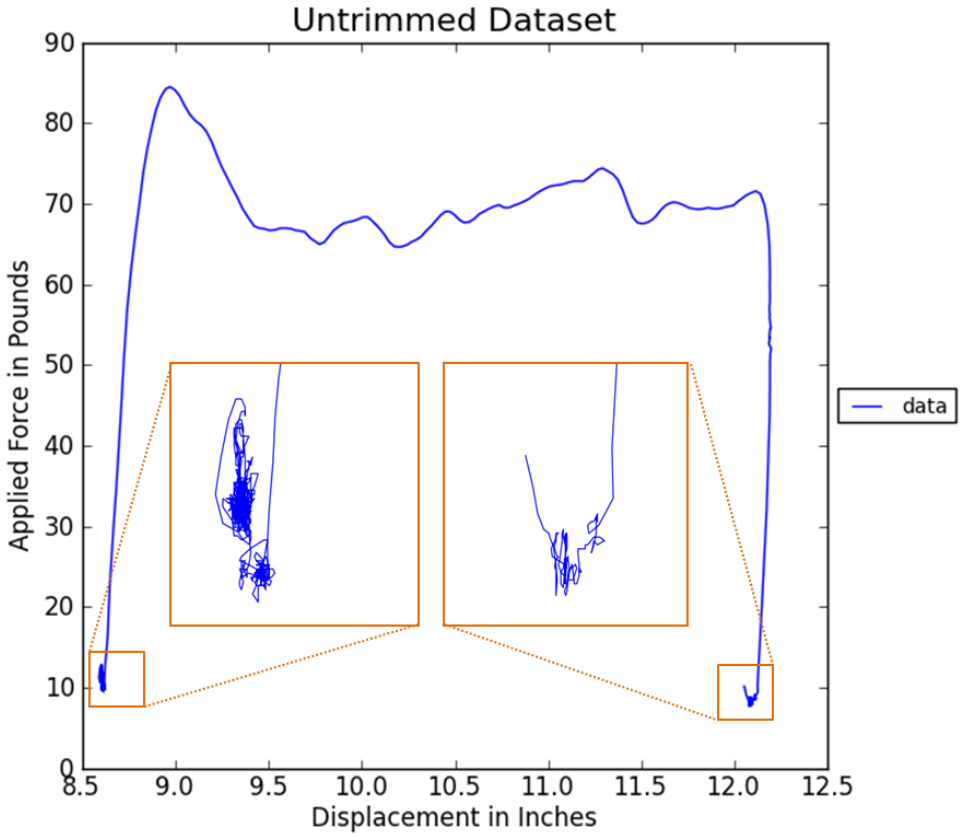

At the end of the data conditioning, the program verified that a usable data array existed in order to prevent errors in following steps. To determine whether the dataset was usable after conditioning, the number of rows in the dataset had to contain a minimum of two points; the minimum of two points was critical to ensure the existence of both maximum and minimum forces and positions.

5.1.2.4 Start Point and Peaks in Force

As discussed in MacDonald et al. (2012), one primary point of interest was the first peak in the displacement-force graph. The first peak was identified by comparing the f_n force to f_{n+1}

force where n was the row number. If $f_n > f_{n+1}$ was true, then the force and position associated with f_n was recorded as a point of interest. After the first maximum was found, the next maximum was a point of interest only if: $f_n > f_{n+1}$ and $f_n > previous\ maximum\ force$ held true. In order to avoid false maximums before the test began, the array of maximums was tested against the dataset's global minimum and an absolute start force value of 20 lb. If any of the maximums had a force within 10 lb. or were within 5% of the global minimum or were less than 20 lb., they were discarded. An example of an array of maximums as determined by the program is illustrated in Figure 5.6.

Figure 5.6: Example of complied maximums

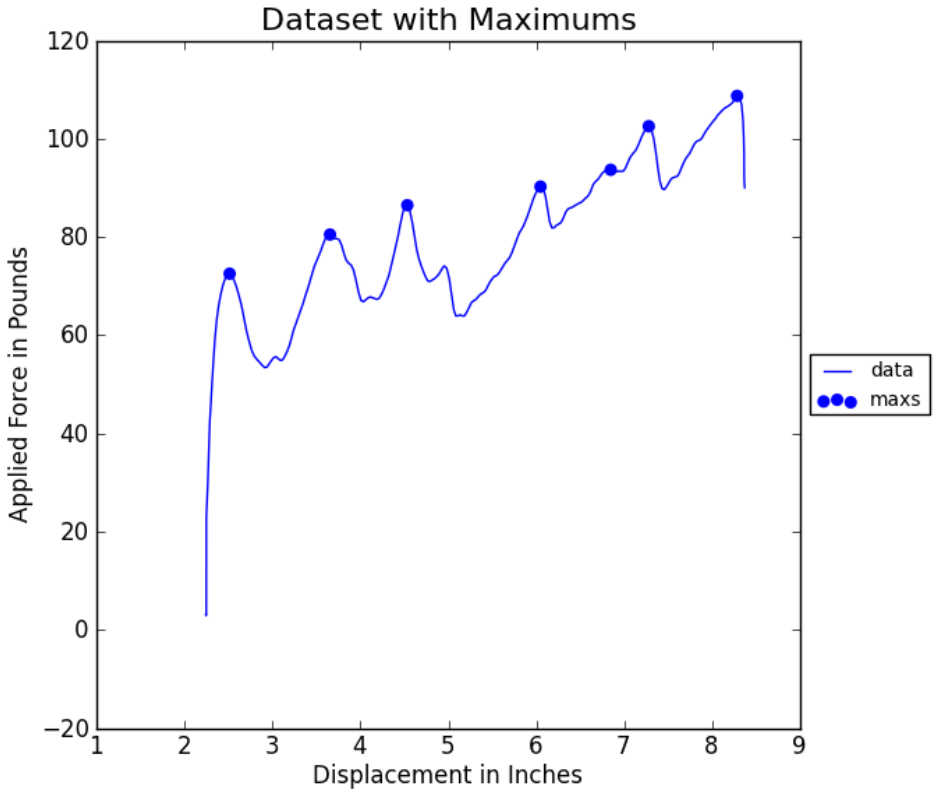

A start point was added to the array containing maximums, referred to as points of interest, using a logic search similar to the one implemented to find the maximums. The search was conducted in the direction of descending displacement from the first maximum until the

force criteria $f_{n-1} > f_n$ or $n = 0$ was met. The addition of the start point to the array containing points of interest aided in the calculation of soil displacement at shear failure.

5.1.2.5 Identifying Cases Requiring Human Input

Though the program was designed to automate the process of analyzing data obtained from the VASST, three special cases were identified in which the program could not correctly determine shear failure. For these special cases, the program prompted the user to identify the point of interest that corresponded to the shear failure using a GUI.

5.1.2.5.1 Special Case 1: Rapid Change in the Force/Displacement Ratio

In some cases, especially when dealing with fine-grained soil, the point at which shear failure occurred was not defined as a peak force. This was a result of the sheared soil pushing, commonly termed plowing, intact soil forward. The occurrence of plowing was identified using the force/displacement ratio, referred to as slope. To identify rapid changes in the slope, the program created an array of the slopes using $(f_{n+2} - f_n)/(p_{n+2} - p_n)$ where f = force and p = displacement. Once an array of slope values was created, each slope was compared to the average of the previous slopes and the relative error was used to determine whether a sudden slope change occurred. If a rapid slope change was identified before a maximum was reached, the point was added to the array containing points of interest. Figure 5.7 demonstrates a sudden change in slope before the first maximum, the red point on the graph.

Figure 5.7: Example of special case 1, sudden slope change

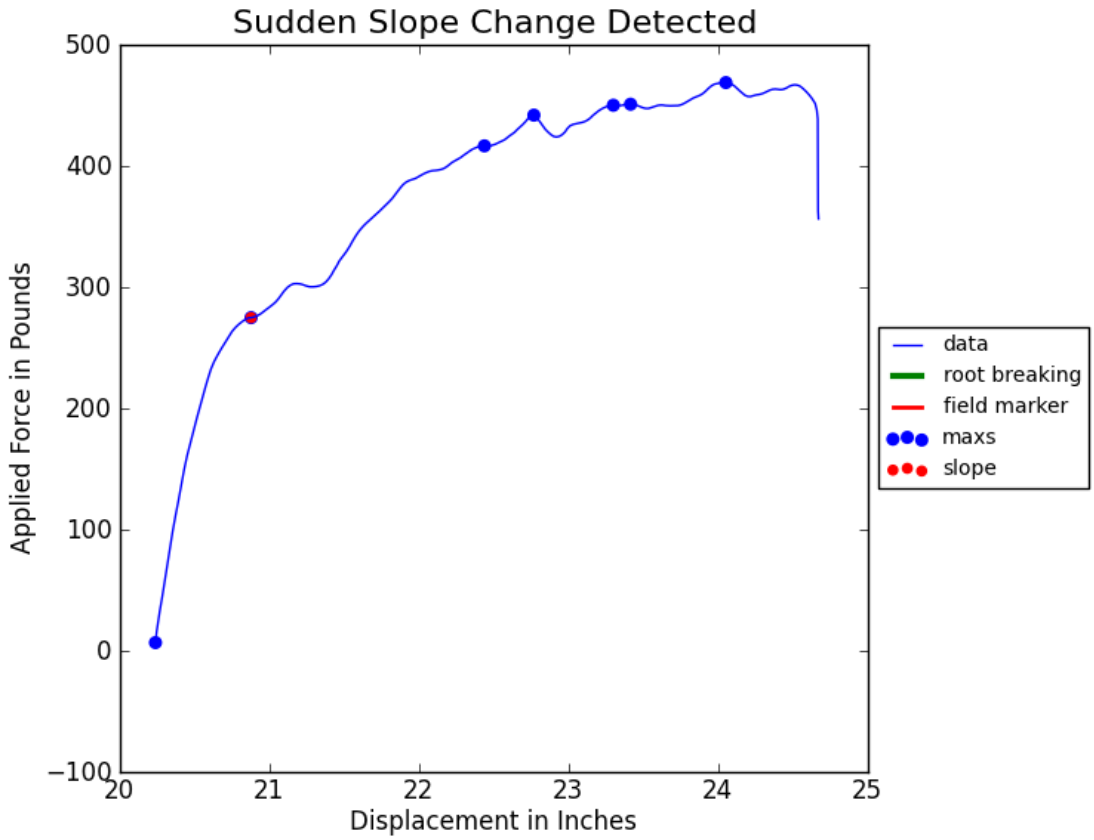

5.1.2.5.2 Special Case 2: Inflection Points

Similar to rapid changes in slope, inflection points were identified as an indicator of shear failure. Because the program looked for inflection points associated with shear failure, only inflection points on positive force-displacement slopes shifting from decreasing slope to increasing slope were calculated. The method used to find inflection points was a series of logic tests: if $f_n < f_{n+3} < f_{n+5}$ was true, then test whether $s_{n+1} > (1.25 * s_{n+2})$ and $(1.25 * s_{n+3}) < s_{n+4}$ were true with s_n being the slope between f_n and f_{n+1}. These logic tests were chosen to limit the number of inflection points to just those that are likely due shear failure. If an inflection point, as defined by the logic tests, occurred in the dataset at a displacement less than the first maximum, all inflection points for the dataset are added to the points of interest array.

The user was then prompted to choose the point of shear failure. Figure 5.8 illustrates how inflection points of interest are displayed on the graphical output.

Figure 5.8: Example of special case 2, inflection points of interest

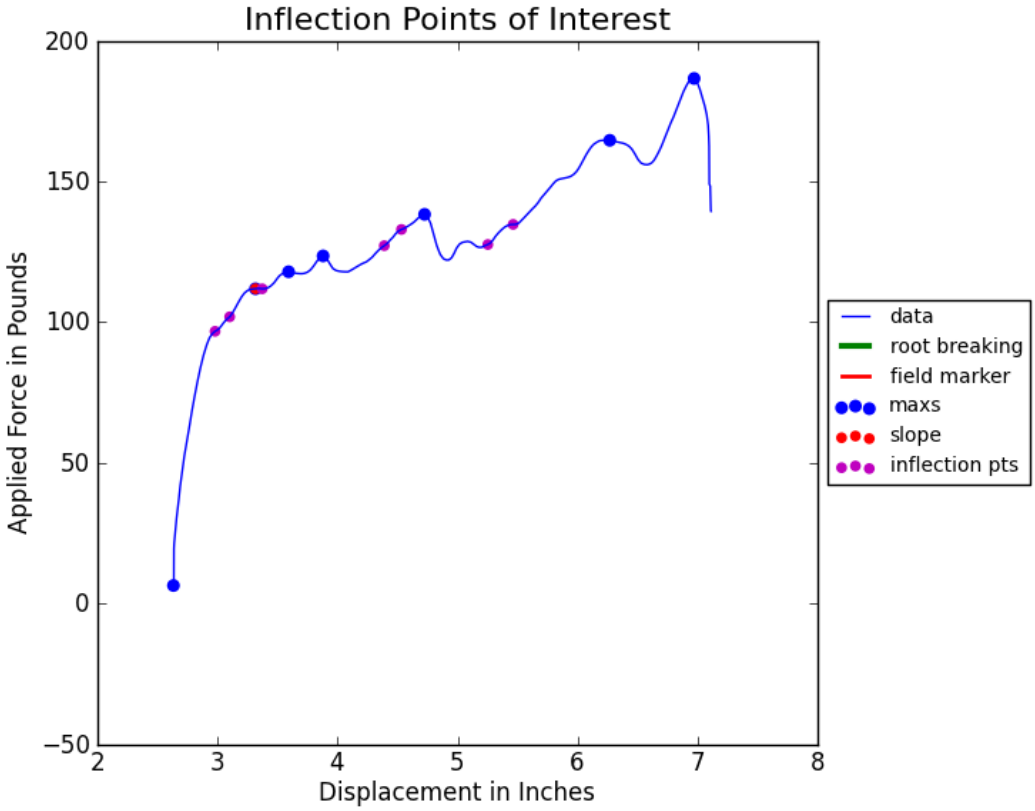

5.1.2.5.3 Special Case 3: Root Breaks

Roots could cause false maximums if they broke before the soil had experienced complete shear failure. A root break could be observed in the dataset as a series of 4 to 10 measurements that had the following pattern: a steep positive slope initially, followed by a steep negative slope, and a return to a steep positive slope. When this pattern was detected anywhere in the conditioned dataset, the program prompted the user to identify the point of interest that corresponded to the shear failure. Figure 5.9 displays how the root break pattern appeared on the graphical output.

Figure 5.9: Example of special case 3, detected root breaks

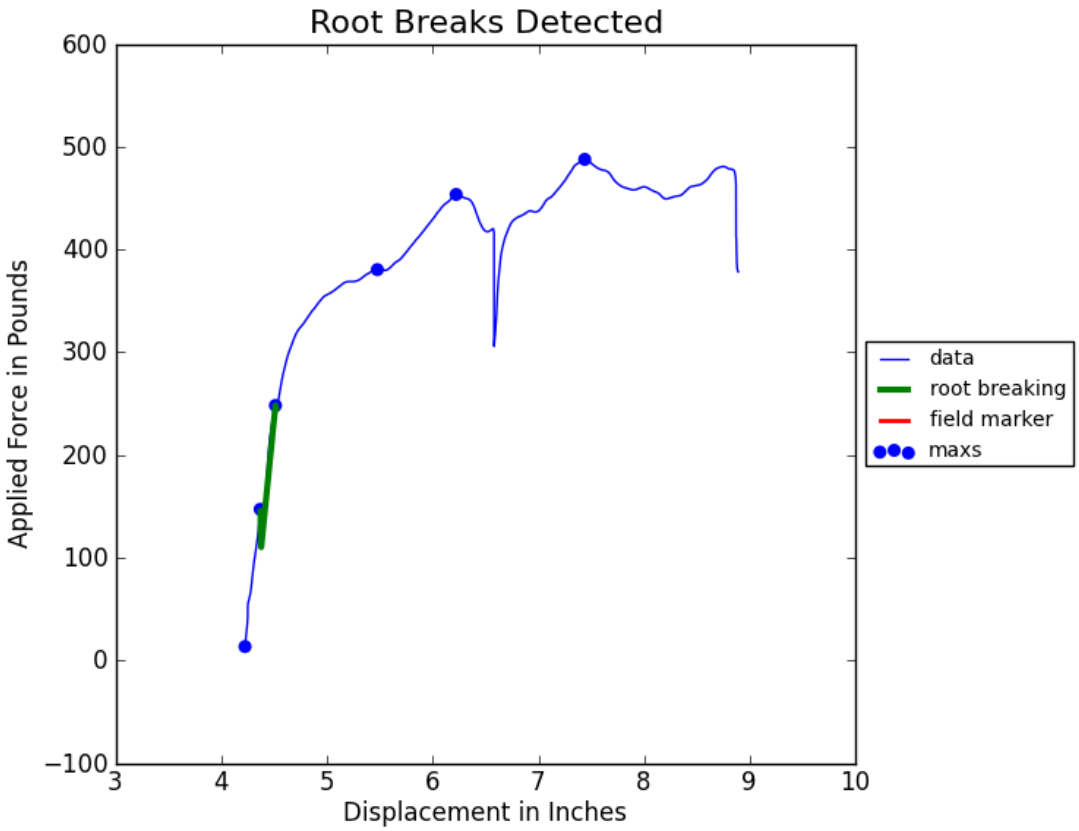

5.1.2.5.4 Special Case 4: Event Marker Present

In the case of an event marker, the program automatically displayed the force-displacement graph and prompted the user for input. This was done as a precaution, since event markers may have indicated problems with the test or equipment. These issues may have resulted in a false reading. Figure 5.10 demonstrates what an event marker was displayed as. However, from visual inspection, the data used in the example appeared to be accurate. In this situation, field notes from the operator were reviewed to explain the purpose of the event marker.

Figure 5.10: Example of special case 4, event marker being triggered

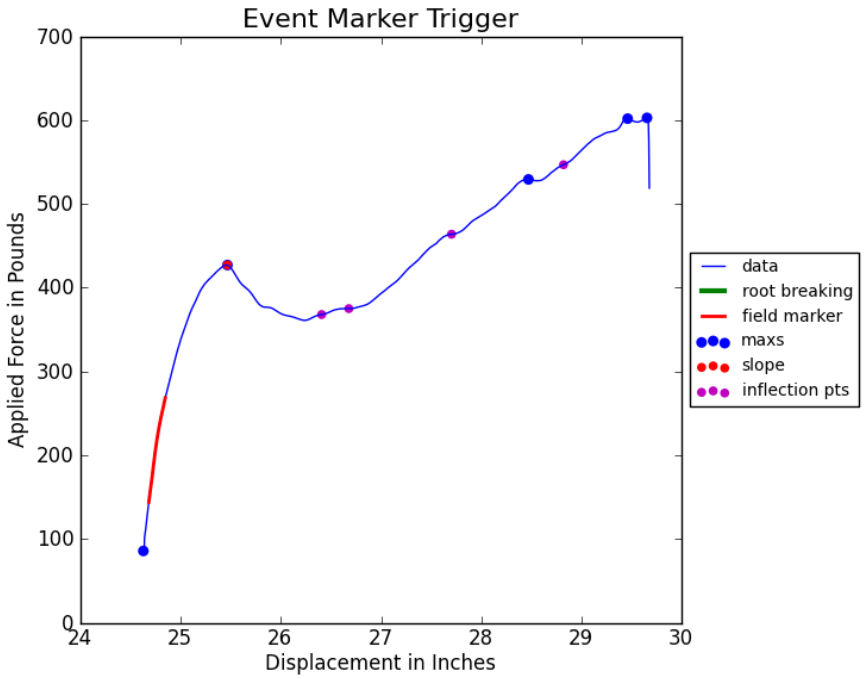

5.1.2.6 Reporting Data

A combined CSV file containing relevant numeric information for all data sets within the folder and individual images of the graphical output were created. The CSV file contained numerical values that described key attributes from the data sets; attributes included were: data directory, file name, force at initial soil failure, displacement required for soil failure, and slope created by force/displacement. The CSV file of complied data was chosen to allow for efficient data transfer to spreadsheets, databases, and statistical programs.

Images of each force-displacement graph were generated during the analysis and saved. The graphs contained possible points of interest, as well as the point identified as the initial soil failure. Although the images were not required for the analysis of the data, they offered an easy way to verify that data reported in the CSV file accurately described the features of the data collected from the VASST. Images were also produced to aid in further developments of the program as more tests are conducted with the VASST. Figures 5.11 and 5.12 show examples of

the program's graphical output for both the automated and manual decision making process respectively.

Figure 5.11: Graphical output for program determined shear failure

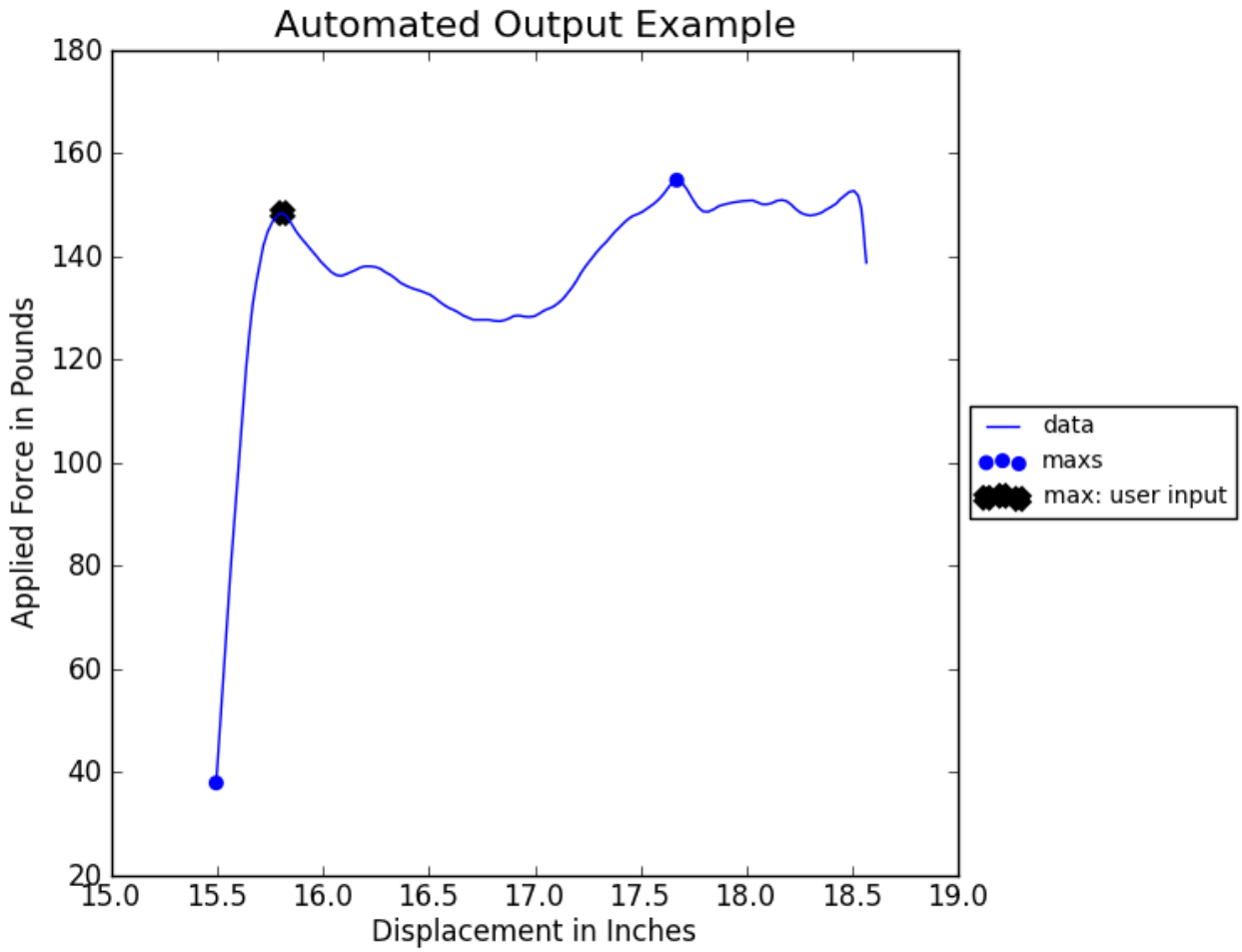

Figure 5.12: Graphical output for user determined shear failure

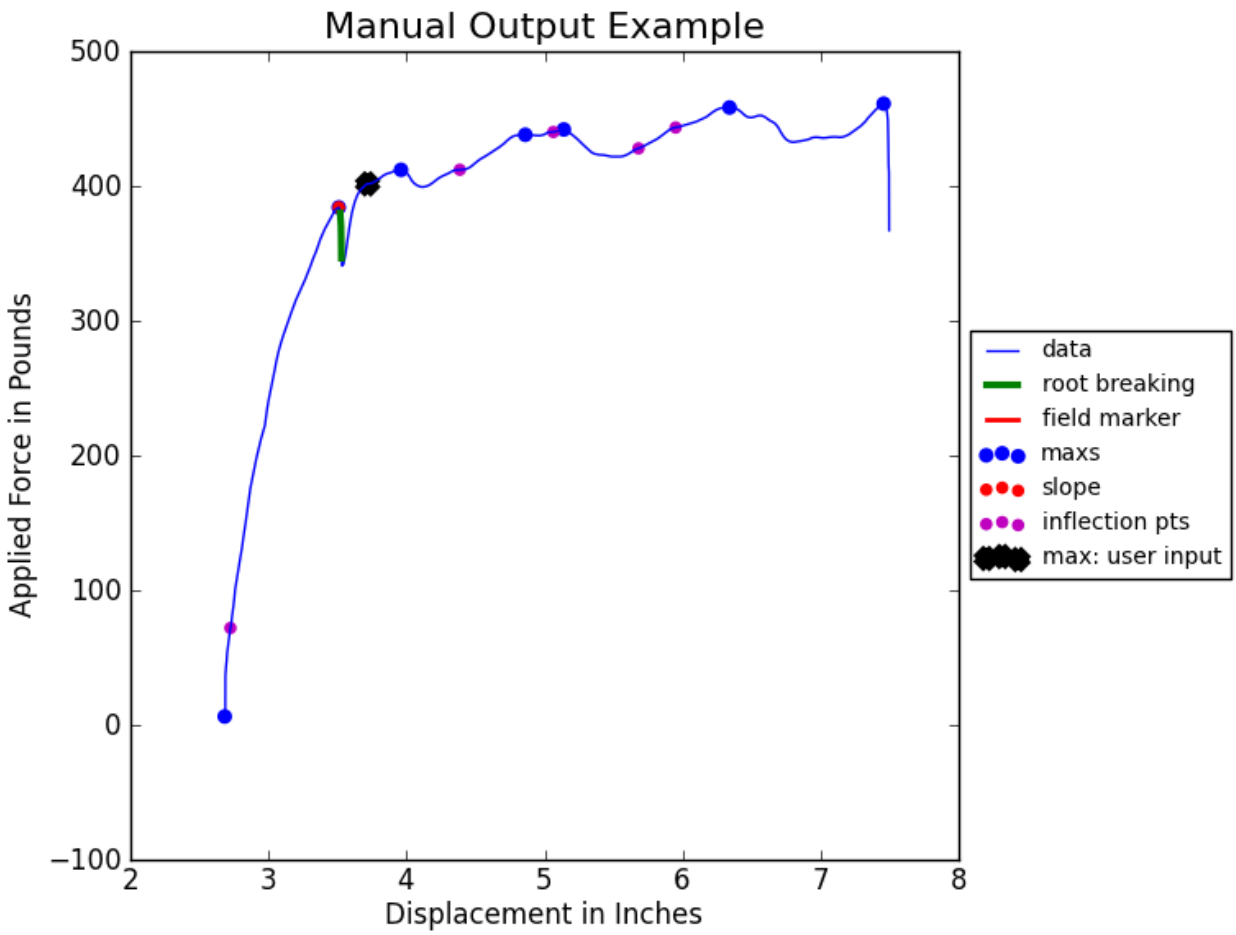

5.2 Development of Mohr-Coulomb Theory for Validation of VASST Measurements

The measurements taken with the VASST were explained theoretically with the modified Mohr-Coulomb, Equation 1.2. It was observed that unlike the experimental apparatuses used by Waldon (1977), Wu et al. (1979), and Endo (1980), the soil samples being sheared by the VASST were not subjected to a vertical loading force. This lack of vertical loading, unique to the VASST, led to the assumption that the normal force, σ in the modified Mohr-Coulomb equation, would become negligible due to the mass of soil being the only vertical force acting at the shearing plane. Under this assumption, the VASST was theoretically much less sensitive to

fictional forces present at the shearing plane compared to effects from cohesion and root reinforcements on soil shear strength. Rohani and Baladi (1981) also stated that it can be assumed that the tangent of the internal angle of friction is negligible, $tan\phi = 0$, for cohesive soils. From Peterson (1988), the effects of soil moisture on shear strength could be accounted for by changes in soil cohesion. Therefore, the modified Mohr-Coulomb equation hypothetically developed for the forces present during VASST testing simplified to Equation 5.1.

$$\tau = c + \Delta s \qquad \text{Eq. 5.1}$$

Rohani and Baladi (1981) found that soil cohesion does not significantly contribute to shear strength in granular soils. The lack of an applied normal force at the soil surface and insignificant soil cohesion led to a further simplification of Equation 5.1 to form Equation 5.2 for granular soils. This equation implied that root reinforcement within the soil matrix was the only parameter affecting VASST measured shear strength at the soil surface in non-cohesive soils.

$$\tau = \Delta s \qquad \text{Eq. 5.2}$$

To test the model developed for the VASST measurements in course grained soils, CBR was determined using Equation 3.11, $CBR = 0.1691 * (CIV)^{1.695}$ (Al-Amoudi et al., 2002b). The shear strength was then calculated from Equation 5.3, developed by Garcia and Thompson (2004). To prove the theoretically developed equation, the VASST shear strength measurements had to be highly correlated to the effects of roots in the soil matrix and insensitive to variations in soil parameters.

$$\tau = 2.25 * CBR \qquad \text{Eq. 5.3}$$

For fine grained soils, CBR was estimated using Equation 3.12, $CBR = a * (CI)^b$ (Shoop et al., 2008), with coefficients from Table 3.1. Shear strength was again calculated using

Equation 5.3. This allowed for the comparison of the VASST measured shear force to the shear force derived from CI.

5.3 Statistical Analysis

The entire statistical analysis for this research was performed using SAS/STAT(R) and SAS/GRAPH software, Version 9.3 of the SAS System for Windows. (SAS Institute Inc., 2014)

5.3.1 Data Exploration

Collected field data was first used to generate several scatter plots in order to determine which class variables would best describe changes in the VASST measurements due to soil type. Scatter plots were produced using SAS 9.3 and the classes compared were soil plasticity (high, medium, none), average particle size (coarse, fine), USCS soil type, and United States Department of Agriculture (USDA) soil texture. It was determined that plasticity was able to describe the behavior of the soil during VASST testing while maintaining a large enough sample size per class to perform statistical analysis.

As a complement to the scatter plots, the same class variables were tested to determine number of observations, means, standard deviations, minimums, and maximums for VASST measurements. This information confirmed the viability of using plasticity as a class variable for further analysis.

Once plasticity was determined to be an important descriptive class variable, box plots of shearing forces were generated to confirm the differences in VASST measurements in soils with different plasticities. Box plots contained several useful pieces of information such as 25^{th} and 75^{th} percentiles as well as the median and mean values for each class. Box plots were also used to identify potential outliers in the data, points that lie outside of the box plot's whiskers. If an

outlier was determined to be caused by human errors or equipment failures, the observation related to the outlier was dropped from the data set.

To identify soil parameters related to VASST measurements, a correlation tool was used to create a matrix of Pearson correlation coefficients. Additionally, the tool provided simple statistics for each variable investigated. The Pearson correlation coefficients provided valuable insight as to which soil and vegetation parameters had the largest impact on VASST measurements per soil plasticity class. Furthermore, the tool was used to check for correlations between soil shear strength, as calculated by methods described in section 5.2, and various parameters measured by the VASST. The correlation results determined whether the VASST could be used as a direct measure of soil shear strength.

Information from the exploratory statistics was applied to more suitable tests for investigating soil and vegetation parameters that affect the measurements obtained using the VASST. Survival analysis was chosen to carry out the statistical analysis as the dataset and characteristics of shear failure share many qualities with clinical trials, experiments that often investigate survival times. VASST induced shear failure, similar to clinical trials, was seen as a measure of life expectancy but by applied force rather than event time. Survival analysis was used to determine which soil and vegetation parameters have significant effects on soil strength measured with the VASST. The survival analysis was conducted each level of soil plasticity previously identified. Another advantage of using survival statistics was that unequal replications were accounted for, a condition often occurring in clinical trials as well as this study. The survival analysis provided valuable insight as to how the VASST performs in various soil plasticities and how its measurements relate to the Mohr-Coulomb failure criterion.

CHAPTER 6: RESULTS AND DISCUSSION

A thorough investigation of the VASST's capabilities as a tool for measuring vegetated soil shear strength was conducted. The VASST measurements were compared to vegetation and soil parameters to gain a better understanding of how the VASST's performance varied under a range of conditions. The existence of correlations between the VASST's measurements, common in-situ soil strength measurements, and calculated soil shear strength was also investigated to determine its capabilities of measuring soil trafficability. Finally, survival analysis was performed to determine which soil and vegetation parameters the VASST was sensitive to.

6.1 Descriptive Parameters of Soil and Vegetation Condition

Field and laboratory measured parameters were used to classify/quantify soil and vegetation characteristics that would likely affect VASST testing results. The parameters were categorized as either class variables or continuous variables. All SAS outputs from the statistical analysis conducted during this research are found in Appendices C though G.

6.1.1 Class Variables

The statistical data set contained the following class variables: plasticity (high, medium, and none), average particle size (coarse and fine), USCS soil type, and USDA soil texture. To determine which class variable described the results by soil type, simple statistics and scatter plots for each class variable were generated. These statistics were used to determine which class variable to use. Scatter plots, found in appendix C, allowed for visual inspection of the data set to identify groups of similar observations that could be accounted for by the class variables. Similarly, the simple statistics provided summary tables that included number of observations,

mean, standard deviation, and maximum and minimum values associated with each level of each class.

The scatter plots showed potential correlations between vegetation parameters, common soil strength tests, and VASST measurements. The presence of a relationship between CI and CIV as well as drop-cone values was visible in each scatter plot, a relationship that has been documented in previous research. Also, the plots showed that trends exist between the VASST force measurements and the various soil strength tests, the CIV in particular. Furthermore, moderate correlations were visible between the VASST force and displacement measurements and the vegetation quantification parameters: aboveground biomass, belowground biomass, and root weight. It was also noted that soil moisture has the biggest effect on strength measurements in high plasticity soil with little visible impact on non-plastic soils.

Comparing the simple statistics produced for each class variable tested helped determine the appropriate variable to classify the behavior of different soil types during VASST testing. When choosing the class variable to describe the soil type, it was important to capture how the different soils failed without creating unequal class sizes.

The simple statistics by plasticity, shown in Table 6.1, indicated that non-plastic and highly plastic soil classes contain nearly the same number of observations with very different means and standard deviations. However, the medium-plasticity soils class only had 21 sets of VASST measurements. The lack of observations increased the potential of Type II errors during statistical analysis and was dropped from the remaining statistical analysis.

Table 6.1: Simple statistics by plasticity

The MEANS Procedure

Plasticity	N Obs	Variable	Label	N	Mean	Std Dev	Minimum	Maximum
High	137	VM	VASST Force	137	364.5845594	153.5812551	25.4444828	762.7454834
		VD	VASST Displacement	137	0.9380158	0.3808606	0.1435471	2.4884300
		VS	VASST Slope	137	0.0034466	0.0026026	0.0012065	0.0226033
Medi	21	VM	VASST Force	21	314.4932122	141.4968736	45.2991219	618.8851929
		VD	VASST Displacement	21	0.8036778	0.3813570	0.0191422	1.5992355
		VS	VASST Slope	21	0.0032353	0.0016150	0.000791560	0.0082558
None	141	VM	VASST Force	141	101.5190929	36.2218727	34.2382317	264.0436401
		VD	VASST Displacement	141	0.4044636	0.2166795	0.1088059	1.3560429
		VS	VASST Slope	141	0.0053580	0.0023880	0.0016281	0.0132764

Simple statistics were also produced for average grain size to provide a summary of the VASST measurements by coarse and fine particle sizes, shown in Table 6.2. When compared to the classification by plasticity, the medium and high plasticity soils were combined in the fine particle class. Although Tables 6.1 and 6.2 are very similar, observations made in the field indicated that medium and high plasticity soils behaved quite differently when being sheared with the VASST. Due to the differing behavior of these soils, it was determined that classifying the soils by average grain size was inappropriate for the study.

Table 6.2: Simple statistics by average grain size

The MEANS Procedure

Average Particle Size	N Obs	Variable	Label	N	Mean	Std Dev	Minimum	Maximum
Coarse	141	VM	VASST Force	141	101.5190929	36.2218727	34.2382317	264.0436401
		VD	VASST Displacement	141	0.4044636	0.2166795	0.1088059	1.3560429
		VS	VASST Slope	141	0.0053580	0.0023880	0.0016281	0.0132764
Fine	158	VM	VASST Force	158	357.9268487	152.5572964	25.4444828	762.7454834
		VD	VASST Displacement	158	0.9201607	0.3824554	0.0191422	2.4884300
		VS	VASST Slope	158	0.0034185	0.0024910	0.000791560	0.0226033

Although the methods described in the USCS were used to derive the class variables for plasticity and average grain size, using USCS soil types created too many classes, as illustrated

in Table 6.3. The USCS classes accurately captured the presence of groups in the data set, however the number of classes greatly and unevenly divided the observations. The small observation numbers per class could have caused a Type II error when comparing multiple continuous variables within a class. Therefore, the classification by USCS soil types was not suitable for this study.

Table 6.3: Simple statistics by USCS soil type

The MEANS Procedure

USCS Classification	N Obs	Variable	Label	N	Mean	Std Dev	Minimum	Maximum
ClayeySand	8	VM	VASST Force	8	65.3684506	13.9693767	42.8945808	83.0847626
		VD	VASST Displacement	8	0.2108117	0.0788858	0.1259327	0.3697395
		VS	VASST Slope	8	0.0062569	0.0021983	0.0042139	0.0111944
InorganicClays	134	VM	VASST Force	134	347.0474863	156.8364727	25.4444828	762.7454834
		VD	VASST Displacement	134	0.9125402	0.3894812	0.0191422	2.4884300
		VS	VASST Slope	134	0.0035808	0.0026530	0.000791560	0.0226033
InorganicSilts_	8	VM	VASST Force	8	413.4687080	135.3342673	261.5704041	638.1902466
		VD	VASST Displacement	8	1.1268950	0.3758532	0.6692123	1.7630005
		VS	VASST Slope	8	0.0031362	0.000964869	0.0023198	0.0053756
Sand	28	VM	VASST Force	28	91.1890507	35.0245563	34.2382317	180.0221252
		VD	VASST Displacement	28	0.4490040	0.1881763	0.1289558	0.9621258
		VS	VASST Slope	28	0.0058972	0.0023159	0.0019696	0.0121620
Sand_ClayeySand	36	VM	VASST Force	36	96.9872114	26.2232666	37.4671860	150.1371155
		VD	VASST Displacement	36	0.3479378	0.1983587	0.1088059	0.8523130
		VS	VASST Slope	36	0.0051692	0.0020087	0.0027001	0.0110554
Sand_SiltySand	69	VM	VASST Force	69	112.2668327	38.9145359	51.6883316	264.0436401
		VD	VASST Displacement	69	0.4383334	0.2315710	0.1974630	1.3560429
		VS	VASST Slope	69	0.0051335	0.0025984	0.0016281	0.0132764

The classes assigned by USDA soil texture also indicated the presence of groups in the data set. Like the classes formed using the USCS soil type, the classes designated by USDA soil texture created a large number of classes, as shown in Figure 6.4; this increased the risk of a Type II error. Furthermore, Table 6.4 shows that sample sizes are very unequal.

Table 6.4: Simple statistics by USDA texture

The MEANS Procedure

USDA Texture	N Obs	Variable	Label	N	Mean	Std Dev	Minimum	Maximum
Clay_Loam	26	VM	VASST Force	26	230.7394377	79.8856115	115.0995102	417.4533691
		VD	VASST Displacement	26	0.8079069	0.4549285	0.2861195	2.4884300
		VS	VASST Slope	26	0.0045802	0.0033352	0.0014391	0.0194712
Loamy_Sand	52	VM	VASST Force	52	88.6508818	27.1892716	34.2382317	180.0221252
		VD	VASST Displacement	52	0.4258462	0.1766973	0.1289558	0.9621258
		VS	VASST Slope	52	0.0065281	0.0026016	0.0019696	0.0132764
Sand	67	VM	VASST Force	67	114.3089354	40.5584559	37.4671860	264.0436401
		VD	VASST Displacement	67	0.3889553	0.2457269	0.1088059	1.3560429
		VS	VASST Slope	67	0.0042653	0.0017864	0.0016281	0.0110554
Sandy_Clay_Loam	22	VM	VASST Force	22	92.9839802	27.8078509	42.8945808	150.1371155
		VD	VASST Displacement	22	0.4011529	0.2132914	0.1259327	0.8523130
		VS	VASST Slope	22	0.0059202	0.0020045	0.0027001	0.0111944
Silt_Loam	102	VM	VASST Force	102	397.4296737	154.2716273	25.4444828	762.7454834
		VD	VASST Displacement	102	0.9921238	0.3628662	0.1435471	1.7892836
		VS	VASST Slope	102	0.0033197	0.0024072	0.0012493	0.0226033
Silty_Clay_Loam	16	VM	VASST Force	16	421.2705793	99.8459413	235.5326691	589.6185303
		VD	VASST Displacement	16	0.8806156	0.3082889	0.3538132	1.4900589
		VS	VASST Slope	16	0.0022008	0.000496654	0.0012065	0.0028683
Very_stony_clay	14	VM	VASST Force	14	233.9329096	79.3815367	45.2991219	361.5993042
		VD	VASST Displacement	14	0.6495246	0.2987081	0.0191422	1.0669017
		VS	VASST Slope	14	0.0033726	0.0019083	0.000791560	0.0082558

Based on the results from simple statistical analysis of each class variable, it was determined that classifying the soils by plasticity was appropriate for the scope of this study. Plasticity classes captured differences in VASST measurements without introducing many classes which would have decreased the number of observations per class.

After simple statistics indicated plasticity as the proper class variable, box plots were produced to visually inspect differences in the classification variables. The box plot of VASST measured shear strength classified by plasticity, Figure 6.1, echoed the results of the simple statistical analyses. The box plot showed that as plasticity decreased, variations in the VASST measured shear strength decreased. Furthermore, the plot indicated the presence of outliers in the

high and non-plastic soils classes, likely a result of higher sampling rates when compared to medium plasticity soils. Box plots for all class variables are found in Appendix D.

Figure 6.1: Box plots of VASST measured shear strength by plasticity class

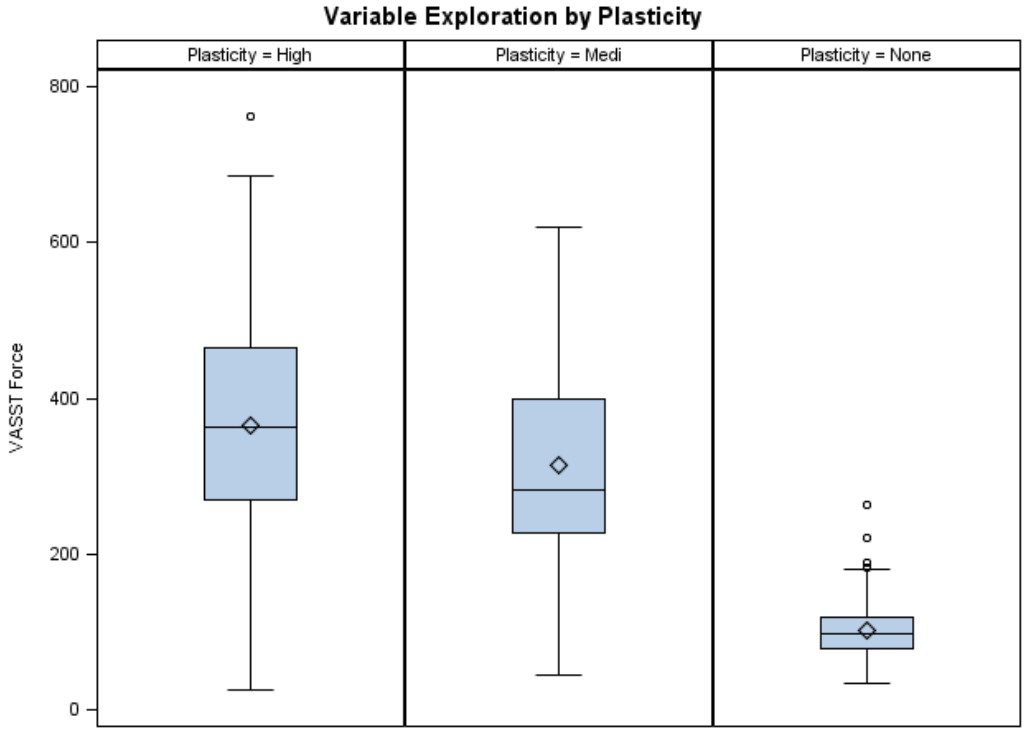

Scatter plots classified by plasticity were also produced to verify the existence of trends for vegetation parameters and soil strength measurements compared to VASST measured soil strength. Additional, parameters from the VASST, force, displacement, and slope, were compared to observe trends within plasticity.

Figure 6.2 illustrates how vegetation parameters form groups when compared to VASST measured soil shear strength. General trends for high and medium plasticity soils showed that as all vegetation measures increase so did VASST measured shear strength. However, there was high variability in individual observations. VASST strength measurements in non-plastic soils appeared less sensitive to root mass and only moderately sensitive to belowground biomass. On

the other hand, VASST shear strength measurements tended to increase as aboveground biomass increased for all soil plasticity classes.

Figure 6.2: Vegetation parameters compared to VASST measured soil strength, classified by plasticity

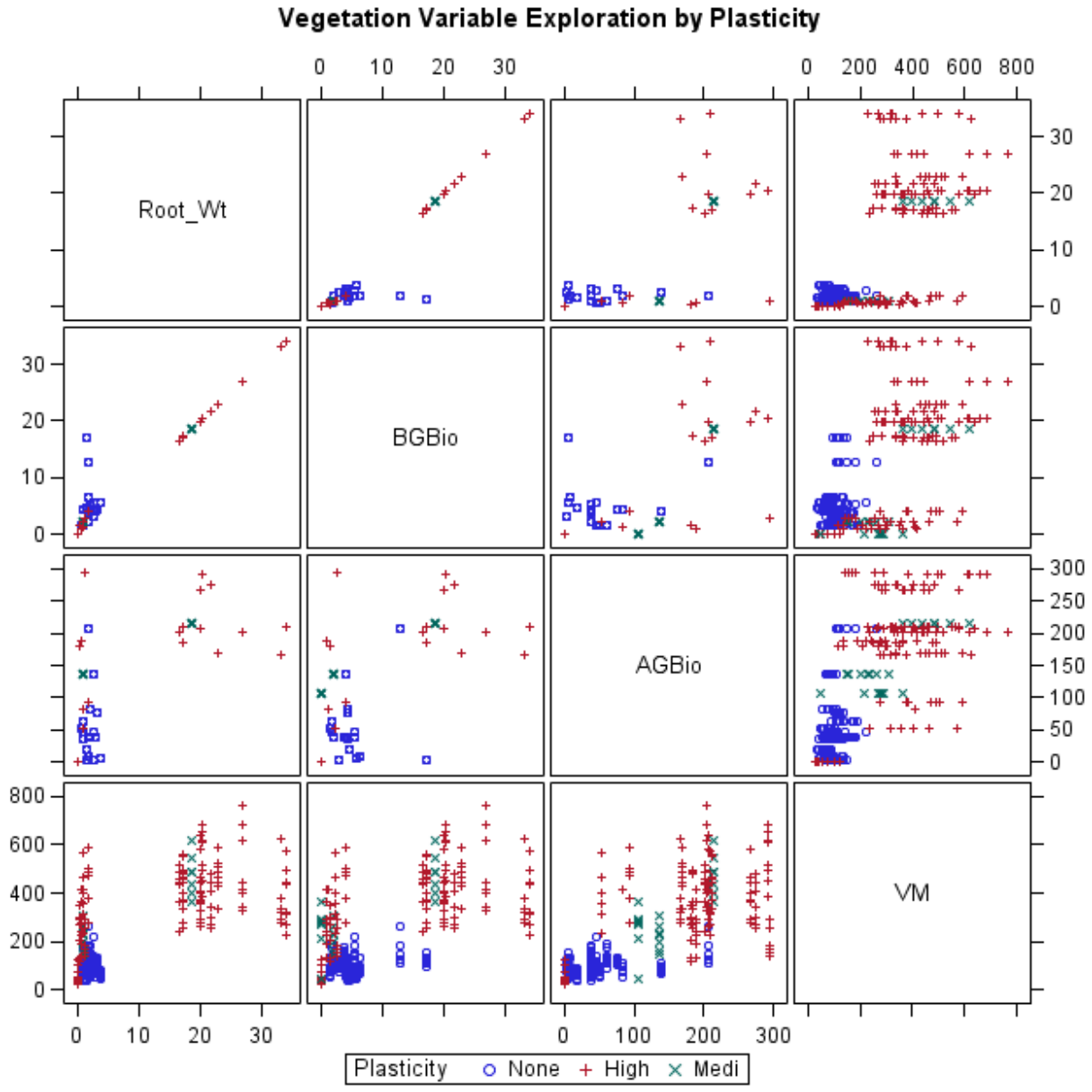

Similarly, it was noted that when comparing the VASST measured soil strength to other common soil strength measurements, groups of observations coincided with soil plasticity levels. Figure 6.3 illustrates the trends found between CI, CIV, drop-cone penetration, and VASST

shear strength measurements. The relationships showed that the VASST was more sensitive to plasticity, as indicated by the strong emergence of plasticity groups, than the other three soil strength measurements.

Figure 6.3: Common soil strength measurements compared to VASST measured soil strength, classified by plasticity

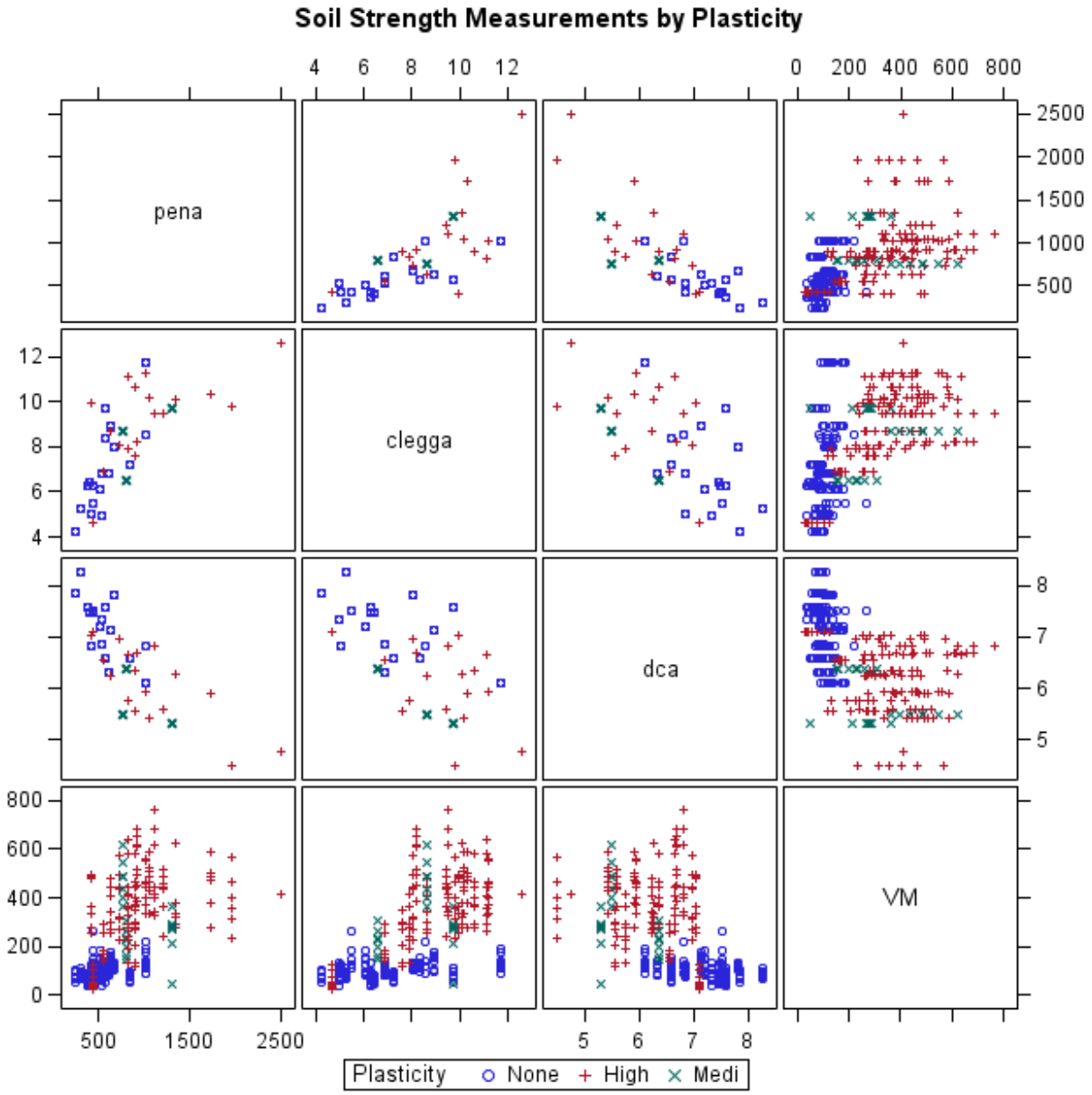

6.1.2 Continuous Variables

Continuous variables were parameters measured using a continuous scale and included measurements quantifying soil particle diameters, root weight, belowground biomass, aboveground biomass, CI, SMC, CIV, drop-cone penetration, and bulk density. Variables also included measurements obtained from the VASST (maximum force, displacement, and force-displacement slope). These parameters were then placed into two categories, measures of soil strength and variables affecting soil strength. This was done to compare the VASST measurements against other measures of soil strength and test which soil and vegetation parameters have the greatest impact on VASST measurements.

6.2 Correlations of the VASST Maximum Force Measurement to Common In-situ Soil Strength Tests

The VASST maximum force measurements were compared to other in-situ measurements of soil strength, CI, CIV, and drop-cone values, to investigate possible correlations between measurements. Previous research (Koch et al., 2010; Shoop et al., 2008) showed strong correlations between the mentioned common in-situ measurements and land trafficability, research that led to the development of the VASST. Correlations between the VASST and previously mentioned measurements are presented in Tables 6.5 through 6.8.

6.2.1 High Plasticity Soils

In high plasticity soils, the Pearson correlation coefficients, illustrated in Table 6.5, showed that VASST maximum force measurements were strongly correlated with CIV and CI. Strong correlations to other soil strength measurements that are used to quantify soil trafficability suggest that the VASST can be used as a tool to quantify trafficability.

Table 6.5: Pearson correlation coefficients for high plasticity soils

Pearson Correlation Coefficients, N = 137 Prob > |r| under H0: Rho=0				
	pena	**clegga**	**dca**	**VM**
pena	1.00000	0.53265	-0.71347	0.36404
Cone Index		<.0001	<.0001	<.0001
clegga	0.53265	1.00000	-0.34005	0.61013
Clegg Impact Value	<.0001		<.0001	<.0001
dca	-0.71347	-0.34005	1.00000	-0.13593
Drop Cone Value	<.0001	<.0001		0.1132
VM	0.36404	0.61013	-0.13593	1.00000
VASST Force	<.0001	<.0001	0.1132	

However, the drop cone was weakly correlated with the VASST when compared to correlations between drop-cone values to CI and CIV. This alluded to differences in soil parameter sensitivities between the VASST and drop-cone. Figure 6.4 presents the data used to calculate the correlation coefficients for high plasticity soils and shows the distribution of data for common in-situ measurements.

Figure 6.4: Observations used for correlation coefficients of high plasticity soils

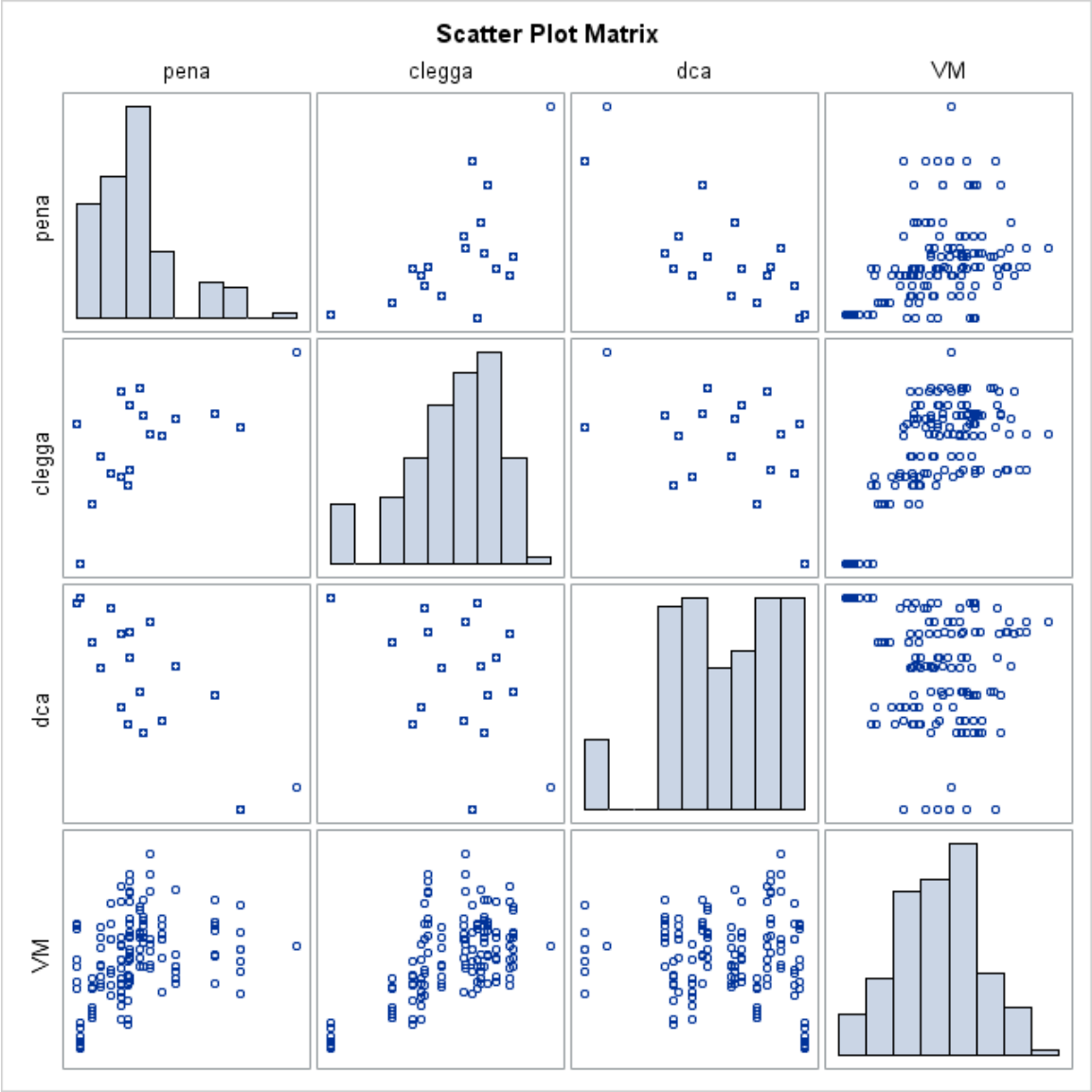

6.2.2 Medium Plasticity Soils

The medium plasticity soils, according to the Pearson correlation coefficients shown in Table 6.6, suggested that VASST maximum force measurements were moderately correlated with CIV, drop-cone values, and CI. However, p-values revealed that the confidence of this correlation is weak. With only 23 samples used to predict the correlation coefficients, low sample numbers for medium plasticity soils severely limited statistical rigor.

Table 6.6: Pearson correlation coefficients for medium plasticity soils

Pearson Correlation Coefficients, N = 21 Prob > |r| under H0: Rho=0				
	pena	**clegga**	**dca**	**VM**
pena	1.00000	0.71720	-0.59122	-0.38311
Cone Index		0.0003	0.0048	0.0865
clegga	0.71720	1.00000	-0.98605	0.23790
Clegg Impact Value	0.0003		<.0001	0.2991
dca	-0.59122	-0.98605	1.00000	-0.36683
Drop Cone Value	0.0048	<.0001		0.1019
VM	-0.38311	0.23790	-0.36683	1.00000
VASST Force	0.0865	0.2991	0.1019	

The scatter plot, shown in Figure 6.5, emphasized the limitations of the medium plasticity class. It revealed that only three observations were used for CIV, drop cone values, and CI measurements. Unlike the high plasticity and non-plastic soils, the data was so limited that well-distributed data was not possible within the medium plasticity class. Conclusions on the VASST's performance in medium plasticity could not be drawn with the current data set.

Figure 6.5: Observations used for correlation coefficients of medium plasticity soils

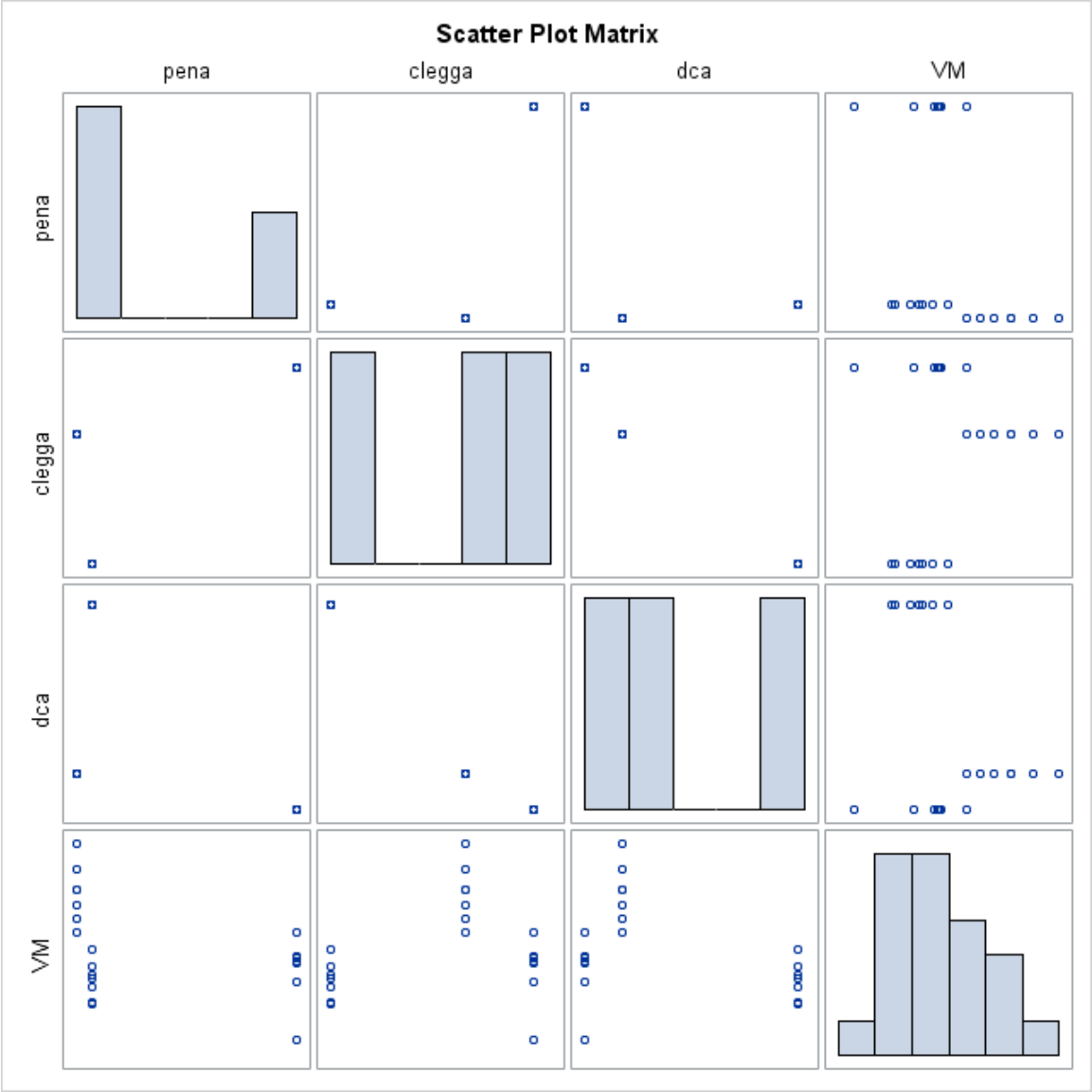

6.2.3 Non-Plastic Soils

As with high plasticity soils, the Pearson correlation coefficients for non-plastics showed that VASST maximum force measurements were moderately correlated with CIV and CI and weakly correlated with drop-cone (Table 6.7). The correlation coefficients in non-plastic soil compared to high plasticity soil indicates a limitation in the soil types the VASST can be used to quantify trafficability. Many of the current trafficability models are based on CI; a stronger

correlation between the VASST maximum force and CI would be expected if the VASST was measuring the same aspect of soil trafficability.

Table 6.7: Pearson correlation coefficients for non-plastic soils

Pearson Correlation Coefficients, N = 141 Prob > |r| under H0: Rho=0				
	pena	**clegga**	**dca**	**VM**
pena	1.00000	0.80363	-0.70742	0.36664
Cone Index		<.0001	<.0001	<.0001
clegga	0.80363	1.00000	-0.50902	0.31113
Clegg Impact Value	<.0001		<.0001	0.0002
dca	-0.70742	-0.50902	1.00000	-0.26520
Drop Cone Value	<.0001	<.0001		0.0015
VM	0.36664	0.31113	-0.26520	1.00000
VASST Force	<.0001	0.0002	0.0015	

The data used to calculate the correlation coefficients for non-plastic soils presented in Figure 6.6, showed the distribution of data for common in-situ measurements. Similar to the observations for high plasticity soils, the data points were fairly well distributed across the range of the data with the exception of the VASST measurements that are left skewed.

Figure 6.6: Observations used for correlation coefficients of non-plastic soils

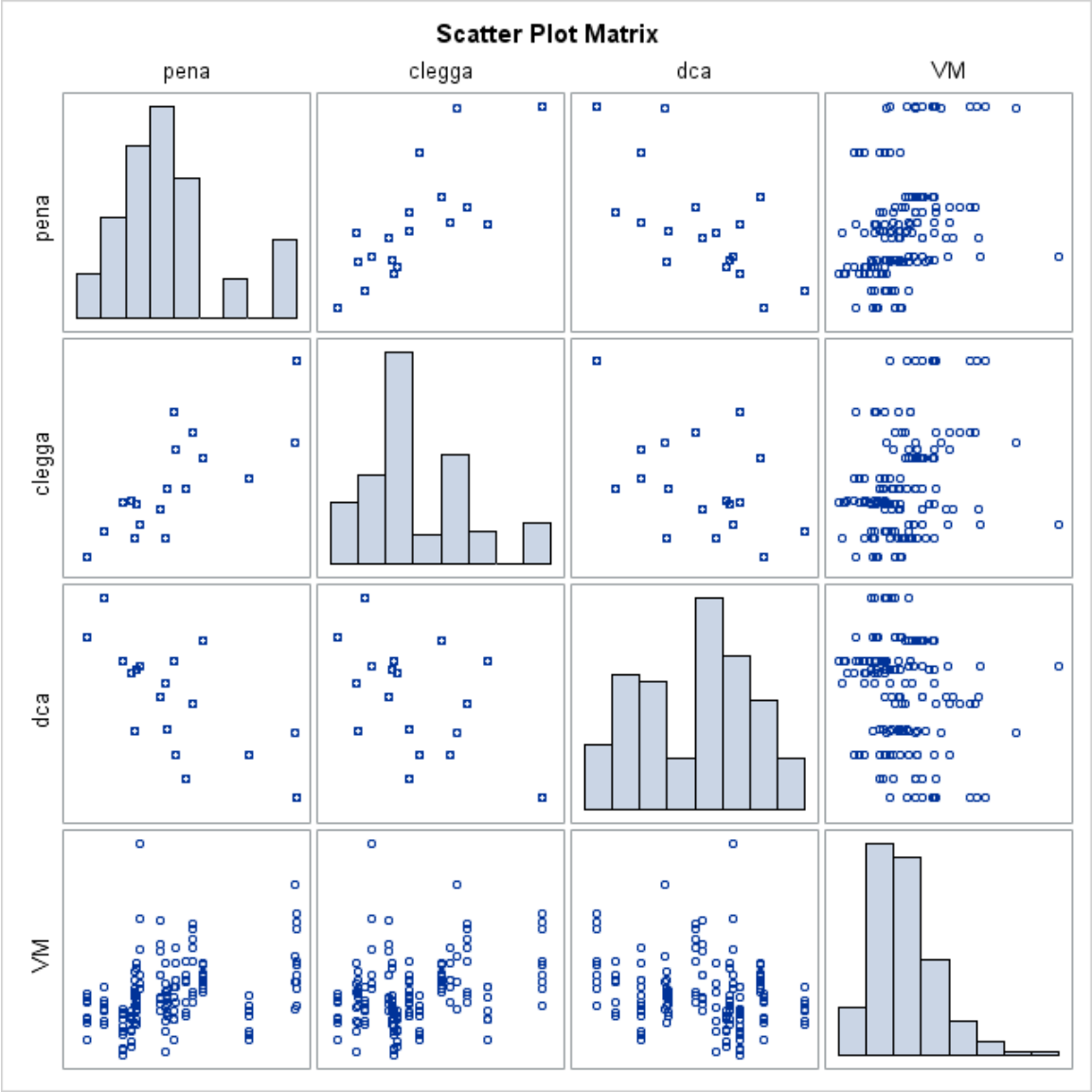

6.3 Comparison of VASST Measurements to Estimated Soil Shear Strength

Pearson correlation coefficients for the estimated soil shear strength, calculated for each of the three plasticity classes were compared (Tables 6.8 through 6.10). Estimated soil shear strength was moderately to strongly correlated to all of the VASST measured shearing parameters for each plasticity class. Only soil displacement in high plasticity and non-plastic soils was not correlated.

In highly cohesive soils, the VASST maximum force applied was strongly correlated with the calculated shear strength, as shown in Figure 6.6. The correlation indicated that the VASST's applied force measurements were a potential indicator of in-situ soil shear strength of high plasticity soils. Displacement distances were also correlated with the calculated shear strength, likely a result of organic fibers increasing the tensile strength of the soil matrix. Due to the elastic nature of organic fibers, they achieved their maximum tensile strength after being stretched as described in Waldron (1977).

Table 6.8: Pearson correlation coefficients for high plasticity soils

Pearson Correlation Coefficients, N = 137 Prob > |r| under H0: Rho=0				
	Tau	**VM**	**VD**	**VS**
Tau	1.00000	0.39126	0.13584	-0.35773
Calculated Shear Strength		<.0001	0.1135	<.0001
VM	0.39126	1.00000	0.65881	-0.53512
VASST Force	<.0001		<.0001	<.0001
VD	0.13584	0.65881	1.00000	0.00532
VASST Displacement	0.1135	<.0001		0.9508
VS	-0.35773	-0.53512	0.00532	1.00000
VASST Slope	<.0001	<.0001	0.9508	

For medium plasticity soils, the Pearson correlation coefficients indicated that shearing parameters were moderately to strongly correlated to calculated soil shear strength (Table 6.9). However, the 21 observations that occurred in medium plasticity soils were limited when compared to the 121 and 141 observations for highly plastic and non-plastic soils respectively. The lack of observations was reflected by the limited confidence in rejecting the null hypothesis (Table 6.9).

Table 6.9: Pearson correlation coefficients for medium plasticity soils

Pearson Correlation Coefficients, N = 21 Prob > |r| under H0: Rho=0				
	Tau	**VM**	**VD**	**VS**
Tau	1.00000	-0.38696	-0.66895	-0.53104
Calculated Shear Strength		0.0831	0.0009	0.0132
VM	-0.38696	1.00000	0.71416	-0.17620
VASST Force	0.0831		0.0003	0.4449
VD	-0.66895	0.71416	1.00000	0.49519
VASST Displacement	0.0009	0.0003		0.0225
VS	-0.53104	-0.17620	0.49519	1.00000
VASST Slope	0.0132	0.4449	0.0225	

The analysis highlighted a lack of correlation between calculated soil shear strength and displacement for non-cohesive soils measured by the VASST, as illustrated in Table 6.10. When compared to cohesive soils, the correlation difference was a result of the VASST test spikes' interaction with the two types of soil when a load was applied. As the spikes applied force to cohesive soils, it was observed that the soil surrounding all five spikes was displaced, as a unit, forming a single continuous shearing surface. On the other hand, as non-cohesive soils were subjected to lateral forces via the spikes, soil particles moved around individual spikes; this

resulted in small, consistent displacement values. Therefore, the short, uniform displacement values observed in non-cohesive soil did not relate to the calculated shear strength.

Table 6.10: Pearson correlation coefficients for non-plastic soils

Pearson Correlation Coefficients, N = 141 Prob > |r| under H0: Rho=0				
	Tau	**VM**	**VD**	**VS**
Tau	1.00000	0.31712	-0.14602	-0.53614
Calculated Shear Strength		0.0001	0.0840	<.0001
VM	0.31712	1.00000	0.59394	-0.35969
VASST Force	0.0001		<.0001	<.0001
VD	-0.14602	0.59394	1.00000	0.37452
VASST Displacement	0.0840	<.0001		<.0001
VS	-0.53614	-0.35969	0.37452	1.00000
VASST Slope	<.0001	<.0001	<.0001	

6.4 Survival Analysis of VASST Measured Shear Strength

Survival analysis was performed on each plasticity class, of the data set, to identify key soil and vegetation parameters influencing VASST soil shear strength. The limited number of observations for medium plasticity soil did not result in an accurate depiction of the VASST's performance. Medium plasticity soil observations were not used in the final analysis.

The parameters initially analyzed as affecting the VASST measured shear strength were root weight, belowground biomass, aboveground biomass, soil moisture, 30% finer particle diameter, 60% finer particle diameter, and soil bulk density. Proc lifetest highlighted that the addition of bulk density as a parameter caused confounding among the variables. This resulted in no parameters being significant predictors of the VASST measured shear strength in high plasticity soil. The significance of parameters in non-plastic soils was unaffected by the inclusion of bulk density, so bulk density was removed from the survival analysis as a predictor. The

complete results of the survival analysis both with and without bulk density as a predicting parameter, can be found in Appendices F and G.

6.4.1 High Plasticity Soils

The survival analysis for high plasticity soils showed that when covariates were individually evaluated aboveground and belowground biomass were the only significant variables affecting VASST force measurements (Table 6.11). However, when analyzing the covariates in a forward stepwise sequence, as shown in Table 6.12, the significant parameters became aboveground biomass, 60% finer particle diameter, root weight, and soil moisture content.

Table 6.11: Rank test for the association of VASST shear force with covariates in high plasticity soils

Univariate Chi-Squares for the Wilcoxon Test					
Variable	Test Statistic	Standard Error	Chi-Square	Pr > Chi-Square	Label
Root_Wt	110.2	59.3923	3.4434	0.0635	Root Wt
BGBio	114.2	56.4720	4.0865	0.0432	Below Ground Biomass
AGBio	1805.6	417.6	18.6965	<.0001	Above Ground Biomass
tdra	-21.2920	29.3911	0.5248	0.4688	Soil Moisture
D30	-0.00119	0.00351	0.1144	0.7351	30% Finer Diameter
D60	0.0266	0.0255	1.0958	0.2952	60% Finer Diameter

Table 6.12: Stepwise test results of associated covariates in high plasticity soils

Forward Stepwise Sequence of Chi-Squares for the Wilcoxon Test						
Variable	DF	Chi-Square	Pr > Chi-Square	Chi-Square Increment	Pr > Increment	Label
AGBio	1	18.6965	<.0001	18.6965	<.0001	Above Ground Biomass
D60	2	59.1087	<.0001	40.4121	<.0001	60% Finer Diameter
Root_Wt	3	65.8502	<.0001	6.7415	0.0094	Root Wt
tdra	4	72.7190	<.0001	6.8688	0.0088	Soil Moisture
BGBio	5	72.7771	<.0001	0.0580	0.8096	Below Ground Biomass
D30	6	72.7862	<.0001	0.00916	0.9237	30% Finer Diameter

The significant effect of aboveground biomass on the VASST was the result of the shallow depth at which the soil was being sheared. During field testing, it was observed that the root crowns did not shear through their interior; in other words, the root crowns were displaced, not broken. This caused an increased surface area of the shearing plane. The root crowns' effect on the area of the shearing plane was directly related to the amount of aboveground biomass and had a large impact on the VASST force measurements. This observation was reflected in the data with aboveground biomass being the leading contributor to soil shear strength near the surface. The results implied that aboveground biomass had the most significant effect on lateral shearing resistance of all the parameters tested in high plasticity soils.

Though the measurement of 60% finer particle diameter was not significant in the individual association analysis, it was significant in the forward stepwise sequence. The significance of the 60% finer particle diameter in the stepwise sequence was likely the result of the parameter's association with cohesion rather than particle size. As described in literature, cohesion is the major contributing factor for soil shear strength in fine grained soils (Rohani et al., 1981). It is also important to note why the 60% finer particle diameter was not significant in the individual association test but became significant in the stepwise test. This difference

occurred because the 60% finer particle diameter described a soil parameter independent of aboveground biomass. For the same reason, belowground biomass went from being significant as an individual parameter to being insignificant when the parameters were analyzed as a group (Table 6.12). This change in significance is due to the dependence of belowground biomass on aboveground biomass.

As expected, the amount of roots, as measured by dry weight for this study, had a significant effect on the soil shear strength obtained with the VASST. The roots acted as reinforcing members within the soil matrix effectively adding tensile strength which resisted shearing.

Lastly, SMC played a significant role in VASST shear strength measurements. The effect was the result of water within the soil matrix acting as a lubricant between soil particles, thus requiring less force to be displaced. Increased soil water content also reduced adhesion between roots and soil particles. The reduction in adhesion caused roots to slip through the soil matrix rather than be loaded to their ultimate tensile strength. Increased SMC resulted in reduced cohesion between soil particles and adhesion between soil particles and roots, which caused a decrease in the soil's shear strength.

Concluding the results of the VASST testing in high-plasticity soils, the VASST was affected by the same soil and vegetation parameters as the direct shear tests performed in vegetated soils during previous studies. The forward stepwise survival analysis confirmed that VASST performance was significantly associated with aboveground biomass, 60% finer particle diameter, root weight, and soil moisture and implied that the VASST can be successfully used as a device to measure in-situ soil shear strength of highly plastic, vegetated soils.

6.4.2 Non-Plastic Soils

The survival analysis for non-plastic soils showed that when covariates were individually evaluated, 60% finer particle diameter, 30% finer particle diameter, aboveground biomass, and belowground biomass were significantly associated with VASST force measurements (Table 6.13). In order for the theoretically developed equation, $\tau = \Delta s$ (Equation 5.2), to be valid, the only significant parameters in non-plastic soils should have been related to vegetation. Statistical analysis of individual soil and vegetation parameters proved the influence of particle size on VASST measurements and suggested that the Equation 5.2 does not hold true with the assumption of a zero normal force at the shearing plane.

Table 6.13: Rank test for the association of VASST maximum force with covariates in non-plastic soils

Univariate Chi-Squares for the Wilcoxon Test					
Variable	Test Statistic	Standard Error	Chi-Square	Pr > Chi-Square	Label
Root_Wt	-6.1632	5.6791	1.1778	0.2778	Root Wt
BGBio	53.5098	23.5356	5.1691	0.0230	Below Ground Biomass
AGBio	803.5	303.5	7.0119	0.0081	Above Ground Biomass
tdra	16.9234	19.1138	0.7839	0.3759	Soil Moisture
D30	-0.7363	0.2442	9.0908	0.0026	30% Finer Diameter
D60	-2.2581	0.5646	15.9968	<.0001	60% Finer Diameter

Field observations offered an explanation as to why the normal force was not zero. As the test spikes were dragged through the soil, non-plastic soils behaved similarly to a high viscosity fluid with increased internal pressures immediately forward of the spikes. These internal pressures created normal forces acting on the individual soil particles and were present in the direction parallel to the spikes' motion. The normal forces among particles increased frictional forces within the soil matrix, a soil property directly related to internal angle of friction.

When reviewing the forward stepwise sequence of covariates in Table 6.14, the significant parameters were 60% finer particle diameter, aboveground biomass, and root weight, parameters also significant in describing high plasticity soils. But, unlike highly plastic soils, the SMC was not identified as an associated covariate of the VASST shearing force.

Table 6.14: Stepwise test results of associated covariates in non-plastic soils

Forward Stepwise Sequence of Chi-Squares for the Wilcoxon Test						
Variable	DF	Chi-Square	Pr > Chi-Square	Chi-Square Increment	Pr > Increment	Label
D60	1	15.9968	<.0001	15.9968	<.0001	60% Finer Diameter
Root_Wt	2	28.5321	<.0001	12.5353	0.0004	Root Wt
AGBio	3	39.0752	<.0001	10.5431	0.0012	Above Ground Biomass
BGBio	4	42.1703	<.0001	3.0951	0.0785	Below Ground Biomass
tdra	5	43.9207	<.0001	1.7504	0.1858	Soil Moisture
D30	6	45.8424	<.0001	1.9217	0.1657	30% Finer Diameter

The significance of the 60% finer particle diameter in coarse grained soils was likely the parameter's association with internal angle of friction rather than particle size. The 30% finer particle diameter was not identified as significant by the stepwise analysis because of strong correlation between 60% and 30% diameters. This meant that only one parameter quantifying particle size was needed to account for the effect of internal angle of friction associated with soil shear strength.

Similar to high plasticity soils, the VASST force measurements in non-plastic soils were affected by aboveground biomass. The shallow depth at which the VASST sheared the soil explained this result. Once again, root crowns remained intact during testing, causing the surface area of the shearing plane to increase. The increased surface area of the shearing plane directly impacted the amount of applied force required for the VASST to shear the soil.

Roots within the soil matrix, though not significant during individual associated covariate analysis, were considered significant during forward stepwise sequence analysis. The result was due to roots' tensile strength increasing the tensile strength of the soil matrix as it was being sheared. Comparing the roots' individual effect in non-plastic soil to highly plastic soils, it was observed that the roots had a larger effect on shear strength in high plasticity soil. Roots tended to slip through the non-plastic soil, rather than break, indicating that the roots did not reach ultimate tensile strength before shear failure occurred. This scenario mirrors root loading in high moisture content, high plasticity soils.

Unlike VASST shear measurements taken in high plasticity soils, SMC did not significantly affect soil shear strength in the non-plastic soils used for this study. The soils used for non-plastic soil tests were sandy with negligible cohesion. SMC mainly reduced cohesion which was assumed to be zero in sand as indicated in research performed by Rohani and Baladi (1981).

Summarizing the results of the VASST testing in non-plastic soils, the VASST measurements of vegetated soil shear strength could not be described using the theoretical modified Mohr-Coulomb equation developed within this study. The assumption of a zero normal force was inaccurate as proven by the significance of particle size within the survival analysis. Although the developed equation did not produce an accurate description of the VASST measured shear strength, the VASST should still be considered effective at measuring soil shear strength. The significant parameters from the forward stepwise sequence test, 60% finer particle diameter, root weight, and aboveground biomass, are important factors in the modified Mohr-Coulomb proposed by Waldron (1977) when 60% finer particle diameter is considered as being correlated to internal angle of friction.

CHAPTER 7: CONCLUSIONS

The VASST was tested at five geographic locations across five ecoregions. Soils ranged from high plasticity inorganic clays to non-plastic sands. Soil strength measurements were taken concurrent with the VASST to evaluate the use of the VASST for trafficability studies. Using a static penetrometer, drop-cone penetrometer, and Clegg impact tester, tools commonly used for in-situ trafficability quantification, VASST performance was quantified. Measurements of soil and vegetation parameters were taken as well to describe the soil and vegetation characteristics; these measurements included bulk density, soil moisture, and aboveground and belowground biomass. Laboratory analyses of field samples quantified soil parameters for Atterburg limits and particle size descriptors, 60% finer diameter and 30% finer diameter, textural analysis, and above and belowground biomass.

VASST field data had to be interpreted to extract useful information on the force required to shear the soil. Previous work done by McDonald (2012) visually interpreted the VASST data one test at a time by plotting force versus displacement. Determining the force and displacement at which the soil was initially sheared was also performed visually. To quickly analyze the VASST data and ensure that analysis results were repeatable, a Python program was developed to automate the process of extracting important test parameter data at the point of shearing. Although the program was intended to be completely automated, the complexity of the data caused the program to output erroneous results in a few instances. The special cases of inaccurate shearing information were identified by the program but were complex in their solutions. The final program was designed to be semi-automated with user selected shear for failure for special cases identified. Force-displacement plots were automatically generated for each VASST test to provide the user with a method of visual inspection.

With data from field and laboratory testing compiled with VASST data outputted by the Python program, statistical analyses were performed using SAS 9.3 to interpret how the VASST could be implemented as a device to measure in-situ vegetated soil shear strength. Simple statistical analyses and visual inspection of the data revealed that a class variable needed to be implemented as the VASST performed quite differently in various types of soils. Due to a limited number of observations, classification by USCS plasticity classes was used to describe variations in the VASST performance in various soil types; the use of these classes also kept sample sizes reasonable for high and non-plastic soils.

Once a descriptive class variable was established, the shearing force data obtained from the VASST was compared against a static penetrometer, drop-cone penetrometer, and Clegg impact tester, tools that have already been used to quantify land trafficability in previous research. Strong correlations between VASST measured force and CI as well as CIV in highly plastic and non-plastic soils suggested that the VASST can also be implemented to quantify trafficability. The measurements of force, displacement, and force-displacement slope from the VASST were also compared to τ, calculated shear strength, for correlations. It was found that moderate to strong correlations exist between τ and VASST measured force as well as VASST measured force-displacement slope for highly and non-plastic soils. No statements can be made on the application of the VASST in medium and low plasticity soils due to a lack of observations in this study.

An investigation into the soil and vegetation parameters which affect the measurements of the VASST was carried out. The test procedure was performed within each soil plasticity class and determined that in high plasticity soils, vegetation was a key dependent variable of force measurements obtained with the VASST. On the other hand, the key dependent variables

affecting VASST measured shear force in non-plastic soils were more related to soil particle size than biomass. However, biomass variables, aboveground and belowground, were still found to be significant.

When dependent variables were analyzed in a forward stepwise manner, particle size (described by 60% finer by diameter), root weight, and aboveground biomass were key parameters affecting the soil shear strength as measured by the VASST in both highly plastic and non-plastic soils. The exception was the significances of SMC in high plasticity soils which was inversely related to shear strength but not significant in non-plastic soils.

Although the derived models (Equations 5.1 and 5.2) were over-simplified and failed to describe the VASST's measurements of soil shear strength, the VASST was sensitive to biomass and soil parameters. These parameters affect soil shear strength and lead to the conclusion that the VASST measurements were related to soil trafficability. However, the high number of VASST tests within each sample revealed that the VASST measurements were highly variable. This meant that one to two samples would be inadequate for describing soil trafficability. Also, the VASST was a large, cumbersome apparatus that required assembly in the field. While it was suitable for research purposes, the VASST could not be rapidly deployed, a key design flaw when performing quick measurements on an as needed basis is desired.

CHAPTER 8: RECOMMENDATIONS FOR FUTURE WORK

After completing this study, the following are suggestions for further research into the application of the VASST as a tool for measuring in-situ shear strength of vegetation and soil for the purposes of quantifying land trafficability:

- A continuation of this research of this study to include observations for low plasticity and more observations for medium plasticity soils would aid in describing the performance of the VASST across a wider range of soil types. The addition of data for a wider range of plasticity could also result in plasticity being implemented as a continuous variable in future statistical analysis.
- Data on soil cohesion measured with a shear vane was not available at the time of this study but would have been a good soil parameter to investigate. The modified Mohr-Coulomb failure criterion is highly dependent on cohesion, and conclusions drawn in this study about high plasticity soils are limited because cohesion was not directly measured.
- Further research on the effects of SMC on the VASST measured shear force should be conducted. Because this study was focused on soil type, little variation in water content was observed within soil type and location, a potential oversight in fully understanding the soil shear strength data obtained from the VASST.
- Lastly, the VASST may be a useful tool to predict vehicle impacts, especially tracked vehicles that produce a lateral shear at the soil surface during acceleration, deceleration, and turning. Future research into the VASST's accuracy in predicting vehicle impacts could be best achieved by comparing VASST measurement to quantifiable impacts such as rut depth and parameters that describe the vehicle creating the impacts.

CHAPTER 9: REFERENCES

Abe, K., & Ziemer, R. R. (1991). Effect of tree roots on shallow-seated landslides. *(*USDA Forest Service General Technical Report PSQ-GTR-130). Washington, DC: U.S. Government Printing Office.

Al-Amoudi, O. S. B., Asi, I. M., Wahhab, H. I. A., & Khan, Z. A. (2002b). Clegg hammer-California-Bearing ratio correlations. *Journal of Materials in Civil Engineering, 14*(6), 512-523.

ASTM Standard D4318, 2010, "Standard Test Method for Liquid Limit, Plastic Limit, and Plasticity Index of Soils," ASTM International, West Conshohocken, PA, 2010. doi: 10.1520/D4318, www.astm.org

ASTM Standard D 4429, 2009a, "Standard Test for CBR (California Bearing Ratio) of Soils in Place." ASTM International, West Conshohocken, PA, 2009, DOI: 10.1520/D4429-09A, www.astm.org.

ASTM Standard D422, 2007, "Standard Test Methods for Particle-Size Analysis of Soils," ASTM International, West Conshohocken, PA, 2007, DOI: 10.1520/D0422-63R07, www.astm.org.

ASTM Standard E100, 2010, "Standard Specification for ASTM Hydrometers," ASTM International, West Conshohocken, PA, 2010, DOI: 10.1520/E0100-10, www.astm.org.

ASABE Standard 313.2, 1992, "Soil Cone Penetrometer," *ASAE Standards. St. Joseph, MI*, 611.

Braunack, M. (1986). The residual effects of tracked vehicles on soil surface properties. *Journal of Terramechanics, 23*(1), 37-50.

Diersing, V., Shaw, R., & Tazik, D. (1992). US army land condition-trend analysis (LCTA) program. *Environmental Management, 16*(3), 405-414. doi:10.1007/BF02400080

Dilustro, J. J., Collins, B. S., Duncan, L. K., & Sharitz, R. R. (2002). Soil texture, land-use intensity, and vegetation of Fort Benning upland forest sites. *Journal of the Torrey Botanical Society, 129(4),* 289-297.

Directorate of Public Works Environmental Division. (2011). *Supplemental environmental assessment for the repair of training area 41 hilltop access trail (HAT) on Fort Hood, Texas.* Unpublished manuscript.

Endo, T., & Tsuruta, T. (1969). *The effect of the tree's roots upon the shear strength of soil.* (1968 annual report of the Hokkaido branch). Sapporo, Japan: Forest Experiment Station.

Endo, T. (1980). Effect of tree roots upon the shear strength of soil. *Japan Agricultural Research Quarterly, 14,* 112-115.

Evett, S. R. (2003). Soil water measurement by time domain reflectometry. *Encyclopedia of Water Science,* 894-898.

Fredlund, D. G., & Morgenstern, N. R. (1977). Stress state variables for unsaturated soils. *Journal of Geotechnical and Geoenvironmental Engineering, 103* (ASCE 12919)

Fredlund, D. G., Xing, A., Fredlund, M. D., & Barbour, S. (1996). The relationship of the unsaturated soil shear to the soil-water characteristic curve. *Canadian Geotechnical Journal, 33*(3), 440-448.

Fredlund, D., Morgenstern, N., & Widger, R. (1978). The shear strength of unsaturated soils. *Canadian Geotechnical Journal, 15*(3), 313-321.

Freitag, D. R., & Richardson, B. Y. (1968). *Application of Trafficability Analysis to Forestry* (No. AEWES-Misc-Paper-4-9595). Army Engineer Waterway Experiment Station. Vicksburg, MS.

Fulton, A. (2013). *Assessing belowground biomass changes following land management and vehicle disturbance.* (Unpublished Master of Science). University of Illinois Urbana-Champaign, IL

Garcia, G. & Thompson, M. R. (2004) *Subgrade Strength/Stiffness Evaluation* (Project IHR-30, Technical Note 6) University of Illinois Urbana-Champaign, IL

Godwin, R. J., Warner, N. L., & Smith, D. L. O. (1991). The development of a dynamic drop-cone device for the assessment of soil strength and the effects of machinery traffic. *Journal of Agricultural Engineering Research, 48*(2), 123-131. doi: http://dx.doi.org/10.1016/0021-8634(91)80009-4

Gray, D. H., & Leiser, A. T. (1982). *Biotechnical slope protection and erosion control.* New York, NY: Van Nostrand Reinhold Company.

Gray, D. H., & Sotir, R. B. (1996). *Biotechnical and soil bioengineering slope stabilization: A practical guide for erosion control*. New York, NY: John Wiley & Sons.

Gray, D. H. (1974). Reinforcement and stabilization of soil by vegetation. *Journal of the Geotechnical Engineering Division, 100*(6), 695-699.

Greenway, D. (1987). *Vegetation and slope stability.* Anderson M. G., Richards K. S. (Eds.), Slope Stability. New York, NY: John Wiley & Sons Ltd.

Guretzky, J. A., Fehmi, J. S., & Anderson, A. B. *Cattle Grazing and Tracked Vehicle Training on Central and Southwestern U.S. Army Lands* (CERL-05-33). Engineering Research and Development Center. Champaign, IL: Construction Engineering Research Lab.

Holtz, R. D., Kovacs, W. D., & Sheahan, T. C. (2010). *An introduction to geotechnical engineering*. Stark H., Rand K. (Eds.). Upper Saddle River, NJ: Pearson Education, Limited.

Jones, D., & Kunze, M. (2004). Guide to sampling soil compaction using hand-held soil penetrometers. *Center for Environmental Management of Military Lands (CEMML),* Fort Collins, CO: Colorado State University

Kansas Sampler Foundation. (2007). *Tall grass prairie national preserve and the flint hills, chase county*. Retrieved from http://www.kansassampler.org/8wonders/8wondersofkansas-view.php?id=17

Kato, N., & Shuin, Y. (2002). Effects of root systems on the shear strain in a direct shear apparatus. *Proceedings of International Congress INTERPRAEVENT 2002 in the Pacific Rim,* Matsumoto, Japan. *, 2* 525-530.

Koch, D. J., Gertner, G. Z., Svendsen, N. G., Howard, H. R., Horner, D. A., & Sullivan, P. M. (2010). Cumulative Interactions for Military Vehicle Impact Assessment. Pittsburgh, Pennsylvania, June 20- June 23, 2010 1008489. doi: 10.13031/2013.35790 www.asabe.org

MacDonald, K. A., Coutermarsh, B. A., Shoop, S. A., & Burch, W. T. (2012). A new method to measure vegetated soil shear strength using the vegetation and soil shear tester (VASST). *Proceedings of 12th European Regional Conference of the International Society for Terrain-Vehicle Systems,* Pretoria, South Africa.

MacDonald, K. A. & Shoop, S. A. (2013). Validation of the vegetation and soil shear tester (VASST) with existing soil strength instruments. *Proceedings of 7th Americas Regional Conference of the International Society for Terrain-Vehicle Systems,* Tampa, Florida.

Mathur, T., & Coghlan, G. (1987). The use of the Clegg impact tester in managing and designing aggregate-surfaced roads. *Transportation Research Record, 1*(1106)

Meyer, M., & Knight, S. (1961). *Trafficability of Soils: Soil Classification* (AEWES-TM-3-240-SUPPL-16). Army Engineer Waterway Experiment Station. Vicksburg, MS.

Muller, L., Tille, P., & Kretschmer, H. (1990). Trafficability and workability of alluvial clay soils in response to drainage status. *Soil and Tillage Research, 16*(3), 273-287. doi: http://dx.doi.org/10.1016/0167-1987(90)90101-I

Nam, J. S., Park, Y. J., & Kim, K. U. (2010). Determination of rating cone index using wheel sinkage and slip. *Journal of Terramechanics, 47*(4), 243-248. doi: http://dx.doi.org/10.1016/j.jterra.2010.02.002

Natural Resources Conservation Service. (2001). Chapter 4: Bulk Density Test. *Soil Quality Test Kit Guide* (pp. 10). Washington, DC: United States Department of Agriculture.

Peterson, R. W. (1988). Interpretation of triaxial compression test results on partially saturated soils. *ASTM Special Technical Publication,* (977), 512-538.

Pollen, N., & Simon, A. (2006). Temporal and spatial variability in the root-reinforcement of streambanks: incorporating variations in soil shear strength and soil moisture into the rip root model. *Proceedings of the 2006 World Environmental and Water Resources Congress,* 87-91.

Pollen, N., & Simon, A. (2005). Estimating the mechanical effects of riparian vegetation on stream bank stability using a fiber bundle model. *Water Resources Research, 41*(7): 25 doi: 10.1029/2004WR003801

Pollen, N. (2007). Temporal and spatial variability in root reinforcement of streambanks: Accounting for soil shear strength and moisture. *Catena, 69*(3), 197-205. doi: http://dx.doi.org/10.1016/j.catena.2006.05.004

Rohani, B., & Baladi, G. (1981). *Correlation of Mobility Cone Index with Fundamental Engineering Properties of Soil* (Miscellaneous Paper SL-81-4). Army Engineer Waterway Experiment Station. Vicksburg, MS.

Rostam-Abadi, F., Chaika, M., Lambrecht, S., & Namburu, R. (1993). *M1, IPM1, and M1A1 (Through November 1990) Abrams Tank Lifting Provisions: Nonlinear Finite Element Analysis of Front Lifting Eye* (TARDEC-TR-93-13591). U.S. Army Tank-Automotive Command Research, Development, and Engineering Center. Warren, Michigan.

Semen, P. M. (2006). *A Generalized Approach to Soil Strength Prediction with Machine Learning Methods* (ERDC/CRREL-TR-06-15). Engineering Research and Development Center. Hanover, NH: Cold Regions Research and Engineering Lab

Shoop, S. A. (1993). *Terrain Characterization for Trafficability* (CRREL-93-6). Engineering Research and Development Center. Hanover, NH: Cold Regions Research and Engineering Lab

Shoop, S. A., Diemand, D., Wieder, W. L., Mason, G., & Seman P. (2008). *Predicting California Bearing Ratio from Trafficability Cone Index Values.* (ERDC/CRREL-TR-08-17). Engineering Research and Development Center. Hanover, NH: Cold Regions Research and Engineering Lab.

Soil Survey Staff, Natural Resources Conservation Service, United States Department of Agriculture. Web Soil Survey. Available online at http://websoilsurvey.nrcs.usda.gov/ accessed 2/2/2014

Sorrie, B. A., Eerden, B. V., & Russo, M. J. (1997). Noteworthy plants from Fort Bragg and Camp MacKall, North Carolina. *Castanea, 62*(4), 239-259. doi: 10.2307/4034041

Terzaghi, K. (1936). The shear resistance of saturated soils. *Proceedings from 1st International Conference on Soil Mechanics and Foundation Engineering,* Cambridge, United Kingdom. (Vol. 1, pp. 54-56).

Thorne, C. R. (1990). Effects of vegetation on riverbank erosion and stability. Thornes J. B. (Ed.) *Vegetation and Erosion* (pp. 125-144). Chinchester, West Sussex: John Wiley & Sons Ltd.

U.S. Department of the Army. (1997). *Army ranges and training land program.* (Army Regulation 210-21). Washington D.C.: Headquarters, Department of the Army.

U.S. Department of the Army. (2005). *The army sustainable range program.* (Army Regulation 300-19). Washington D.C.: Headquarters, Department of the Army.

Waldron, L. (1977). The shear resistance of root-permeated homogeneous and stratified soil. *Soil Science Society of America Journal, 41*(5), 843-849.

Wismer, R. D., & Luth, H. J. (1972). *Off-road traction prediction for wheeled vehicles.* (ASAE Paper No. 72-619). St. Joseph, MI: ASAE.

Wong, J. Y. (2001). *Theory of ground vehicles* (3rd ed.). New York, NY: John Wiley & Sons Ltd.

Wootan, Z. (2011, March/April). Blackland prairie harvest. *The Reverchon Naturalist,* pp. 1.

Wu, T. H., Beal, P. E., & Lan, C. (1988). In-situ shear test of soil-root systems. *Journal of Geotechnical Engineering, 114*(12), 1376-1394.

Wu, T. H., McKinnell III, W. P., & Swanston, D. N. (1979). Strength of tree roots and landslides on Prince of Wales Island, Alaska. *Canadian Geotechnical Journal, 16*(1), 19-33.

Zhang, C., Chen, L., Liu, Y., Ji, X., & Liu, X. (2010). Triaxial compression test of soil–root composites to evaluate influence of roots on soil shear strength. *Ecological Engineering, 36*(1), 19-26.

APPENDIX A: TEST AND SAMPLE QUANTITIES BY LOCATION

Table A.1: Test and sample quantities at Champaign, Illinois

Location: Champaign, Illinois											
Site	Rep	Soil Type	Soil Classification	TDR	Penetrometer	Clegg Impact Hammer	Drop Cone	VASST	Below Ground Biomass	Above Ground Biomass	Bulk Density
1	1	Inorganic Clays, High Plasticity	1	1	5	3	10	9	1	1	1
2	1	Inorganic Clays, High Plasticity	1	5	5	3	10	8	1	1	1
2	2	Inorganic Clays, High Plasticity	1	5	5	3	10	7	1	1	1
2	3	Inorganic Clays, High Plasticity	1	5	5	3	10	8	1	1	1
3	1	Inorganic Clays, High Plasticity	1	5	5	3	10	7	1	1	1
3	2	Inorganic Clays, High Plasticity	1	5	5	3	10	8	1	1	1
3	3	Inorganic Clays, Medium Plasticity	1	5	5	3	10	7	1	1	1
4	1	Inorganic Clays, High Plasticity	1	5	5	3	10	8	1	1	1
4	2	Inorganic Clays, High Plasticity	1	5	5	3	10	8	1	1	1
4	3	Inorganic Clays, High Plasticity	1	5	5	3	10	8	1	1	1
5	1	Inorganic Clays, High Plasticity	1	5	5	3	10	8	1	1	1
5	2	Inorganic Clays, High Plasticity	1	5	5	3	10	8	1	1	1
5	3	Inorganic Silts and Organic Clays, High Compressibility	1	5	5	3	10	8	1	1	1
		Totals:	**13**	**61**	**65**	**39**	**130**	**102**	**13**	**13**	**13**

Table A.2: Test and sample quantities at Ft. Benning, Georgia

Location: Ft. Benning, Georgia											
Site	Rep	Soil Type	Soil Classification	TDR	Penetrometer	Clegg Impact Hammer	Drop Cone	VASST	Below Ground Biomass	Above Ground Biomass	Bulk Density
1	1	Poorly Graded Sand-Clayey Sand	1	6	9	5	5	6	1	1	1
1	2	Poorly Graded Sand-Clayey Sand	1	6	9	5	5	8	1	1	1
1	3	Poorly Graded Sand-Clayey Sand	1	6	9	5	5	8	1	1	1
2	1	Poorly Graded Sand-Clayey Sand	1	6	9	5	5	8	1	1	1
2	2	Poorly Graded Sand-Clayey Sand	1	6	9	5	5	8	1	1	1
2	3	Poorly Graded Sand-Clayey Sand	1	6	9	5	5	8	1	1	1
3	1	Poorly Graded Sand-Clayey Sand	1	6	9	5	5	8	1	1	1
3	2	Poorly Graded Sand-Clayey Sand	1	6	9	5	5	7	1	1	1
3	3	Poorly Graded Sand-Clayey Sand	1	6	9	5	5	7	1	1	1
		Totals:	**9**	**54**	**81**	**45**	**45**	**68**	**9**	**9**	**9**

Table A.3: Test and sample quantities at Ft. Riley, KS

Location: Ft. Riley, Kansas											
Site	Rep	Soil Type	Soil Classification	TDR	Penetrometer	Clegg Impact Hammer	Drop Cone	VASST	Below Ground Biomass	Above Ground Biomass	Bulk Density
1	1	Inorganic Clays, High Plasticity	1	1	1	1	3	8	1	1	1
1	2	Inorganic Clays, High Plasticity	1	1	1	1	3	7	1	1	1
1	3	Inorganic Clays, High Plasticity	1	1	1	1	3	1	1	1	1
		Totals:	**3**	**3**	**3**	**3**	**9**	**16**	**3**	**3**	**3**

Table A.4: Test and sample quantities at Ft. Bragg, North Carolina

Location: Ft. Bragg, North Carolina											
Site	Rep	Soil Type	Soil Classification	TDR	Penetrometer	Clegg Impact Hammer	Drop Cone	VASST	Below Ground Biomass	Above Ground Biomass	Bulk Density
1	1	Poorly Graded Sand-Silty Sand	1	5	5	5	9	6	1	1	1
1	2	Poorly Graded Sand-Silty Sand	1	5	6	5	9	8	1	1	1
1	3	Poorly Graded Sand-Silty Sand	1	5	6	5	9	10	1	1	1
2	1	Poorly Graded Sand	1	5	6	5	9	9	1	1	1
2	2	Poorly Graded Sand	1	5	6	5	9	10	1	1	1
2	3	Poorly Graded Sand	1	5	6	5	9	9	1	1	1
3	1	Poorly Graded Sand-Silty Sand	1	5	5	5	9	9	1	1	1
3	2	Poorly Graded Sand-Silty Sand	1	5	6	5	9	9	1	1	1
3	3	Poorly Graded Sand-Silty Sand	1	5	5	5	9	5	1	1	1
		Totals:	**9**	**45**	**51**	**45**	**81**	**75**	**9**	**9**	**9**

Table A.5: Test and sample quantities at Ft. Hood, Texas

Location: Ft. Hood, Texas											
Site	Rep	Soil Type	Soil Classification	TDR	Penetrometer	Clegg Impact Hammer	Drop Cone	VASST	Below Ground Biomass	Above Ground Biomass	Bulk Density
2	2	Inorganic Clays, Medium Plasticity	1	5	7	5	9	7	1	1	1
2	3	Inorganic Clays, Medium Plasticity	1	5	8	5	9	7	1	1	1
3	1	Inorganic Clays, High Plasticity	1	5	6	5	9	10	1	1	1
3	2	Inorganic Clays, High Plasticity	1	5	8	5	9	8	1	1	1
3	3	Inorganic Clays, High Plasticity	1	5	6	5	9	8	1	1	1
		Totals:	**5**	**25**	**35**	**25**	**45**	**40**	**5**	**5**	**5**

APPENDIX B: PYTHON CODE

```
1. # code_complier.py
2. # Developed for: United States Army Corp of Engineers
3. # Created on: 30-May-2013
4. # Created by: Casey Campbell
5. # Last Modified: 19-Feb-2013
6. # Usage: Import, Analyze, and Export VASST Data
7. # Description: This module is used to identify file
8. # directories, import raw data, excute logic
9. # based modules, and export relevant data
10. # from VASST CSV files
11. # ____________________________________________________________
12.
13. import numpy
14. import os
15. import CSV
16. import Tkinter, tkFileDialog
17.
18.
19. #get program dir
20. root=Tkinter.Tk()
21. root.withdraw()
22. prodirname=tkFileDialog.askdirectory(parent=root,initialdir="I:\School\Research\Modified
    Mohr-Coulomb\VASST\VASST Code and Data",title='Select Program Directory')
23.
24. #get data dir
25. root=Tkinter.Tk()
26. root.withdraw()
27. datdirname=tkFileDialog.askdirectory(parent=root,initialdir="I:\School\Research\Modified
    Mohr-Coulomb\VASST\VASST Code and Data\Raw VASST Data",title='Select Data Directory')
28.
29. #get output dir
30. root=Tkinter.Tk()
31. root.withdraw()
32. outdirname=tkFileDialog.askdirectory(parent=root,initialdir="I:\School\Research\Modified
    Mohr-Coulomb\VASST\\VASST Code and Data\Outputs",title='Select Output Directory')
33.
34. #define check file size for compatibility
35. def getSize(fileobject):
36. fileobject.seek(0,2)
37. size = fileobject.tell()
38. return size
39.
40. #get names of all CSV files in directory
41. fileslist=numpy.array([],str)
42. os.chdir(datdirname)
43. for files in os.listdir('.'):
44. if files.endswith('.CSV'):
45. fileslist=numpy.concatenate((fileslist,numpy.array([files],str)))
46. print fileslist
47. numfiles=numpy.size(fileslist)
```

```
48.
49. #execute analysis
50. folder=numpy.array([])
51. filenam=numpy.array([])
52. loadm=numpy.array([])
53. posm=numpy.array([])
54. slopem=numpy.array([])
55.
56. filenumb=0
57. while filenumb<numfiles:
58. print 'Current Analyzing: ',fileslist.item(filenumb)
59. file = open(fileslist.item(filenumb),'rb')
60. if getSize(file)<1048576:
61. try:
62. execfile(prodirname+'/data_import.py')
63. execfile(prodirname+'/maxs.py')
64. execfile(prodirname+'/first_min.py')
65. execfile(prodirname+'/root_detection.py')
66. execfile(prodirname+'/inflection_pts.py')
67. execfile(prodirname+'/slope_change.py')
68. execfile(prodirname+'/decision_plotter.py')
69. print 'Done'
70.
71. #record current output
72. folder=numpy.concatenate((folder,numpy.array([datdirname],dtype=str)))
73. filenam=numpy.concatenate((filenam,numpy.array([fileslist.item(filenumb)],dtype=str)))
74. loadm=numpy.concatenate((loadm,numpy.array([firstloadpeak],dtype=float)))
75. posm=numpy.concatenate((posm,numpy.array([run],dtype=float)))
76. slopem=numpy.concatenate((slopem,numpy.array([slopepeak],dtype=float)))
77. filenumb=filenumb+1
78. except SystemExit:
79. filenumb=filenumb+1
80. print 'Done'
81. else:
82. print 'Error: File Size to Large'
83. filenumb=filenumb+1
84. print 'Done'
85. print''
86.
87. #create output arrays
88. outdat=numpy.vstack((folder,filenam,loadm,posm,slopem))
89. outdat=numpy.transpose(outdat)
90.
91. #write to file
92. f=open('%s\Output.CSV'%outdirname,'wb')
93. try:
94. writer=CSV.writer(f)
95. writer.writerow(('Data Location','File Name','Load at First Peak','Position of First
    Peak','Slope to First Peak'))
96. for i in range(len(loadm)):
97. writer.writerow((outdat[i,0],outdat[i,1],outdat[i,2],outdat[i,3],outdat[i,4]))
98. finally:
99. f.close()
100.  # data_import.py
101.  # Developed for: United States Army Corp of Engineers
```

```
# Created on: 30-May-2013
# Created by: Casey Campbell
# Last Modified: 19-Feb-2013
# Usage: Import and Condition VASST Data
# Description: This module is used as part of the code_complier
# module to read CSV files to an array, check
# for errors in the raw data, and condition the
# raw data from VASST CSV files
# ____________________________________________________________

from numpy import*
from pylab import*
from CSV import*
import sys

#Load Data to ndarray
with open(fileslist.item(filenumb), 'rb') as f:
reader = reader(f)
count=0
for row in reader:
if len(row)>1:
if count==24:
DataA=row
if count>25:
Data=row
DataA=vstack((DataA,Data))
count=count+1
#Detect Multiple Segments
if count>25 and size(row)==1:
is_valid=0
print 'Warning: Multiple Segments Detected'
print '1. Use First Segment'
print '2. Skip to Next File'
print ''
while not is_valid:
try:
choice=int(raw_input('Enter choice [1,2]:'))
if choice==1 or choice==2:
is_valid = 1
except ValueError, e:
print 'Invalid Entry, Please Try Again'
if choice==1:
print 'Processing Continued'
if choice==2:
print 'Skipping to Next File'
sys.exit()
break
else:
count=count+1
DataA=DataA.astype(float)

#Detect Loadcell
if max(DataA[:,4])--min(DataA[:,4])<=5:
print 'Error: No Loadcell Detected'
sys.exit()
```

```
157.
158.  #Detect Stringpot
159.  if max(DataA[:,5])-min(DataA[:,5])<=0.25:
160.  print 'Error: No Stringpot Detected'
161.  sys.exit()
162.
163.  #Detect Markers
164.  amarpos=array([])
165.  amark=array([])
166.  count=0
167.  for row in DataA:
168.  if abs(row.item(3))>=4:
169.  mark=DataA[count,4]
170.  marpos=DataA[count,5]
171.  amarpos=concatenate((amarpos,array([marpos])))
172.  amark=concatenate((amark,array([mark])))
173.  count=count+1
174.
175.  #Detect Marker Failure
176.  if len(amark)==len(DataA):
177.  is_valid=0
178.  print 'Warning: Marker Failure'
179.  print '1. Override Warning'
180.  print '2. Accept Warning'
181.  print '3. Skip to Next File'
182.  print ''
183.  while not is_valid:
184.  try:
185.  choice=int(raw_input('Enter choice [1,2]:'))
186.  if choice==1 or choice==2:
187.  is_valid = 1
188.  except ValueError, e:
189.  print 'Invalid Entry, Please Try Again'
190.  if choice==1:
191.  amarpos=array([])
192.  amark=array([])
193.  print 'Warning Overridden, Processing Continued'
194.  if choice==2:
195.  print 'Warning Accepted, Processing Continued'
196.  if choice==3:
197.  print 'Skipping to Next File'
198.  sys.exit()
199.  print ''
200.
201.  #Removing Backward Motion
202.  k0position=0
203.  trDataA=ones(6)
204.  for row in DataA:
205.  k1position=row.item(5)
206.  if k0position<k1position:
207.  k0position=k1position
208.  trDataA=vstack((trDataA,row))
209.  trDataA=delete(trDataA,0,0)
210.  DataA=trDataA
211.
```

```
#Remove Negative Loads
count=0
sizeDataA=size(DataA[:,4])
while sizeDataA>count:
if DataA[count,4]<=0:
DataA=delete(DataA,count,0)
sizeDataA=size(DataA[:,4])
else:
count=1+count
#Remove Loads at VASST stop
count=0
sizeDataA=size(DataA[:,4])
while sizeDataA>count:
if DataA[count,5]>=37.5:
DataA=delete(DataA,count,0)
sizeDataA=size(DataA[:,4])
else:
count=1+count

#Detect No Positive Load+Motion
if len(DataA)<=2:
print 'Error: No Data Found'
sys.exit()
```

```
# maxs.py
# Developed for: United States Army Corp of Engineers
# Created on: 30-May-2013
# Created by: Casey Campbell
# Last Modified: 19-Feb-2013
# Usage: Determine Maximums from VASST Data
# Description: This module is used as part of the code_complier
# module to determine the force and position of
# increasing local maximums with respect to the
# start of a VASST test. Points of interest are
# stored in an array outside of the data array.
# ____________________________________________________________

from numpy import*
from pylab import*

count=0
countmax=0
loadmax=-10.0
aloadmax=array([])
apositionmax=array([])
loadgobmax=max(DataA[:,4])
loadgobmin=min(DataA[:,4])

#find maximums/create array of them
for row in DataA:
loadk0=DataA[:,4].item(count)
positionk0=DataA[:,5].item(count)
if positionk0==max(DataA[:,5]):
break
try:
if loadmax<loadk0 and loadk0>DataA[:,4].item(count+1) or loadk0==loadgobmax:
aloadmax=concatenate((aloadmax,array([loadk0])))
apositionmax=concatenate((apositionmax,array([DataA[count,5]])))
loadmax=loadk0
count=count+1
except (count+1)==len(DataA):
break

#remove false maximums at start
if max(aloadmax)>30.0:
sizea=size(aloadmax)
count=1
while count<sizea:
if 0.95<abs(loadgobmin/aloadmax[0]):
aloadmax=delete(aloadmax,0,0)
apositionmax=delete(apositionmax,0,0)
if abs(aloadmax.item(0)-loadgobmin)<=10:
aloadmax=delete(aloadmax,0,0)
apositionmax=delete(apositionmax,0,0)
if aloadmax.item(0)<=20:
aloadmax=delete(aloadmax,0,0)
apositionmax=delete(apositionmax,0,0)
count=count+1
```

```
# first_min.py
# Developed for: United States Army Corp of Engineers
# Created on: 31-May-2013
# Created by: Casey Campbell
# Last Modified: 19-Feb-2013
# Usage: Define the Start of a VASST Test
# Description: This module is used as part of the code_complier
# module to determine the start point of VASST
# tests. The start point is then added to an
# array with other points of interest.
# ____________________________________________________________

from numpy import*
from pylab import*


DataB=DataA
#Remove Data After First Peak
DataB=flipud(DataB)

for row in DataB:
if row.item(5)>=apositionmax.item(0):
DataB=delete(DataB,0,0)

if size(DataB[:,4])<=1:
print 'Error: No Minimum Detected'
sys.exit()

#Find Start Point
loadk0=DataB[0,4]
loadk1=DataB[1,4]
count=0
while loadk1<=loadk0:
if count+2==size(DataB)/6:
break
loadmin=DataB[count+1,4]
positionmin=DataB[count+1,5]
count=count+1
if loadk1==loadgobmin:
break
loadk0=DataB[count,4]
loadk1=DataB[count+1,4]

#Add Start Point Min to Critical Point Data
aloadmax=insert(aloadmax,0,loadmin)
apositionmax=insert(apositionmax,0,positionmin)

#Remove Data Previous of Start Point
DataB=flipud(DataB)
for row in DataB:
if row.item(5)<apositionmax.item(0):
DataA=delete(DataA,0,0)
DataB=delete(DataB,0,0)
```

```
# root_detection.py
# Developed for: United States Army Corp of Engineers
# Created on: 9-June-2013
# Created by: Casey Campbell
# Last Modified: 19-Feb-2013
# Usage: Check for Root Breaks in the VASST Data
# Description: This module is used as part of the code_complier
# module to identify if root breaking is present
# before soil failure that may lead to false
# points of interest being recorded.
# ____________________________________________________________

loada=DataA[:,4]
posa=DataA[:,5]

count=0
rbc=0
rbla=array([])
rbpa=array([])
slopea=array([])
maxcount=size(loada)/3

while count<maxcount:
rise1=loada.item(count+1)-loada.item(count)
run1=posa.item(count+1)-posa.item(count)
slope=rise1/run1
slopea=concatenate((slopea,array([slope])))
slopeavg=average(slopea)
if slope<0 and slopeavg<=abs(slope*0.75):
rbc=1+rbc
rbla=concatenate((rbla,array([loada.item(count)])))
rbpa=concatenate((rbpa,array([posa.item(count)])))
count=count+1
```

```
# inflection_pts.py
# Developed for: United States Army Corp of Engineers
# Created on: 15-June-2013
# Created by: Casey Campbell
# Last Modified: 19-Feb-2013
# Usage: Identify Inflection Point in the VASST Data
# Description: This module is used as part of the code_complier
# module to determine major inflection point.
# Depending on the location of the inflection
# point, they may be points of interest
# _____________________________________________________________

from numpy import*

loada=DataA[:,4]
positiona=DataA[:,5]
timea=DataA[:,0]

#find the slope a each pt
slopea=array([])
count=0
while count<size(loada)-1:
sfor= (loada.item(count+1)-loada.item(count))/(positiona.item(count+1)-
  positiona.item(count))
slopea=concatenate((slopea,array([sfor])))
count=count+1
slopea=concatenate((slopea,array([0])))

#find inflection points in positive slopes
loadb=array([])
positionb=array([])
count=0
while count<size(loada)-6:
if loada.item(count)<loada.item(count+3) and
  loada.item(count+3)<loada.item(count+5):
if slopea.item(count+1)>slopea.item(count+2) and
  slopea.item(count+3)<slopea.item(count+4):
if slopea.item(count+1)>1.25*slopea.item(count+2)and
  slopea.item(count+4)>1.25*slopea.item(count+3):
inflecload=array([loada.item(count+3)])
inflecpos=array([positiona.item(count+3)])
loadb=concatenate((loadb,inflecload))
positionb=concatenate((positionb,inflecpos))
count=count+1

#delete points within 0.625 inches of max points
count=0
while count<size(loadb):
if len(positionb)==0:
break
fastcount=0
while fastcount<len(apositionmax):
if len(positionb)<=count:
break
if abs(positionb[count]-apositionmax[fastcount])<=.125:
```

```
loadb=delete(loadb,count,0)
positionb=delete(positionb,count,0)
fastcount=fastcount+1
count=count+1

count=0
while count<size(positionb)-1:
if len(positionb)==0:
break
if positionb.item(count+1)-positionb.item(count)<=.125:
loadb=delete(loadb,count+1,0)
positionb=delete(positionb,count+1,0)
count=count+1
```

```
#Developed for United States Army Corp of Engineers
# slope_change.py
# Developed for: United States Army Corp of Engineers
# Created on: 22-June-2013
# Created by: Casey Campbell
# Last Modified: 19-Feb-2013
# Usage: Critical Slope Changes in the VASST Data
# Description: This module is used as part of the code_complier
# module to identify a point of interest being a
# critical slope change before a maximum is
# reached.
# ____________________________________________________________

from numpy import*

loada=DataA[:,4]
positiona=DataA[:,5]
timea=DataA[:,0]

#find the 2nd slope at each pt

slopea2=array([])
countsc=0

while countsc<size(loada)-2:
sfor= (loada.item(countsc+2)-loada.item(countsc))/(positiona.item(countsc+2)-
  positiona.item(countsc))
slopea2=concatenate((slopea2,array([sfor])))
countsc=countsc+1
slopea2=concatenate((slopea2,array([0])))

countsc=1
while countsc<size(loada)-2:
if DataA[countsc-1,4]>=2+DataA[0,4] and DataA[countsc-1,5]>=0.25+DataA[0,5]:
break
countsc=countsc+1

avgslope=0
relerror=0
saloadmax=size(aloadmax)

while DataA[countsc-1,4]<=aloadmax.item(saloadmax-1):
loadc=DataA[countsc-1,4]
positionc=DataA[countsc-1,4]
avgslope=(slopea2.item(countsc)+(countsc-1)*avgslope)/countsc
if avgslope>0 or avgslope<0:
relerror=(avgslope-slopea2.item(countsc))/avgslope
countsc=countsc+1
if relerror>=0.8:
break

if DataA[countsc,4]<aloadmax.item(1)and DataA[countsc,5]<apositionmax.item(1):
if DataA[countsc,5]-DataA[0,5]>=0.125:
aloadmax[1]=DataA[countsc,4]
apositionmax[1]=DataA[countsc,5]
```

```
# decision_plotter.py
# Developed for: United States Army Corp of Engineers
# Created on: 30-May-2013
# Created by: Casey Campbell
# Last Modified: 19-Feb-2013
# Usage: Determine if a Human Decision is Required and
# Create and Save Graphical Data from the VASST
# Description: This module is used as part of the code_complier
# module to determine the point of shear failure.
# Human decisions may be required to identify the
# point of shear failure. This module also creates
# and saves all graphical VASST data.
# ____________________________________________________________

from numpy import*
import Tkinter, tkSimpleDialog
from multiprocessing import Process
import sys

#Determine if conditioned data set is complete
if size(aloadmax)<=1:
print 'Error: Conditioned Data Set too Small'
sys.exit()

#Determine if marker is of interest
if size(amarpos)>0:
if (max(amarpos)-.125)<=min(apositionmax)or (min(amarpos)-
  .125)>=max(apositionmax):
amarpos=array([])
amark=array([])
else:
print amark
print 'Notice: Marker(s) at', amarpos.item(0)

#Determine number of points and how to handle them
numbcritpts=size(aloadmax)
if numbcritpts==2:
rise=aloadmax.item(1)-aloadmax.item(0)
run=apositionmax.item(1)-apositionmax.item(0)
slope=rise/run
firstloadpeak=aloadmax.item(1)
firstloadposition=apositionmax.item(1)
slopetopeak=slope

if DataA[countsc,5]<apositionmax.item(1) or len(positionb)>0 and
  positionb.item(0)<apositionmax.item(1) or size(amark)>0 or rbc>=1:
#Display graph in question
ion()
title('Force-Displacement: %s' %(fileslist.item(filenumb)),fontsize=16)
scatter(apositionmax,aloadmax,color='b',linewidths='2',label='maxs')
scatter(DataA[countsc,5],DataA[countsc,4],color='r',label='slope')
plot(DataA[:,5],DataA[:,4],color='b',label='data')
scatter(positionb,loadb,color='m',label='inflection pts')
plot(rbpa,rbla,color='g',linewidth=3,label='root breaking')
plot(amarpos,amark,color='r',linewidth=2,label='field marker')
```

```
#Stack/sort pts of user input
allptsload=hstack((aloadmax,loadb))
allptsposition=hstack((apositionmax,positionb))
allpts=transpose(vstack((allptsload,allptsposition)))
order=allpts[:,1].argsort()
allpts=transpose(take(allpts,order,0))
allptsload,allptsposition=vsplit(allpts,2)
#Prompt for user input
root=Tkinter.Tk()
root.withdraw()
ptselect=tkSimpleDialog.askinteger('Point Selection', 'Select First Peak')
scatter(allptsposition.item(ptselect),allptsload.item(ptselect),color='k',
  marker='x',linewidths=10, label='max: user input')
ax=subplot(111)
box=ax.get_position()
ax.set_position([box.x0,box.y0,box.width*0.8, box.height])
legend(loc='center left',bbox_to_anchor=(1,0.5), prop={'size':10})
xlabel('Displacement in Inches',fontsize=12)
ylabel('Applied Force in Pounds',fontsize=12)
savefig('%s\%s.png'%(outdirname,fileslist.item(filenumb)),dpi=400)
close()
firstloadpeak=allptsload.item(ptselect)
firstloadposition=allptsposition.item(ptselect)
rise=(firstloadpeak-aloadmax.item(0))
run=(firstloadposition-apositionmax.item(0))
slopepeak=arctan(run/rise)
else:
firstloadpeak=aloadmax.item(1)
firstloadposition=apositionmax.item(1)
rise=aloadmax.item(1)-aloadmax.item(0)
run=apositionmax.item(1)-apositionmax.item(0)
slopepeak=arctan(run/rise)
title('Force-Displacement: %s' %(fileslist.item(filenumb)), fontsize=16)
scatter(firstloadposition,firstloadpeak,color='k',marker='x',linewidths=10,
  label='max used')
scatter(apositionmax,aloadmax,color='b',linewidths='2',label='maxs')
plot(DataA[:,5],DataA[:,4],color='b',label='data')
ax=subplot(111)
box=ax.get_position()
ax.set_position([box.x0,box.y0,box.width*0.8, box.height])
legend(loc='center left',bbox_to_anchor=(1,0.5), prop={'size':10})
xlabel('Displacement in Inches',fontsize=12)
ylabel('Applied Force in Pounds',fontsize=12)
savefig('%s\%s.png'%(outdirname,fileslist.item(filenumb)),dpi=150)
close()
```

APPENDIX C: PROC SGSCATTER RESULTS FOR CLASS VARIABLES

Figure C.1: Scatter plot matrix of variables by plasticity

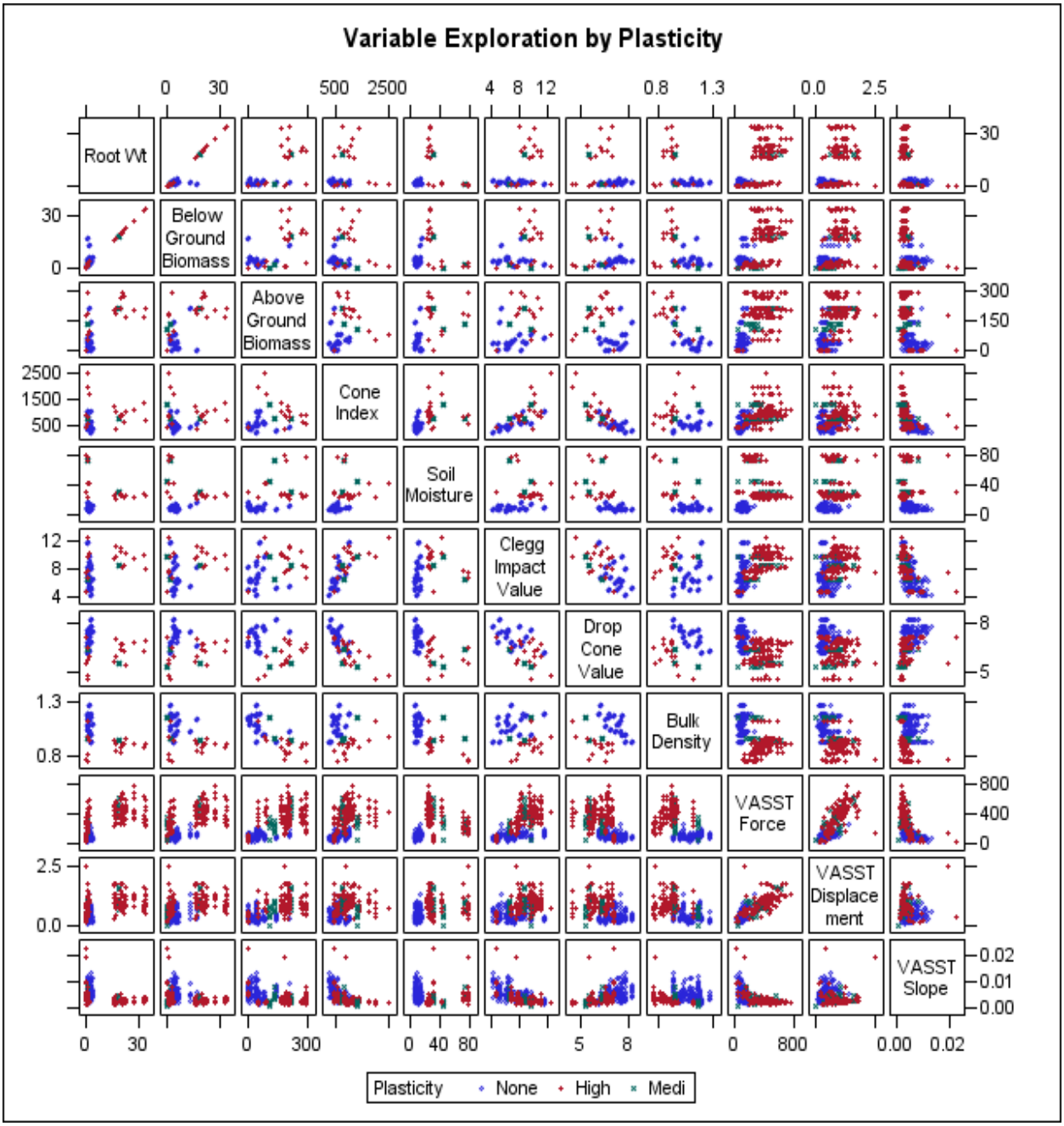

Figure C.2: Scatter plot matrix of variables by average grain size

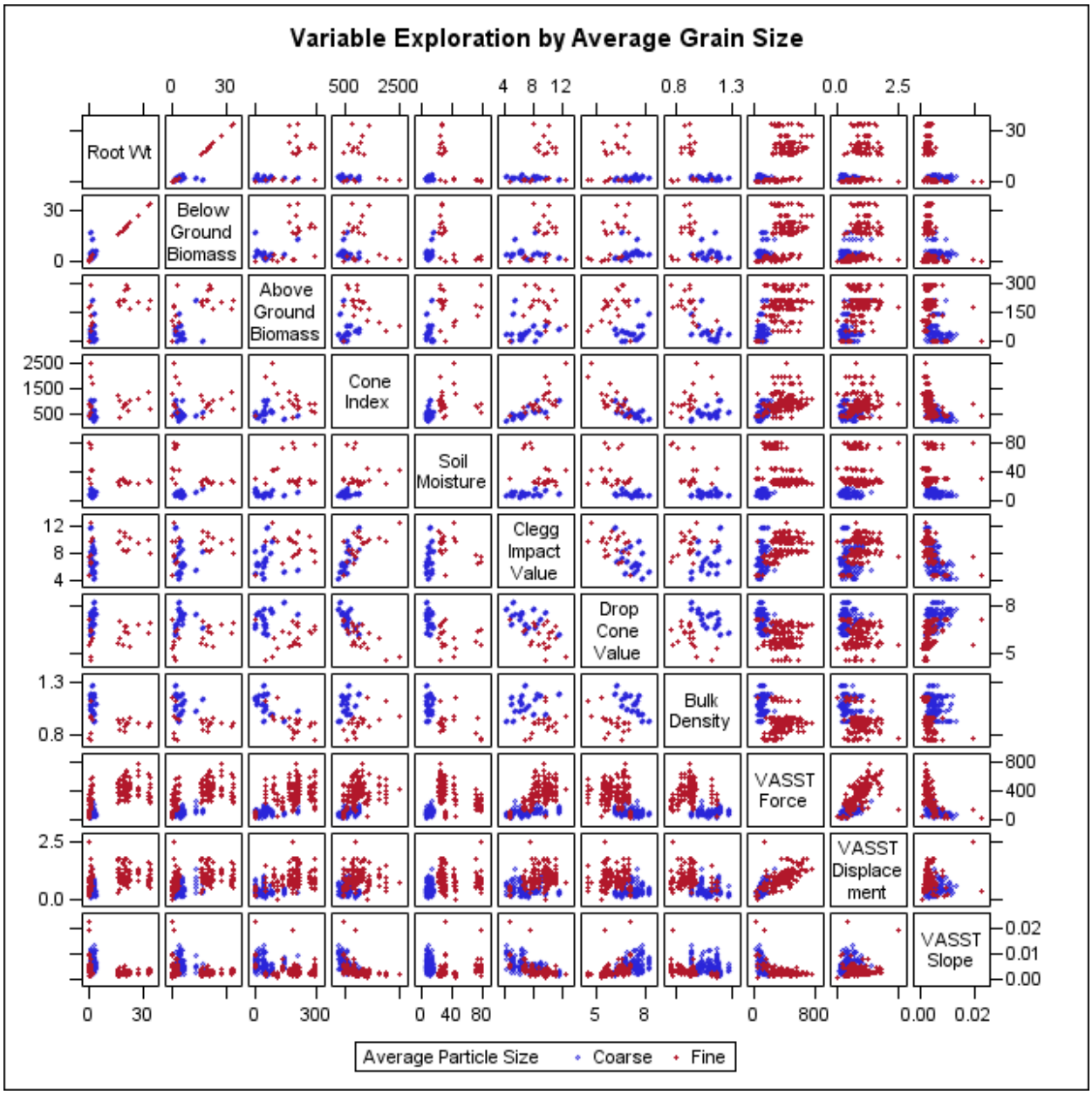

Figure C.3: Scatter plot matrix of variables by USCS

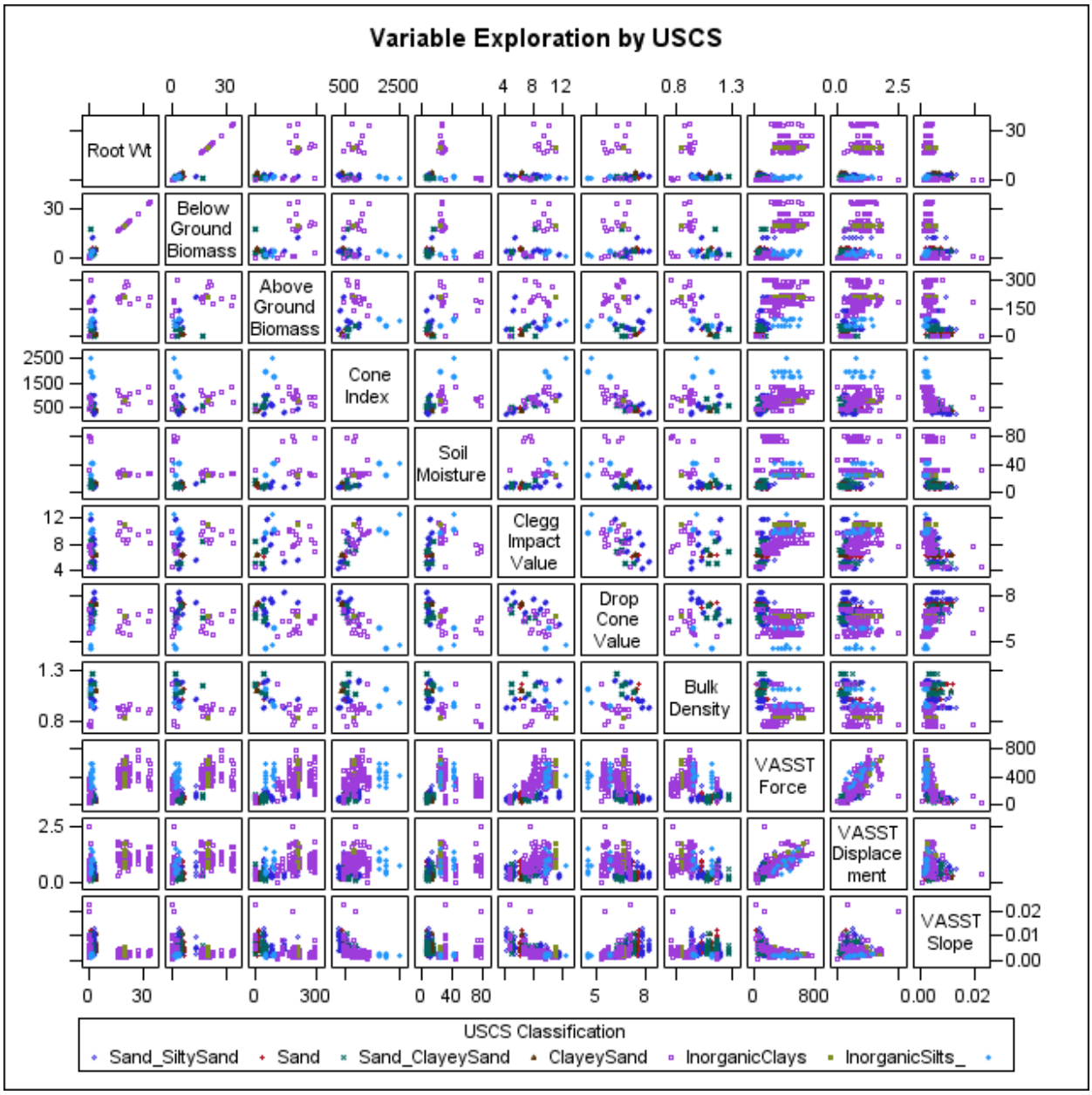

Figure C.4: Scatter plot matrix of variables by USDA texture

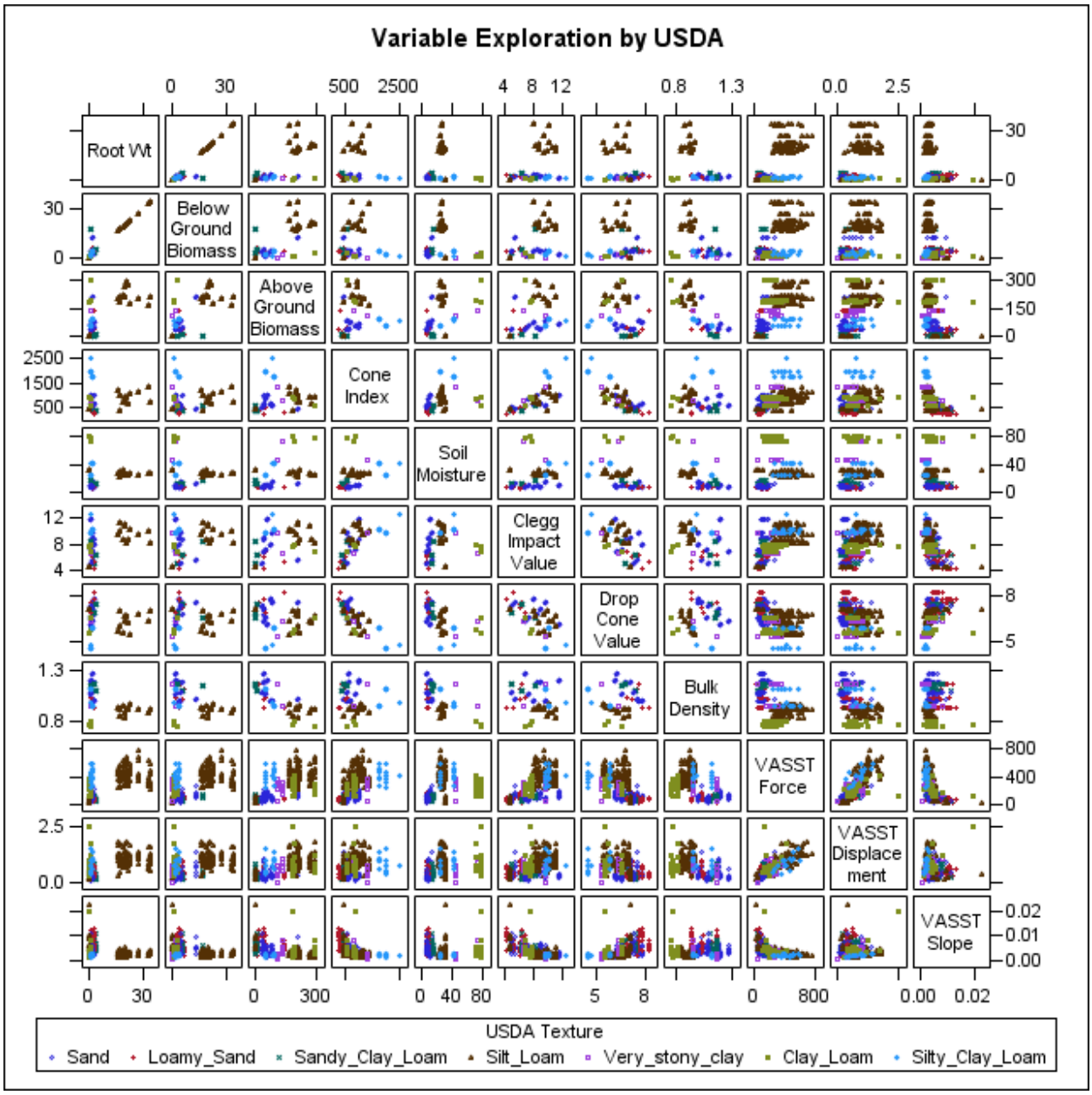

APPENDIX D: PROC SGPANEL RESULTS FOR CLASS VARIABLES

Figure D.1: Box plots of VASST force measurements by plasticity

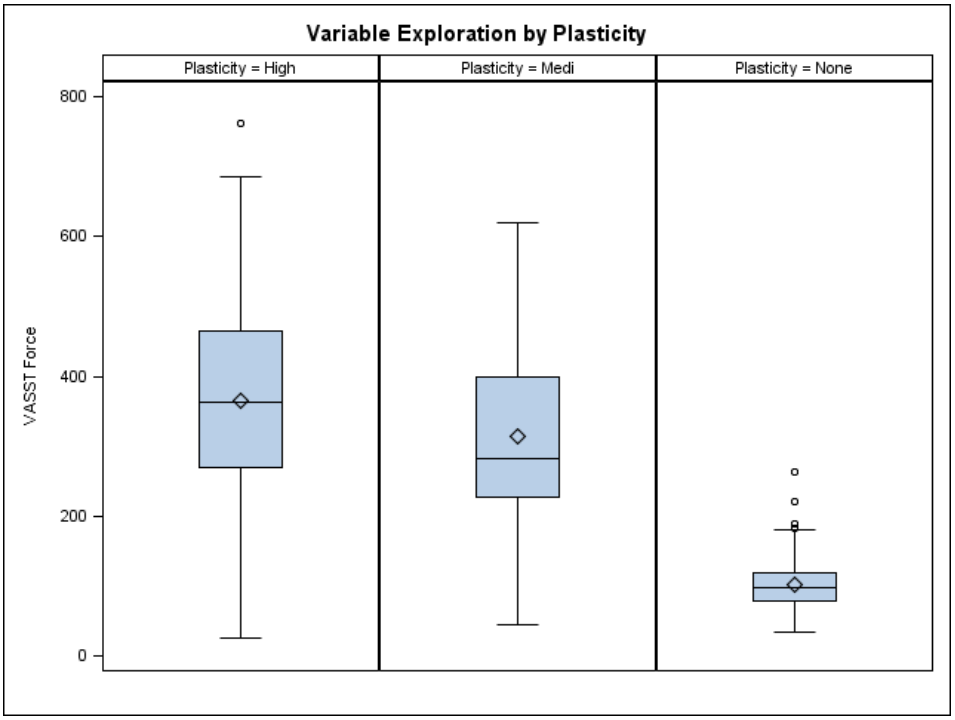

Figure D.2: Box plots of VASST force measurements by USCS

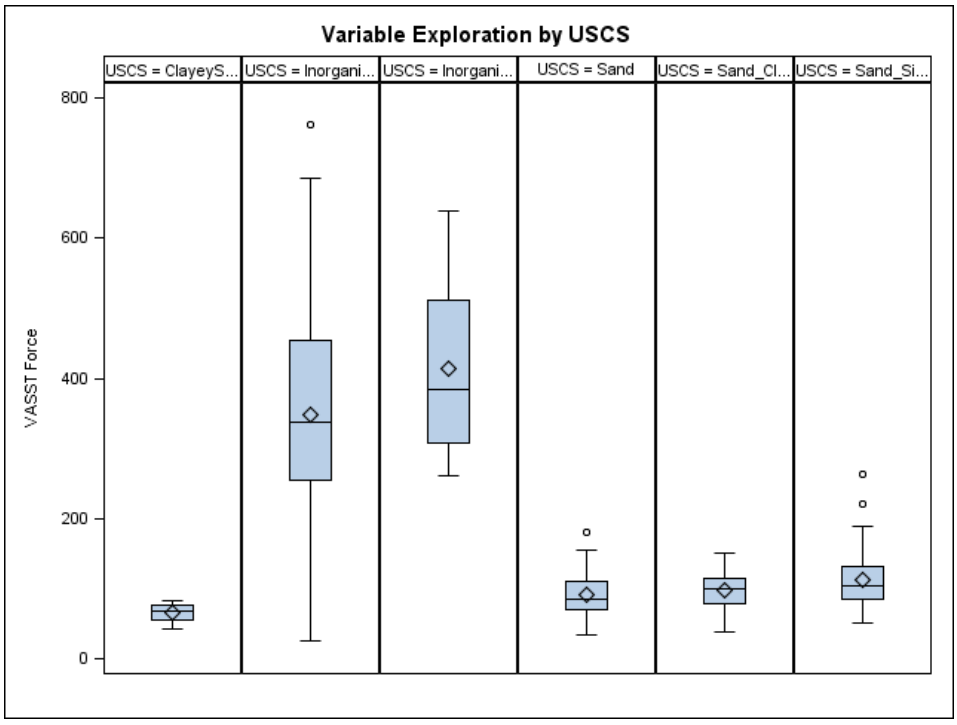

Figure D.3: Box plots of VASST force measurements by average grain size

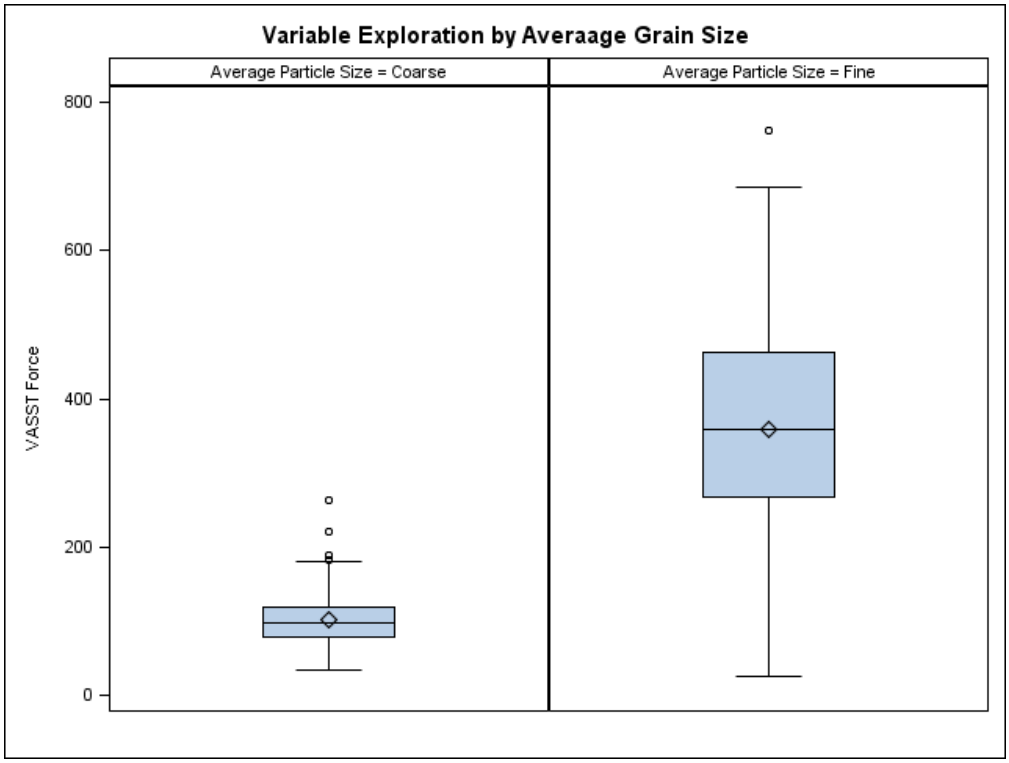

Figure D.4: Box plots of VASST force measurements by USDA texture

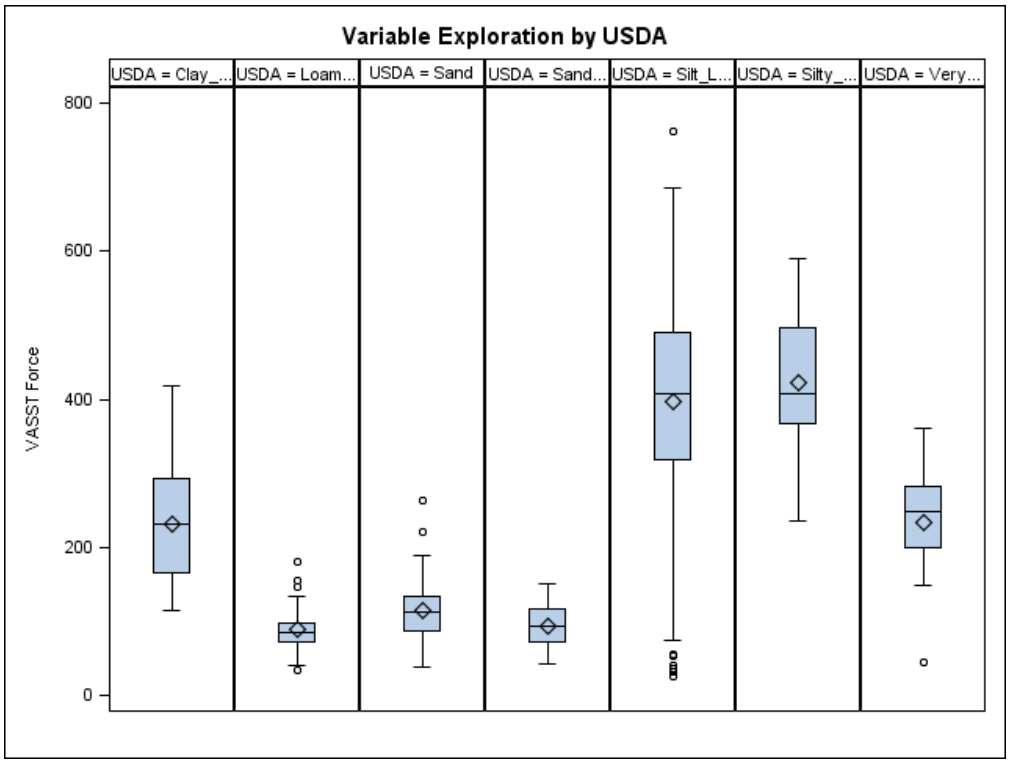

APPENDIX E: PROC CORR RESULTS

Figure E.1: Proc corr results for high plasticity soils

Correlation Ranks

The CORR Procedure

Plasticity=High

10 Variables:	Root_Wt BGBio AGBio pena tdra clegga dca VM VD VS

Simple Statistics

Variable	N	Mean	Std Dev	Sum	Minimum	Maximum	Label
Root_Wt	137	14.64584	11.67344	2006	0	34.06000	Root Wt
BGBio	137	15.04774	11.21913	2062	0	34.06000	Below Ground Biomass
AGBio	137	188.48752	79.48922	25823	0	294.55000	Above Ground Biomass
pena	137	968.87672	418.68487	132736	407.13333	2492	Cone Index
tdra	137	36.44124	19.65846	4992	22.38000	78.58000	Soil Moisture
clegga	137	9.02355	1.73903	1236	4.66667	12.60000	Clegg Impact Value
dca	137	6.21109	0.66610	850.91889	4.50000	7.10000	Drop Cone Value
VM	137	364.58456	153.58126	49948	25.44448	762.74548	VASST Force
VD	137	0.93802	0.38086	128.50816	0.14355	2.48843	VASST Displacement
VS	137	0.00345	0.00260	0.47218	0.00121	0.02260	VASST Slope

Pearson Correlation Coefficients, N = 137
Prob > |r| under H0: Rho=0

	Root_Wt	BGBio	AGBio	pena	tdra	clegga	dca	VM	VD	VS
Root_Wt	1.00000	0.99884	0.39707	-0.06438	-0.64608	0.43327	0.34423	0.46335	0.33343	-0.30529
Root Wt		<.0001	<.0001	0.4548	<.0001	<.0001	<.0001	<.0001	<.0001	0.0003
BGBio	0.99884	1.00000	0.40137	-0.04139	-0.63728	0.44464	0.33511	0.47282	0.33847	-0.31746
Below Ground Biomass	<.0001		<.0001	0.6311	<.0001	<.0001	<.0001	<.0001	<.0001	0.0002
AGBio	0.39707	0.40137	1.00000	-0.35537	0.14462	0.18402	0.22942	0.27007	0.27726	-0.26869
Above Ground Biomass	<.0001	<.0001		<.0001	0.0918	0.0314	0.0070	0.0014	0.0010	0.0015
pena	-0.06438	-0.04139	-0.35537	1.00000	-0.19562	0.53265	-0.71347	0.36404	0.11019	-0.34154
Cone Index	0.4548	0.6311	<.0001		0.0220	<.0001	<.0001	<.0001	0.1999	<.0001
tdra	-0.64608	-0.63728	0.14462	-0.19562	1.00000	-0.45243	-0.14461	-0.44329	-0.18615	0.23300
Soil Moisture	<.0001	<.0001	0.0918	0.0220		<.0001	0.0918	<.0001	0.0294	0.0061
clegga	0.43327	0.44464	0.18402	0.53265	-0.45243	1.00000	-0.34005	0.61013	0.37794	-0.52961
Clegg Impact Value	<.0001	<.0001	0.0314	<.0001	<.0001		<.0001	<.0001	<.0001	<.0001
dca	0.34423	0.33511	0.22942	-0.71347	-0.14461	-0.34005	1.00000	-0.13593	-0.02912	0.22132
Drop Cone Value	<.0001	<.0001	0.0070	<.0001	0.0918	<.0001		0.1132	0.7355	0.0093
VM	0.46335	0.47282	0.27007	0.36404	-0.44329	0.61013	-0.13593	1.00000	0.65881	-0.53512
VASST Force	<.0001	<.0001	0.0014	<.0001	<.0001	<.0001	0.1132		<.0001	<.0001
VD	0.33343	0.33847	0.27726	0.11019	-0.18615	0.37794	-0.02912	0.65881	1.00000	0.00532
VASST Displacement	<.0001	<.0001	0.0010	0.1999	0.0294	<.0001	0.7355	<.0001		0.9508
VS	-0.30529	-0.31746	-0.26869	-0.34154	0.23300	-0.52961	0.22132	-0.53512	0.00532	1.00000
VASST Slope	0.0003	0.0002	0.0015	<.0001	0.0061	<.0001	0.0093	<.0001	0.9508	

Figure E.2: Proc corr results for medium plasticity soils

Plasticity=Medi

10 Variables:	Root_Wt BGBio AGBio pena tdra clegga dca VM VD VS

Simple Statistics

Variable	N	Mean	Std Dev	Sum	Minimum	Maximum	Label
Root_Wt	14	9.65500	9.18927	135.17000	0.80000	18.51000	Root Wt
BGBio	21	6.87333	8.47764	144.34000	0	18.51000	Below Ground Biomass
AGBio	21	152.34667	47.46018	3199	105.38000	215.37000	Above Ground Biomass
pena	21	950.39118	256.37419	19958	755.53333	1304	Cone Index
tdra	21	49.49333	17.70971	1039	31.04000	72.60000	Soil Moisture
clegga	21	8.31556	1.36262	174.62667	6.54000	9.74000	Clegg Impact Value
dca	21	5.72593	0.47094	120.24444	5.31111	6.36667	Drop Cone Value
VM	21	314.49321	141.49687	6604	45.29912	618.88519	VASST Force
VD	21	0.80368	0.38136	16.87723	0.01914	1.59924	VASST Displacement
VS	21	0.00324	0.00162	0.06794	0.0007916	0.00826	VASST Slope

Pearson Correlation Coefficients
Prob > |r| under H0: Rho=0
Number of Observations

	Root_Wt	BGBio	AGBio	pena	tdra	clegga	dca	VM	VD	VS
Root_Wt	1.00000	1.00000	1.00000	-1.00000	-1.00000	1.00000	-1.00000	0.88220	0.45730	-0.58646
Root Wt		<.0001	<.0001	<.0001	<.0001	<.0001	<.0001	<.0001	0.1002	0.0275
	14	14	14	14	14	14	14	14	14	14
BGBio	1.00000	1.00000	0.98531	-0.63462	-0.68262	0.08340	-0.24809	0.81168	0.62563	-0.04753
Below Ground Biomass	<.0001		<.0001	0.0020	0.0007	0.7193	0.2782	<.0001	0.0024	0.8379
	14	21	21	21	21	21	21	21	21	21
AGBio	1.00000	0.98531	1.00000	-0.75729	-0.54778	-0.08802	-0.07899	0.77059	0.67622	0.07778
Above Ground Biomass	<.0001	<.0001		<.0001	0.0102	0.7044	0.7336	<.0001	0.0008	0.7376
	14	21	21	21	21	21	21	21	21	21
pena	-1.00000	-0.63462	-0.75729	1.00000	-0.13156	0.71720	-0.59122	-0.38311	-0.66759	-0.53367
Cone Index	<.0001	0.0020	<.0001		0.5697	0.0003	0.0048	0.0865	0.0009	0.0127
	14	21	21	21	21	21	21	21	21	21
tdra	-1.00000	-0.68262	-0.54778	-0.13156	1.00000	-0.78516	0.87728	-0.67889	-0.17123	0.56560
Soil Moisture	<.0001	0.0007	0.0102	0.5697		<.0001	<.0001	0.0007	0.4580	0.0075
	14	21	21	21	21	21	21	21	21	21
clegga	1.00000	0.08340	-0.08802	0.71720	-0.78516	1.00000	-0.98605	0.23790	-0.29669	-0.73099
Clegg Impact Value	<.0001	0.7193	0.7044	0.0003	<.0001		<.0001	0.2991	0.1916	0.0002
	14	21	21	21	21	21	21	21	21	21
dca	-1.00000	-0.24809	-0.07899	-0.59122	0.87728	-0.98605	1.00000	-0.36683	0.18393	0.71855
Drop Cone Value	<.0001	0.2782	0.7336	0.0048	<.0001	<.0001		0.1019	0.4248	0.0002
	14	21	21	21	21	21	21	21	21	21
VM	0.88220	0.81168	0.77059	-0.38311	-0.67889	0.23790	-0.36683	1.00000	0.71416	-0.17620
VASST Force	<.0001	<.0001	<.0001	0.0865	0.0007	0.2991	0.1019		0.0003	0.4449
	14	21	21	21	21	21	21	21	21	21
VD	0.45730	0.62563	0.67622	-0.66759	-0.17123	-0.29669	0.18393	0.71416	1.00000	0.49519
VASST Displacement	0.1002	0.0024	0.0008	0.0009	0.4580	0.1916	0.4248	0.0003		0.0225
	14	21	21	21	21	21	21	21	21	21
VS	-0.58646	-0.04753	0.07778	-0.53367	0.56560	-0.73099	0.71855	-0.17620	0.49519	1.00000
VASST Slope	0.0275	0.8379	0.7376	0.0127	0.0075	0.0002	0.0002	0.4449	0.0225	
	14	21	21	21	21	21	21	21	21	21

Figure E.2: Proc corr results for non-plastic soils

Correlation Ranks

The CORR Procedure

Plasticity=None

10 Variables:	Root_Wt BGBio AGBio pena tdra clegga dca VM VD VS

Simple Statistics

Variable	N	Mean	Std Dev	Sum	Minimum	Maximum	Label
Root_Wt	141	1.90035	0.85118	267.95000	0.72000	3.77000	Root Wt
BGBio	141	4.83184	3.48111	681.29000	1.56000	17.18000	Below Ground Biomass
AGBio	141	50.45716	46.48222	7114	3.44000	207.31000	Above Ground Biomass
pena	141	551.36701	206.99713	77743	240.48148	1020	Cone Index
tdra	141	9.46149	2.79181	1334	5.72000	16.20000	Soil Moisture
clegga	141	7.03660	1.92896	992.16000	4.26000	11.70000	Clegg Impact Value
dca	141	7.20050	0.57107	1015	6.12222	8.26000	Drop Cone Value
VM	141	101.51909	36.22187	14314	34.23823	264.04364	VASST Force
VD	141	0.40446	0.21668	57.02937	0.10881	1.35604	VASST Displacement
VS	141	0.00536	0.00239	0.75548	0.00163	0.01328	VASST Slope

Pearson Correlation Coefficients, N = 141
Prob > |r| under H0: Rho=0

	Root_Wt	BGBio	AGBio	pena	tdra	clegga	dca	VM	VD	VS
Root_Wt	1.00000	0.07054	-0.00236	-0.41202	0.07037	-0.30065	0.53439	-0.08820	0.11025	0.22488
Root Wt		0.4058	0.9778	<.0001	0.4070	0.0003	<.0001	0.2983	0.1931	0.0073
BGBio	0.07054	1.00000	0.14906	-0.23621	0.43968	-0.10704	0.14813	0.20038	0.26429	-0.00500
Below Ground Biomass	0.4058		0.0777	0.0048	<.0001	0.2065	0.0796	0.0172	0.0015	0.9530
AGBio	-0.00236	0.14906	1.00000	0.01736	0.08782	0.02247	0.31481	0.27103	0.17576	-0.11389
Above Ground Biomass	0.9778	0.0777		0.8381	0.3004	0.7914	0.0001	0.0012	0.0371	0.1787
pena	-0.41202	-0.23621	0.01736	1.00000	0.14679	0.80363	-0.70742	0.36664	-0.17030	-0.57428
Cone Index	<.0001	0.0048	0.8381		0.0824	<.0001	<.0001	<.0001	0.0435	<.0001
tdra	0.07037	0.43968	0.08782	0.14679	1.00000	0.31074	-0.24717	0.08941	-0.03821	-0.15092
Soil Moisture	0.4070	<.0001	0.3004	0.0824		0.0002	0.0031	0.2917	0.6528	0.0740
clegga	-0.30065	-0.10704	0.02247	0.80363	0.31074	1.00000	-0.50902	0.31113	-0.15387	-0.55672
Clegg Impact Value	0.0003	0.2065	0.7914	<.0001	0.0002		<.0001	0.0002	0.0685	<.0001
dca	0.53439	0.14813	0.31481	-0.70742	-0.24717	-0.50902	1.00000	-0.26520	0.12504	0.36949
Drop Cone Value	<.0001	0.0796	0.0001	<.0001	0.0031	<.0001		0.0015	0.1396	<.0001
VM	-0.08820	0.20038	0.27103	0.36664	0.08941	0.31113	-0.26520	1.00000	0.59394	-0.35969
VASST Force	0.2983	0.0172	0.0012	<.0001	0.2917	0.0002	0.0015		<.0001	<.0001
VD	0.11025	0.26429	0.17576	-0.17030	-0.03821	-0.15387	0.12504	0.59394	1.00000	0.37452
VASST Displacement	0.1931	0.0015	0.0371	0.0435	0.6528	0.0685	0.1396	<.0001		<.0001
VS	0.22488	-0.00500	-0.11389	-0.57428	-0.15092	-0.55672	0.36949	-0.35969	0.37452	1.00000
VASST Slope	0.0073	0.9530	0.1787	<.0001	0.0740	<.0001	<.0001	<.0001	<.0001	

APPENDIX F: PROC LIFETEST RESULTS WITH BULK DENSITY

Figure F.1: Proc lifetest results for high plasticity soils

Parameters Affecting VASST Force Measurements with Bulk Density

The LIFETEST Procedure
Plasticity=High

Quartile Estimates				
Percent	**Point Estimate**	**95% Confidence Interval**		
		Transform	**[Lower**	**Upper)**
75	465.132	LOGLOG	443.079	494.536
50	362.699	LOGLOG	333.501	400.965
25	270.364	LOGLOG	237.250	292.142

Mean	**Standard Error**
364.585	13.121

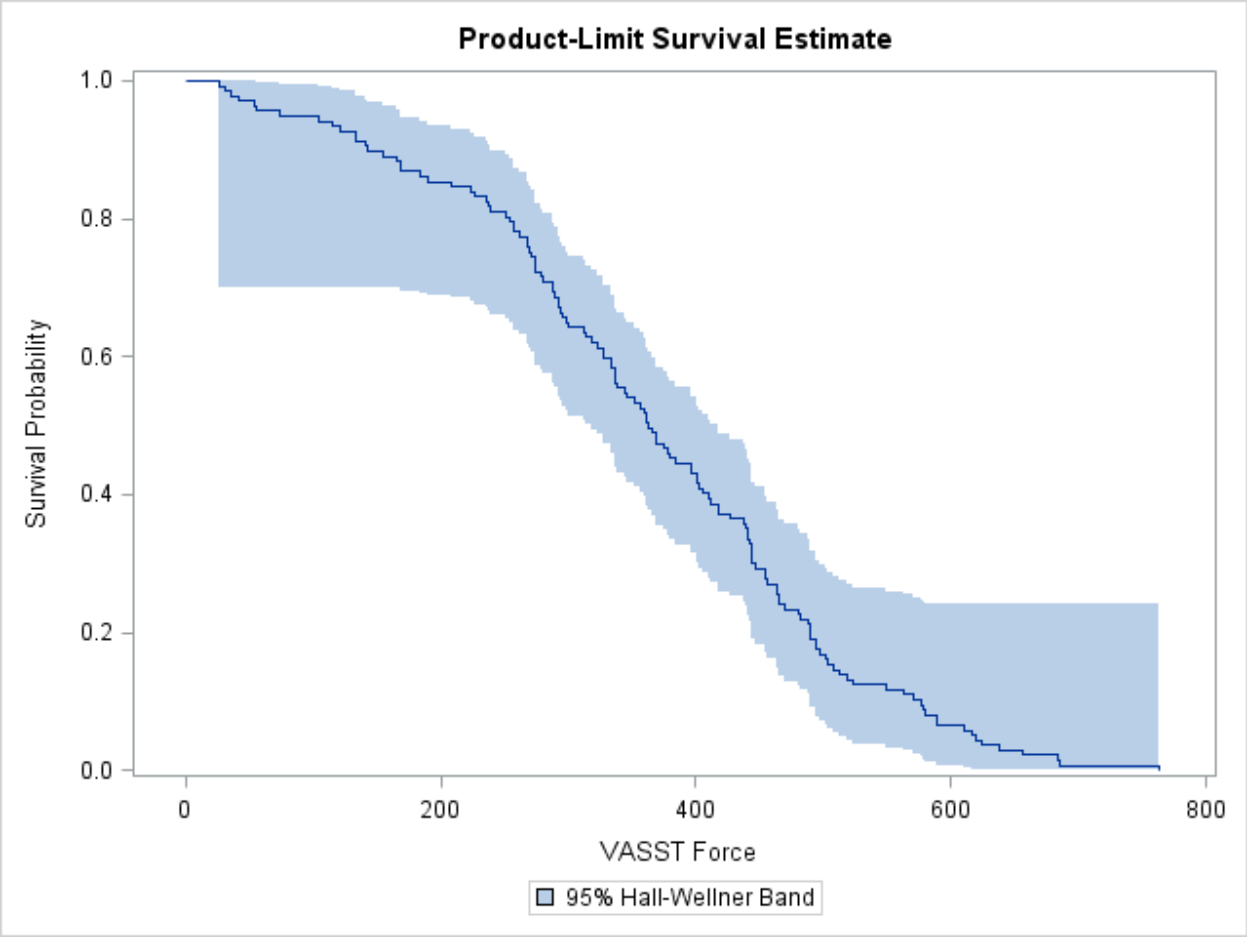

Figure F.1 (cont.)

Summary of the Number of Censored and Uncensored Values			
Total	**Failed**	**Censored**	**Percent Censored**
137	137	0	0.00

Rank Tests for the Association of VM with Covariates

Univariate Chi-Squares for the Wilcoxon Test					
Variable	**Test Statistic**	**Standard Error**	**Chi-Square**	**Pr > Chi-Square**	**Label**
Root_Wt	-53.7449	54.6642	0.9666	0.3255	Root Wt
BGBio	-51.9384	51.5964	1.0133	0.3141	Below Ground Biomass
AGBio	222.8	375.6	0.3519	0.5530	Above Ground Biomass
tdra	8.1571	28.9164	0.0796	0.7779	Soil Moisture
D30	0.00308	0.00337	0.8373	0.3602	30% Finer Diameter
D60	0.00668	0.0248	0.0725	0.7878	60% Finer Diameter
Bulk_Den	0.2237	0.3722	0.3611	0.5479	Bulk Density

Covariance Matrix for the Wilcoxon Statistics							
Variable	**Root_Wt**	**BGBio**	**AGBio**	**tdra**	**D30**	**D60**	**Bulk_Den**
Root_Wt	2988	2817	12491	-720	0	-1	-12
BGBio	2817	2662	11368	-637	0	-1	-11
AGBio	12491	11368	141070	-4706	0	-8	-89
tdra	-720	-637	-4706	836	-0	0	-0
D30	0	0	0	-0	0	-0	-0
D60	-1	-1	-8	0	-0	0	0
Bulk_Den	-12	-11	-89	-0	-0	0	0

Forward Stepwise Sequence of Chi-Squares for the Wilcoxon Test						
Variable	**DF**	**Chi-Square**	**Pr > Chi-Square**	**Chi-Square Increment**	**Pr > Increment**	**Label**
BGBio	1	1.0133	0.3141	1.0133	0.3141	Below Ground Biomass
D30	2	4.6885	0.0959	3.6752	0.0552	30% Finer Diameter
AGBio	3	6.8543	0.0767	2.1658	0.1411	Above Ground Biomass
Bulk_Den	4	8.7306	0.0682	1.8763	0.1708	Bulk Density
tdra	5	10.4986	0.0623	1.7679	0.1836	Soil Moisture
D60	6	12.9960	0.0431	2.4975	0.1140	60% Finer Diameter
Root_Wt	7	15.3887	0.0313	2.3926	0.1219	Root Wt

Figure F.1 (cont.)

Univariate Chi-Squares for the Log-Rank Test					
Variable	**Test Statistic**	**Standard Error**	**Chi-Square**	**Pr > Chi-Square**	**Label**
Root_Wt	7.1488	86.4994	0.00683	0.9341	Root Wt
BGBio	6.3140	81.0656	0.00607	0.9379	Below Ground Biomass
AGBio	708.8	639.2	1.2294	0.2675	Above Ground Biomass
tdra	-14.6230	49.0493	0.0889	0.7656	Soil Moisture
D30	0.00562	0.00533	1.1112	0.2918	30% Finer Diameter
D60	-0.0188	0.0407	0.2130	0.6445	60% Finer Diameter
Bulk_Den	0.00897	0.5508	0.000265	0.9870	Bulk Density

Covariance Matrix for the Log-Rank Statistics							
Variable	**Root_Wt**	**BGBio**	**AGBio**	**tdra**	**D30**	**D60**	**Bulk_Den**
Root_Wt	7482	7003	29845	-2335	0	-3	-24
BGBio	7003	6572	26674	-2060	0	-3	-22
AGBio	29845	26674	408601	-15225	1	-21	-194
tdra	-2335	-2060	-15225	2406	-0	1	1
D30	0	0	1	-0	0	-0	-0
D60	-3	-3	-21	1	-0	0	0
Bulk_Den	-24	-22	-194	1	-0	0	0

Forward Stepwise Sequence of Chi-Squares for the Log-Rank Test						
Variable	**DF**	**Chi-Square**	**Pr > Chi-Square**	**Chi-Square Increment**	**Pr > Increment**	**Label**
AGBio	1	1.2294	0.2675	1.2294	0.2675	Above Ground Biomass
Bulk_Den	2	1.7946	0.4077	0.5651	0.4522	Bulk Density
D30	3	2.7940	0.4245	0.9994	0.3174	30% Finer Diameter
tdra	4	3.7499	0.4409	0.9559	0.3282	Soil Moisture
Root_Wt	5	4.0505	0.5422	0.3006	0.5835	Root Wt
BGBio	6	4.6895	0.5842	0.6389	0.4241	Below Ground Biomass
D60	7	7.5412	0.3748	2.8518	0.0913	60% Finer Diameter

Figure F.2: Proc lifetest results for non-plastic soils

Parameters Affecting VASST Force Measurements with Bulk Density

The LIFETEST Procedure
Plasticity=None

Quartile Estimates				
Percent	**Point Estimate**	**95% Confidence Interval**		
		Transform	**[Lower**	**Upper)**
75	119.771	LOGLOG	112.489	131.656
50	96.688	LOGLOG	89.337	102.871
25	77.863	LOGLOG	72.505	82.466

Mean	**Standard Error**
101.519	3.050

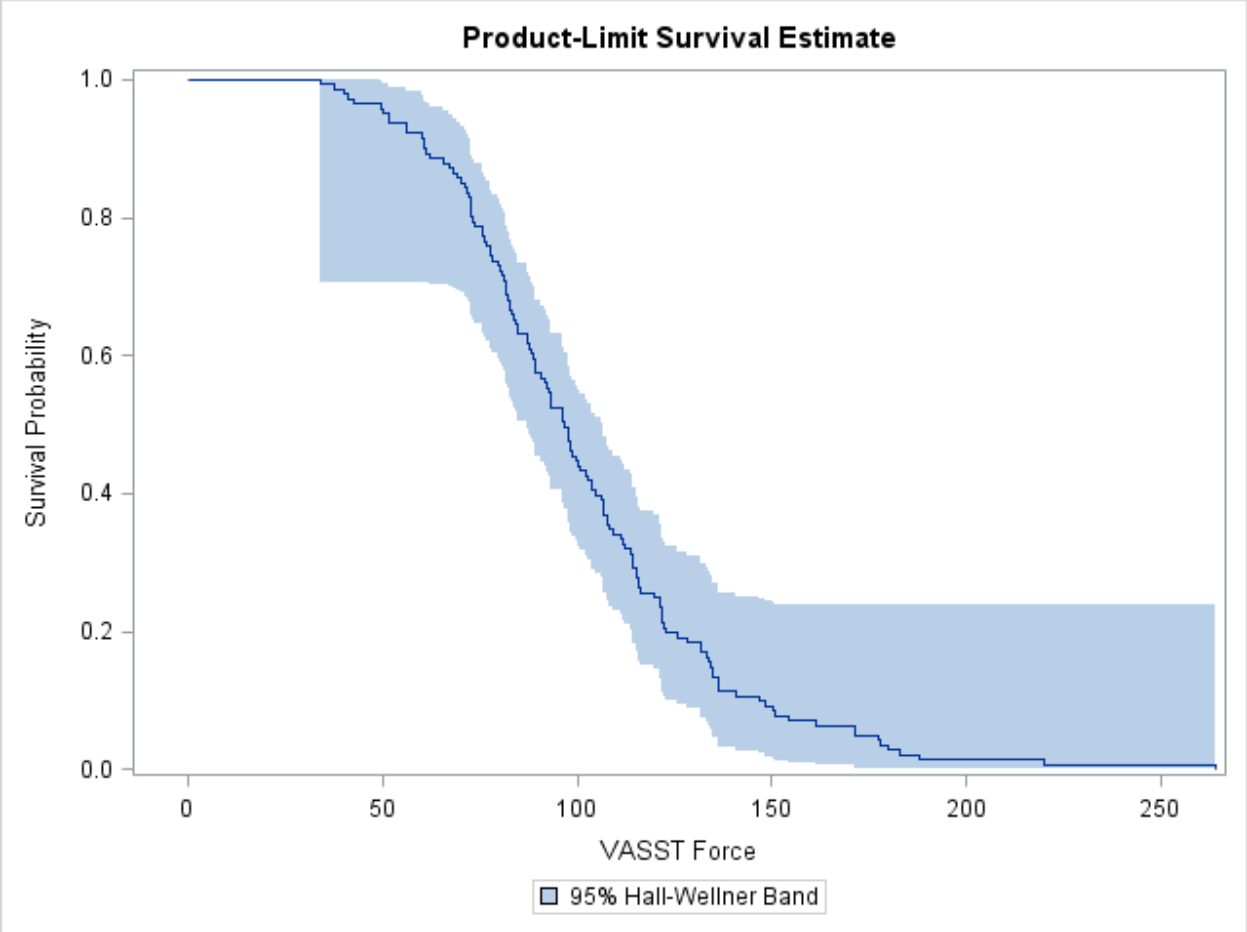

Figure F.2 (cont.)

Summary of the Number of Censored and Uncensored Values			
Total	**Failed**	**Censored**	**Percent Censored**
141	141	0	0.00

Rank Tests for the Association of VM with Covariates

Univariate Chi-Squares for the Wilcoxon Test					
Variable	**Test Statistic**	**Standard Error**	**Chi-Square**	**Pr > Chi-Square**	**Label**
Root_Wt	-6.1632	5.6791	1.1778	0.2778	Root Wt
BGBio	53.5098	23.5356	5.1691	0.0230	Below Ground Biomass
AGBio	803.5	303.5	7.0119	0.0081	Above Ground Biomass
tdra	16.9234	19.1138	0.7839	0.3759	Soil Moisture
D30	-0.7363	0.2442	9.0908	0.0026	30% Finer Diameter
D60	-2.2581	0.5646	15.9968	<.0001	60% Finer Diameter
Bulk_Den	1.3187	0.6430	4.2058	0.0403	Bulk Density

Covariance Matrix for the Wilcoxon Statistics							
Variable	**Root_Wt**	**BGBio**	**AGBio**	**tdra**	**D30**	**D60**	**Bulk_Den**
Root_Wt	32.3	7.5	95.2	1.3	-0.3	-1.6	-1.1
BGBio	7.5	553.9	390.1	189.9	-0.2	-1.2	-0.8
AGBio	95.2	390.1	92084.7	55.1	1.9	10.0	-101.0
tdra	1.3	189.9	55.1	365.3	-2.6	-2.3	0.8
D30	-0.3	-0.2	1.9	-2.6	0.1	0.1	-0.0
D60	-1.6	-1.2	10.0	-2.3	0.1	0.3	0.0
Bulk_Den	-1.1	-0.8	-101.0	0.8	-0.0	0.0	0.4

Forward Stepwise Sequence of Chi-Squares for the Wilcoxon Test						
Variable	**DF**	**Chi-Square**	**Pr > Chi-Square**	**Chi-Square Increment**	**Pr > Increment**	**Label**
D60	1	15.9968	<.0001	15.9968	<.0001	60% Finer Diameter
Root_Wt	2	28.5321	<.0001	12.5353	0.0004	Root Wt
AGBio	3	39.0752	<.0001	10.5431	0.0012	Above Ground Biomass
Bulk_Den	4	50.2210	<.0001	11.1458	0.0008	Bulk Density
BGBio	5	53.5116	<.0001	3.2906	0.0697	Below Ground Biomass
tdra	6	56.0864	<.0001	2.5748	0.1086	Soil Moisture
D30	7	57.0377	<.0001	0.9513	0.3294	30% Finer Diameter

Figure F.2 (cont.)

Univariate Chi-Squares for the Log-Rank Test					
Variable	**Test Statistic**	**Standard Error**	**Chi-Square**	**Pr > Chi-Square**	**Label**
Root_Wt	-11.2311	8.4415	1.7701	0.1834	Root Wt
BGBio	100.2	50.1127	3.9960	0.0456	Below Ground Biomass
AGBio	1660.0	640.9	6.7094	0.0096	Above Ground Biomass
tdra	32.3441	33.1856	0.9499	0.3297	Soil Moisture
D30	-0.9282	0.4109	5.1039	0.0239	30% Finer Diameter
D60	-3.1869	1.1036	8.3392	0.0039	60% Finer Diameter
Bulk_Den	2.2561	1.0548	4.5753	0.0324	Bulk Density

Covariance Matrix for the Log-Rank Statistics							
Variable	**Root_Wt**	**BGBio**	**AGBio**	**tdra**	**D30**	**D60**	**Bulk_Den**
Root_Wt	71	7	186	-41	-0	-4	-3
BGBio	7	2511	10403	973	1	5	-14
AGBio	186	10403	410732	4470	47	158	-331
tdra	-41	973	4470	1101	-7	-3	3
D30	-0	1	47	-7	0	0	-0
D60	-4	5	158	-3	0	1	-0
Bulk_Den	-3	-14	-331	3	-0	-0	1

Forward Stepwise Sequence of Chi-Squares for the Log-Rank Test						
Variable	**DF**	**Chi-Square**	**Pr > Chi-Square**	**Chi-Square Increment**	**Pr > Increment**	**Label**
D60	1	8.3392	0.0039	8.3392	0.0039	60% Finer Diameter
AGBio	2	19.3436	<.0001	11.0045	0.0009	Above Ground Biomass
Bulk_Den	3	34.6927	<.0001	15.3491	<.0001	Bulk Density
Root_Wt	4	38.8941	<.0001	4.2014	0.0404	Root Wt
D30	5	42.0333	<.0001	3.1392	0.0764	30% Finer Diameter
BGBio	6	45.7060	<.0001	3.6727	0.0553	Below Ground Biomass
tdra	7	51.1677	<.0001	5.4617	0.0194	Soil Moisture

APPENDIX G: PROC LIFETEST RESULTS WITHOUT BULK DENSITY

Figure G.1: Proc lifetest results for high plasticity soils

Parameters Affecting VASST Force Measurements without Bulk Density

The LIFETEST Procedure
Plasticity=High

Quartile Estimates				
Percent	**Point Estimate**	**95% Confidence Interval**		
		Transform	**[Lower**	**Upper)**
75	465.132	LOGLOG	443.079	494.536
50	362.699	LOGLOG	333.501	400.965
25	270.364	LOGLOG	237.250	292.142

Mean	**Standard Error**
364.585	13.121

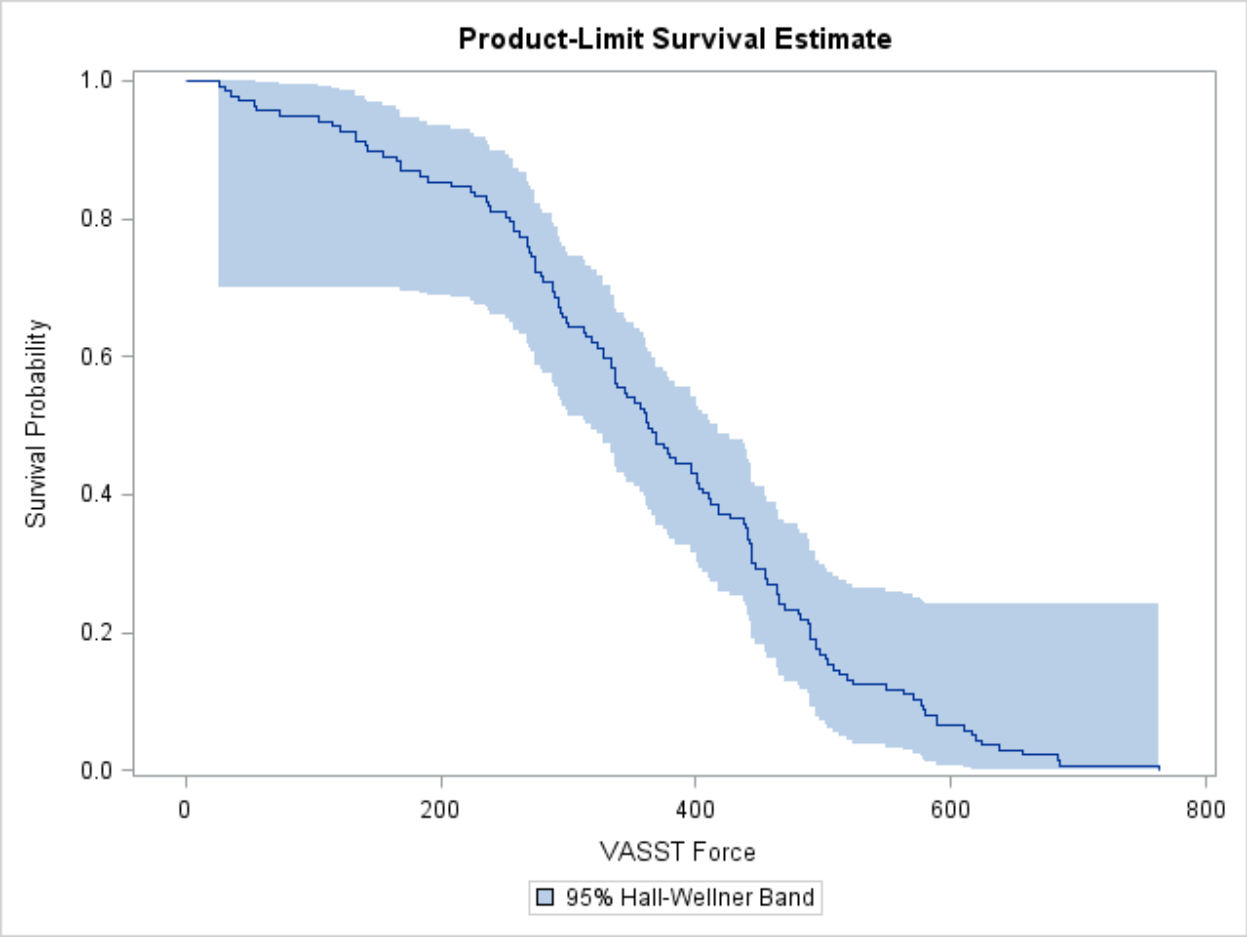

Figure G.1 (cont.)

Summary of the Number of Censored and Uncensored Values			
Total	**Failed**	**Censored**	**Percent Censored**
137	137	0	0.00

Rank Tests for the Association of VM with Covariates

Univariate Chi-Squares for the Wilcoxon Test					
Variable	**Test Statistic**	**Standard Error**	**Chi-Square**	**Pr > Chi-Square**	**Label**
Root_Wt	110.2	59.3923	3.4434	0.0635	Root Wt
BGBio	114.2	56.4720	4.0865	0.0432	Below Ground Biomass
AGBio	1805.6	417.6	18.6965	<.0001	Above Ground Biomass
tdra	-21.2920	29.3911	0.5248	0.4688	Soil Moisture
D30	-0.00119	0.00351	0.1144	0.7351	30% Finer Diameter
D60	0.0266	0.0255	1.0958	0.2952	60% Finer Diameter

Covariance Matrix for the Wilcoxon Statistics						
Variable	**Root_Wt**	**BGBio**	**AGBio**	**tdra**	**D30**	**D60**
Root_Wt	3527	3350	15745	-770	0	-1
BGBio	3350	3189	14600	-687	0	-1
AGBio	15745	14600	174377	-5214	0	-8
tdra	-770	-687	-5214	864	-0	0
D30	0	0	0	-0	0	-0
D60	-1	-1	-8	0	-0	0

Forward Stepwise Sequence of Chi-Squares for the Wilcoxon Test						
Variable	**DF**	**Chi-Square**	**Pr > Chi-Square**	**Chi-Square Increment**	**Pr > Increment**	**Label**
AGBio	1	18.6965	<.0001	18.6965	<.0001	Above Ground Biomass
D60	2	59.1087	<.0001	40.4121	<.0001	60% Finer Diameter
Root_Wt	3	65.8502	<.0001	6.7415	0.0094	Root Wt
tdra	4	72.7190	<.0001	6.8688	0.0088	Soil Moisture
BGBio	5	72.7771	<.0001	0.0580	0.8096	Below Ground Biomass
D30	6	72.7862	<.0001	0.00916	0.9237	30% Finer Diameter

Figure G.1 (cont.)

Univariate Chi-Squares for the Log-Rank Test					
Variable	**Test Statistic**	**Standard Error**	**Chi-Square**	**Pr > Chi-Square**	**Label**
Root_Wt	174.3	91.6831	3.6160	0.0572	Root Wt
BGBio	175.9	86.1244	4.1715	0.0411	Below Ground Biomass
AGBio	2385.3	677.5	12.3943	0.0004	Above Ground Biomass
tdra	-44.7797	51.0505	0.7694	0.3804	Soil Moisture
D30	0.00140	0.00559	0.0628	0.8021	30% Finer Diameter
D60	0.00270	0.0425	0.00402	0.9494	60% Finer Diameter

Covariance Matrix for the Log-Rank Statistics						
Variable	**Root_Wt**	**BGBio**	**AGBio**	**tdra**	**D30**	**D60**
Root_Wt	8406	7885	34318	-2532	0	-3
BGBio	7885	7417	30891	-2238	0	-3
AGBio	34318	30891	459038	-16618	1	-23
tdra	-2532	-2238	-16618	2606	-0	2
D30	0	0	1	-0	0	-0
D60	-3	-3	-23	2	-0	0

Forward Stepwise Sequence of Chi-Squares for the Log-Rank Test						
Variable	**DF**	**Chi-Square**	**Pr > Chi-Square**	**Chi-Square Increment**	**Pr > Increment**	**Label**
AGBio	1	12.3943	0.0004	12.3943	0.0004	Above Ground Biomass
D60	2	33.5742	<.0001	21.1799	<.0001	60% Finer Diameter
Root_Wt	3	53.3908	<.0001	19.8166	<.0001	Root Wt
tdra	4	67.4105	<.0001	14.0197	0.0002	Soil Moisture
D30	5	69.4141	<.0001	2.0036	0.1569	30% Finer Diameter
BGBio	6	69.4332	<.0001	0.0191	0.8899	Below Ground Biomass

Figure G.2: Proc lifetest results for non-plastic soils

Parameters Affecting VASST Force Measurements without Bulk Density

The LIFETEST Procedure
Plasticity=None

Quartile Estimates				
Percent	**Point Estimate**	**95% Confidence Interval**		
		Transform	**[Lower**	**Upper)**
75	119.771	LOGLOG	112.489	131.656
50	96.688	LOGLOG	89.337	102.871
25	77.863	LOGLOG	72.505	82.466

Mean	**Standard Error**
101.519	3.050

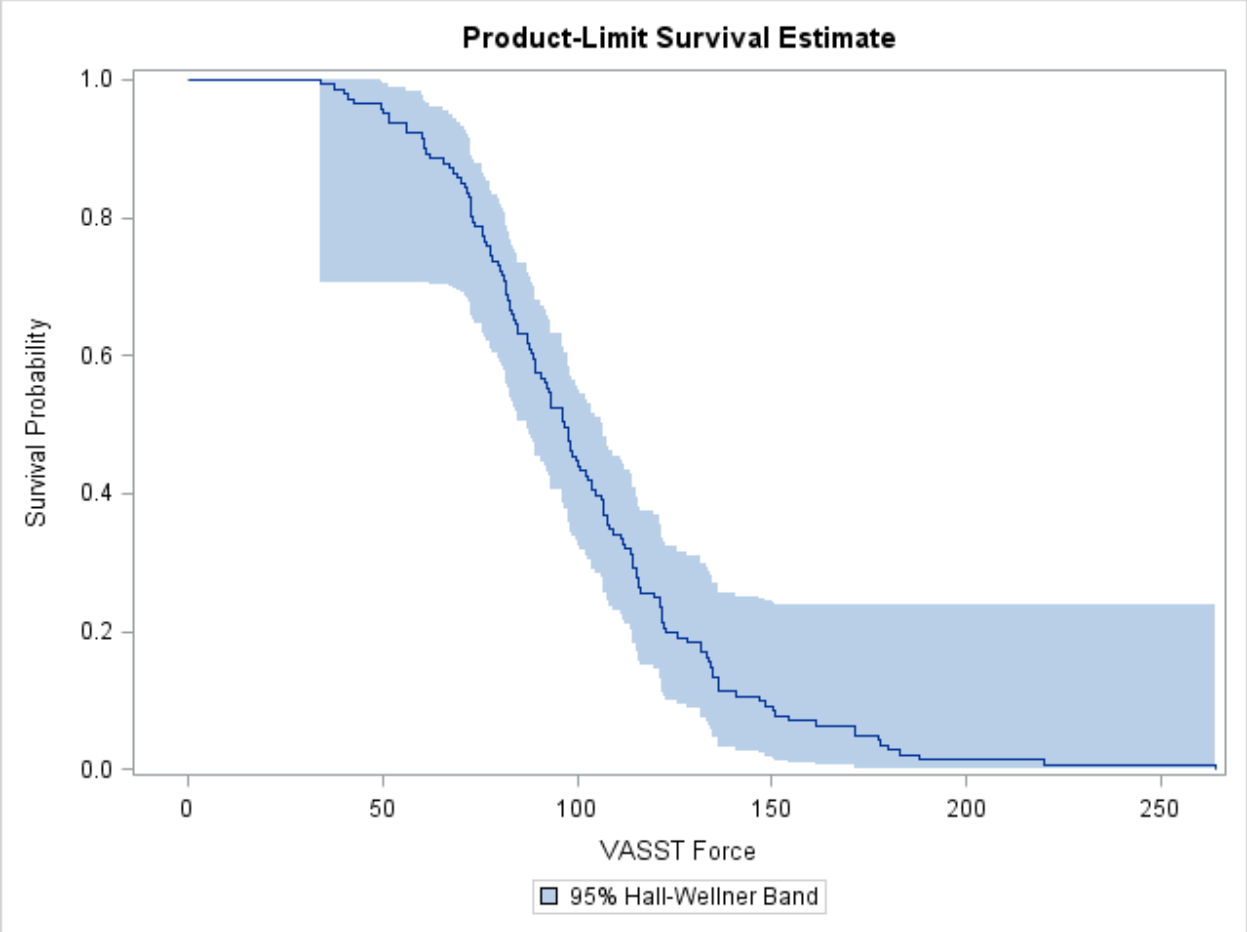

Figure G.2 (cont.)

Summary of the Number of Censored and Uncensored Values			
Total	**Failed**	**Censored**	**Percent Censored**
141	141	0	0.00

Rank Tests for the Association of VM with Covariates

Univariate Chi-Squares for the Wilcoxon Test					
Variable	**Test Statistic**	**Standard Error**	**Chi-Square**	**Pr > Chi-Square**	**Label**
Root_Wt	-6.1632	5.6791	1.1778	0.2778	Root Wt
BGBio	53.5098	23.5356	5.1691	0.0230	Below Ground Biomass
AGBio	803.5	303.5	7.0119	0.0081	Above Ground Biomass
tdra	16.9234	19.1138	0.7839	0.3759	Soil Moisture
D30	-0.7363	0.2442	9.0908	0.0026	30% Finer Diameter
D60	-2.2581	0.5646	15.9968	<.0001	60% Finer Diameter

Covariance Matrix for the Wilcoxon Statistics						
Variable	**Root_Wt**	**BGBio**	**AGBio**	**tdra**	**D30**	**D60**
Root_Wt	32.3	7.5	95.2	1.3	-0.3	-1.6
BGBio	7.5	553.9	390.1	189.9	-0.2	-1.2
AGBio	95.2	390.1	92084.7	55.1	1.9	10.0
tdra	1.3	189.9	55.1	365.3	-2.6	-2.3
D30	-0.3	-0.2	1.9	-2.6	0.1	0.1
D60	-1.6	-1.2	10.0	-2.3	0.1	0.3

Forward Stepwise Sequence of Chi-Squares for the Wilcoxon Test						
Variable	**DF**	**Chi-Square**	**Pr > Chi-Square**	**Chi-Square Increment**	**Pr > Increment**	**Label**
D60	1	15.9968	<.0001	15.9968	<.0001	60% Finer Diameter
Root_Wt	2	28.5321	<.0001	12.5353	0.0004	Root Wt
AGBio	3	39.0752	<.0001	10.5431	0.0012	Above Ground Biomass
BGBio	4	42.1703	<.0001	3.0951	0.0785	Below Ground Biomass
tdra	5	43.9207	<.0001	1.7504	0.1858	Soil Moisture
D30	6	45.8424	<.0001	1.9217	0.1657	30% Finer Diameter

Figure G.2 (cont.)

Univariate Chi-Squares for the Log-Rank Test					
Variable	**Test Statistic**	**Standard Error**	**Chi-Square**	**Pr > Chi-Square**	**Label**
Root_Wt	-11.2311	8.4415	1.7701	0.1834	Root Wt
BGBio	100.2	50.1127	3.9960	0.0456	Below Ground Biomass
AGBio	1660.0	640.9	6.7094	0.0096	Above Ground Biomass
tdra	32.3441	33.1856	0.9499	0.3297	Soil Moisture
D30	-0.9282	0.4109	5.1039	0.0239	30% Finer Diameter
D60	-3.1869	1.1036	8.3392	0.0039	60% Finer Diameter

Covariance Matrix for the Log-Rank Statistics						
Variable	**Root_Wt**	**BGBio**	**AGBio**	**tdra**	**D30**	**D60**
Root_Wt	71	7	186	-41	-0	-4
BGBio	7	2511	10403	973	1	5
AGBio	186	10403	410732	4470	47	158
tdra	-41	973	4470	1101	-7	-3
D30	-0	1	47	-7	0	0
D60	-4	5	158	-3	0	1

Forward Stepwise Sequence of Chi-Squares for the Log-Rank Test						
Variable	**DF**	**Chi-Square**	**Pr > Chi-Square**	**Chi-Square Increment**	**Pr > Increment**	**Label**
D60	1	8.3392	0.0039	8.3392	0.0039	60% Finer Diameter
AGBio	2	19.3436	<.0001	11.0045	0.0009	Above Ground Biomass
Root_Wt	3	32.0531	<.0001	12.7094	0.0004	Root Wt
BGBio	4	33.9652	<.0001	1.9122	0.1667	Below Ground Biomass
tdra	5	38.9261	<.0001	4.9609	0.0259	Soil Moisture
D30	6	39.5281	<.0001	0.6020	0.4378	30% Finer Diameter

APPENDIX H: ACRONYMS

Acronym	Initial Components
AR	Army Regulation
ASABE	American Society of Agricultural and Biological Engineers
ASTM	American Society for Testing and Materials
CBR	California-bearing ratio
CERL	Construction Engineering Research Laboratory
CI	cone index
CIV	Clegg impact value
CRREL	Cold Regions Research and Engineering Laboratory
ERDC	Engineering Research and Development Center
GSL	Geotechnical and Structures Laboratory
GUI	Graphical User Interface
HAT	Hilltop Access Trail
ITAM	Integrated Training Area management
LCTA	Land Condition-Trend Analysis
NRCS	Natural Resources Conservation Service
NRMM	NATO Referenced Mobility Model
OPAL	Optimal Allocation of Training Lands
PVC	poly-vinyl chloride
RTLP	Range and Training Lands Program
SRP	Sustainable Range Program
TDR	time domain reflectometry
UIUC	University of Illinois Urbana-Champaign
USCS	United Soil Classification System
USDA	United States Department of Agriculture
VASST	Vegetation And Soil Shear Tester
WES	Waterways Experimental Station